CATALYTIC OZONATION OF PHARMACEUTICALS IN AQUEOUS SOLUTION

A dissertation submitted to the

ALCALA UNIVERSITY

For the degree of

DOCTOR OF ALCALA UNIVERSITY

Presented by

MARÍA SOLEDAD GONZALO MUÑOZ

Supervised by

ROBERTO ROSAL GARCÍA

ANTONIO RODRÍGUEZ FERNÁNDEZ-ALBA

2010

ACKNOWLEDGMENTS

Thanks to…

…The Spanish Ministry of Education and the Dirección General de Universidades e Investigación de la Comunidad de Madrid for financing the research projects CONSOLIDER INGENIO and REMTAVARES, respectively.

…Prof. Roberto Rosal García and Prof. Antonio Rodríguez Fernández-Alba for supervising my PhD process. They gave me the opportunity of performing this rearch work and achieved my dreams.

…Eloy García Calvo, who made my thesis possible in the department of Analytical and Chemical Engineering and trusted in me for this project.

… The Department of An Analytical Chemistry and Chemical Engineering and IMDEA Agua, to all the staff (Pedro, Karina, Jose Antonio, Irene, etc,), PhD students (Alejandro, Cristina, Javier, Jose Benito, Lety, Raúl, Sara, Susana, etc) and all the people that helped me during these years (Mar, Carol, Ana, Toñi, etc).

…my parents, Jose Antonio y Agustina, who supported me and always helped me either good or bad moments.

…my friends, Karelia, Estefanía, Marta, Irmina, etc., for taking care of my multiple problems and bearing countless hours of talking about this PhD work.

…and David, because he is the greatest.

RESUMEN

La detección de numerosos contaminantes orgánicos de origen antropogénico en masas de agua supone un importante riesgo medioambiental por su posible impacto en los ecosistemas acuáticos y en la salud humana. En particular, se han detectado numerosos fármacos, pesticidas y otros compuestos con actividad biológica algunos de los cuales podrían tener efectos crónicos. La evaluación de la toxicidad a través del uso de diferentes organismos acuáticos permite conocer el riesgo asociado a la presencia de los contaminantes en los diversos ambientes acuáticos naturales, si bien la valoración de los efectos a largo plazo requiere estudios complejos de los que apenas se dispone. La principal fuente de estos contaminantes son los efluentes de las plantas de tratamiento de aguas residuales convencionales, en cuyo proceso no se eliminan completamente y que suponen un aporte constante de contaminantes al medio natural. Los procesos de oxidación avanzada, basados en la generación de radicales hidroxilo, posibilitan la eliminación de contaminantes orgánicos en medio acuoso y en baja concentración. Entre ellos, los procesos basados en el ozono, un agente oxidante utilizado tradicionalmente para desinfección o precipitación de ciertos metales disueltos, suponen una opción particularmente viable que se basa en una tecnología bien establecida. El uso de catalizadores en el proceso de ozonización ha supuesto una mejora notable en la completa mineralización de los contaminantes. Metales, óxidos metálicos y metales soportados pueden acelerar significativamente la velocidad de las reacciones entre el ozono y sus productos de descomposición y los contaminantes presentes. Numerosos grupos de investigación han propuesto diversos mecanismos de actuación del catalizador, aunque aún hoy no hay ninguno que se admita de forma generalizada.

El objetivo de esta tesis doctoral es la caracterización del papel que desempeña el catalizador en las reacciones de ozonización para la eliminación de los compuestos farmacéuticos naproxeno, carbamazepina y ácido clofíbrico, el metabolito ácido fenofíbrico y los pesticidas atrazina y linuron. Para ello se han realizado ensayos en régimen continuo y semicontinuo utilizando catalizadores de óxido de titanio (TiO_2) y de óxido de manganeso soportado sobre alúmina (MnO_x/Al_2O_3), y sobre sílice mesoporosa (MnO_x/SBA15). Se ha determinado el papel del catalizador en la adsorción de los compuestos orgánicos y en la adsorción y

descomposición del ozono en diferentes condiciones de operación. Se han empleado tanto matrices sintéticas como aguas residuales y se han obtenido diversas constantes cinéticas de los procesos de ozonización. Además, se han propuesto mecanismos de actuación del catalizador basados en datos cinéticos, se identificaron varios compuestos intermedios de reacción, y se determinó la ecotoxicidad de las mezclas en función de la duración del tratamiento de ozonización.

En el caso de naproxeno y carbamazepina, compuestos que reaccionan con ozono con constantes cinéticas elevadas, se obtuvieron reducciones del carbono orgánico total de hasta un 75% para 1g/L de TiO_2 en los primeros 20 minutos de reacción. La mineralización presente dos períodos claramente diferenciados, el segundo de los cuales, más lento se ha asociado a la degradación de ácidos carboxílicos y otros productos de oxidación. Se determinó que el catalizador alcanza su máxima actividad en condiciones ácidas, lo que sugiere que los centros ácidos de la superficie desempeñan un papel en la reacción catalítica. En todos los casos se observó una mejora en la degradación del los compuestos orgánicos en presencia de TiO_2 y MnO_x, aunque mediante cinética competitiva se pudo determinar que el catalizador no produce una variación significativa en la constante de reacción entre los radicales hidroxilo y el ozono. Este hecho sugiere que, aunque efectivamente se produce un aumento en la producción de radicales hidroxilo, la interacción con los centros superficiales del catalizador con los compuestos orgánicos es limitada o nula. El incremento en la producción de radicales hidroxilo a partir de ozono se determinó mediante ensayos en régimen semicontinuo y en un reactor de lecho fijo catalítico y alcanzó valores de hasta treinta veces los correspondientes a ensayos sin catalizador. En la ozonización de ácido clofíbrico se observó un fuerte incremento de toxicidad en los primeros minutos de ozonización, siendo este menor en las reacciones catalíticas. Mediante determinación analítica de los intermedios de oxidación, esta toxicidad se ha podido asociar a la formación de intermedios producto de la apertura del anillo aromático. Los resultados obtenidos comparando soportes con distinta superficie específica indican que la dispersión del catalizador desempeña un papel importante en la reacción catalítica.

TABLE OF CONTENTS

CHAPTER 1

INTRODUCTION

1. Introduction

1.1. Background

1.1.1. Ozone in water treatment

The use of ozone for the depletion of pollutants in water treatment has been extensively studied in the last thirty years. In the late seventies, Hoigné and Bader analyzed the role of hydroxyl radicals in the ozonation processes, and studied the use of ozone in treating several natural waters in Switzerland [1, 2]. To determine the amount of ozone in water, both authors developed a method based on indigo, a colorant that reacts in the presence of ozone [3]. In subsequent papers, Hoigné and co-workers studied the reactions of ozone with different organic and inorganic compounds [4-6]. In 1984 Bühler et al. and Staehelin et al. studied the decomposition of ozone in water using the pulse radiolysis method [7, 8]. Stahelin and Hoigné described the effect of several promoters and inhibitors of the radical chain reactions that take place during ozone decomposition [9]. Finally, Tomiyasu et al. developed a complete kinetic for ozone decomposition in basic aqueous solution [10].

The disinfection capacity of ozone has been dealt with in a number of works studying the inactivation of different microorganisms [11-14]. Additional reasons for using ozone in the treatment of drinking water are taste and odour control and decolouration. Traditionally, the use of ozone as a disinfectant and oxidant in water treatment has been associated with a low level of disinfection by-products [15]. This is a key point in the use of ozone, which diminished considerably after bromate formation was discovered during the ozonation of bromide-containing waters [16]. The formation of the carcinogen bromate has also been shown to take place in advanced oxidation processes [17]. Glaze and Weinberg identified a number of polar drinking water disinfection by-products associated with the use of ozone [18].

Ozonation processes have also been proposed for the removal of wastewater pollutants [19]. In this regard, the introduction of anthropogenic pollutants into the aqueous environment has been shown to be largely due to the discharge from Wastewater Treatment Plants (WWTP) [20]. The removal of these compounds and their metabolites, and the study of toxicity evolution associated with effluent and treatment, is one of the key issues in current research [21-23].

Ozone reacts at a high rate with certain organic moieties such as double bounds, and is able to completely remove many organic pollutants from water and wastewater. However, since ozone has a limited capacity to achieve complete mineralization, a more powerful oxidant must be used in order to deplete organic intermediates. Advanced Oxidation Processes (AOP) are defined as those which exploit the high reactivity of hydroxyl radicals when driving oxidation processes; thus they are suitable for achieving the complete mineralization of even the least reactive pollutants [24,25]. These techniques usually operate at near or ambient temperature and pressure and are able to treat dilute streams as indicated in Fig. 1.1.

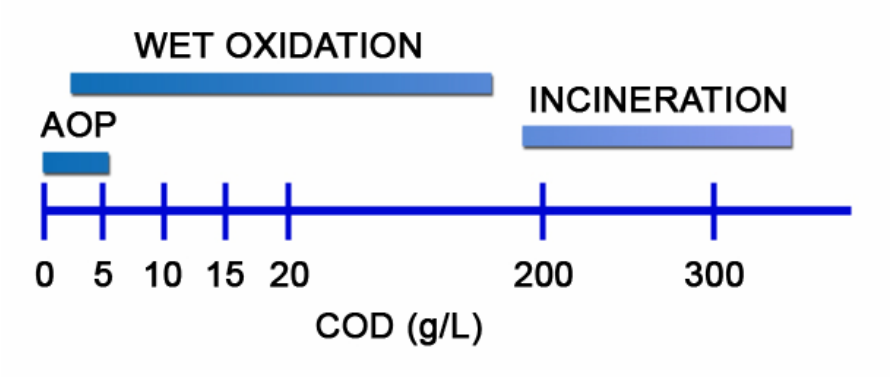

Fig.1.1. Suitability of water treatment technology as a function of chemical oxygen demand (COD); adapted from [24].

The versatility of AOP is enhanced by the fact that they offer a variety of possible ways to produce hydroxyl radicals, thus improving compliance with specific treatment requirements [24]. Hydroxyl radicals can be produced by the direct use of ozone or of ozone and hydrogen peroxide, but also by photocatalytic methods, Fenton-based systems, hydrodynamic or acoustic cavitation, radiolysis and several electrical and electrochemical methods [26, 27]. Table I shows a scheme of the AOP family.

Table I: Classification of Advanced Oxidation Processes based on the way hydroxyl radicals are generated

	Direct energy transfer	**Generation of hydroxyl radicals from ozone**	**Peroxone-based**	**Fenton homogeneous or heterogeneous processes**	**Heterogeneous catalytic processes**
Chemical	-	O_3-OH^- Alkaline ozonation	O_3-H_2O_2 Peroxone process	H_2O_2-Fe(II)/Fe(III) Fenton and Fenton-like processes	Catalytic ozonation (Metals, Metal oxides, Activated Carbon)
Photochemical	Direct photolysis*	O_3-UV Ozone photolysis	O_3-H_2O_2-UV Ultraviolet peroxone	H_2O_2-Fe(II)/Fe(III)-UV Photo-Fenton processes	TiO_2-UV (O_3-H_2O_2) Photocatalysis
Ultrasound	Sonolysis*	O_3-US Ozone-assisted cavitation	O_3-H_2O_2-US Ultrasound Peroxone	H_2O_2-Fe(II)/Fe(III)-US Sono-Fenton and US Fenton-like systems	Catalytic ultrasonic processes
Electrochemical	Anodic oxidation	Electrolytic generation of O_3	Electrolytic generation of O_3 or O_3-H_2O_2	Electro-Fenton methods	Wet electrocatalytic oxidation

* Not advanced oxidation processes

As mentioned above, ozone is a potential oxidation treatment for the removal of many types of organic pollutants in water and a more efficient disinfectant for most microorganisms than chlorine-based disinfectants. However, the direct reaction of ozone is highly selective and despite its substantial reactivity with microbial constituents, it is relatively unreactive towards many inorganic species and classes of organics compounds [28]. The oxidation of these reactants requires the generation of hydroxyl radicals, which are formed from ozone decomposition; as they constitute a highly reactive and nonspecific oxidant, they are chiefly responsible for being the main responsible for the degradation of certain ozone-resistant micropollutants [29].

While studying the generation of hydroxyl radicals from ozone, Elovitz and von Gunten introduced a parameter, R_{ct}, which represents the ratio of hydroxyl radicals and ozone at any time during the reaction [29].

$$R_{ct} = \frac{c_{HO^{\bullet}}}{c_{O_3}}$$

During the ozone treatment of water containing organic pollutants, the depletion of ozone frequently occurs in two reaction stages, the first being associated with the reaction of organic compound with a high second order direct rate constant [29]. According to the literature, R_{ct} varies in the $7 \times 10^{-10} \sim 10^{-7}$ range [29]. For example, in disinfection processes an R_{ct} of 10^{-8} is typical in the secondary phase [30].

While in natural waters R_{ct} is a constant during most of the ozonation process, in the ozonation of wastewater R_{ct} behaves as a parameter that characterizes the oxidation process [31]. Real et al. evaluated the generation of hydroxyl radicals in the elimination of hydrochlorothiazide from different water matrixes (surface water and a secondary effluent from a municipal wastewater treatment plant) [32]. For the initial reaction period, the R_{ct} values were 61.7×10^{-8} for surface water and 82.7×10^{-8} for a secondary effluent; and in the subsequent reaction period, 8.3×10^{-8} and 4.8×10^{-8}, respectively.

But the matrix is not only able to modify the hydroxyl radical-to-ozone ratio. Rosal et al. [67] studied the elimination of fenofibric acid in different matrixes (pure water, phosphate buffered water and wastewater) in the presence of certain catalysts (Al_2O_3 and MnO_x/Al_2O_3). For phosphate buffered water and wastewater, an amount of 1g/l of Al_2O_3 and MnO_x/Al_2O_3 improved the ratio in three and seven-fold respectively, compared to the non-catalytic ozonation.

Pharmaceuticals and personal care products (PPCPs) compose a group of emerging pollutants whose presence in water and wastewater may lead to public health problems even though their concentration is low. Some pharmaceuticals are not totally eliminated because the conventional technology of treatment used in WWTP is inadequate to the task [20, 34]. Although they can be degraded in the environment by biotic [35] or abiotic process [36, 37], it is assumed that pharmaceuticals act as persistent compounds simply because of their continual infusion into aquatic media via WWTP effluents, which sustain a multigenerational expose for the resident organisms [37]. Globally, the concentrations measured in WWTP effluents and in aquatic environment were in the nanograms-per-liter to micrograms-per-liter range [20, 34].

Many pollutants are an environmental risk not only on account of their acute toxicity, but also because they originate pathogen resistance and endocrine disruption [38]. In order to assess the ecotoxicity of PPCPs and other compounds in water and wastewater many tests have been developed using different organisms. Some of them, such as the marine bacteria *Vibrio fischeri*, the crustácea *Daphnia magna*, the algae *Pseudokirchneriella subcapitata*, the plant *Lemna minor* or the fish *Danio rerio*, can detect toxic effects even at considerably low concentrations. Many of these tests are performed according to well-established international protocols such as ISO and OCDE guidelines [39-47].

The use of single organisms to evaluate wastewater ecotoxicity cannot provide a real assessment of risk. A more appropriate way to assess the risk presented by chemicals is the use of a battery of ecotoxicity test with representative organisms from different trophic levels.

The characterization of chemical-associated risk in the environment is assessed in line with two procedures specified by the European Medicines Evaluation Agency (EMEA). The concept Environmental Risk Assessment (ERA) is based in the parameter Risk Quotient (RQ), which is the ratio between the measured or predicted environmental concentrations and the concentration below which the exposure is not expected to cause adverse effects. The RQ parameter defines certain risk levels: "low risk" if $0.01 < RQ < 0.1$, "medium risk" if $0.1 < RQ < 1$ and "high risk" if $RQ > 1$. When the chemical exceeds a cut-off value of 0.01 μg/l in the surface water, EMEA proposes a second-tier procedure based on ecotoxicity, which may be accomplished with the other parameter. For aquatic organisms, the assessment of risk is achieved by comparing PEC (Predicted Environmental Concentrations) or MEC (Measured Environmental Concentration) with PNEC (Predicted No Effect Concentration). If the ratio MEC/PNEC is higher than unity a risk scenario, a third-tier process is included (chronic toxicity tests, bioaccumulation studies, etc.) [48].

Pollutants are not discharged individually to the environment, but forming complex mixtures of compounds from different classes. Current methods of risk assessment focus on single chemicals, in a procedure that assumes additive behaviour and may underestimate the risk associated with the toxic action of mixtures [49]. In fact, the combination of various pharmaceuticals may cause stronger effects than expected from measurements carried out on their individual components. Rodea-Palomares et al. investigated the toxicological interactions of lipid regulators in the aquatic environment with two bioluminescent organisms [50]. They observed the toxicological interactions between pharmaceuticals using the combination index (CI)-isobologram method, and obtained toxicological interactions that changed with the level of effect. Antagonism predominated at low and intermediate levels, while at a high level additive and synergism was more common.

1.1.2. Catalytic ozonation

Ozone is known to be a powerful oxidant, but it reacts slowly with some organic compounds such as inactivated aromatics. As mentioned above, it does not lead to the complete oxidation of organics, which results in the formation of carboxylic acids, carbonyl compounds and many others [51]. In recent years, catalytic ozonation has been attracting the interest of the scientific community dedicated to the study of ozone processes in water treatment. The use of the appropriate catalyst can improve ozone reactions in aqueous solutions. Catalytic ozonation can be performed using catalysts dispersed within the liquid phase or in the form of solid either suspended or in fixed bed.

Homogeneous catalytic ozonation is based on ozone activation by metal ions present in aqueous solution. The catalysts usually used are transition metals such as Fe(II), Mn(II), Ni(II), Co(II), Cd(II), Cu(II), Ag(I), Cr(III) and Zn(II), whose nature determines not only the reaction rate, but also selectivity and ozone consumption [52]. In a possible mechanism to explain the role of homogeneous catalysts, the decomposition of ozone is enhanced by metal ions, thus leading to the generation of free radicals, including hydroxyl radicals.

An example of a homogeneous catalytic ozonation is the mechanism proposed by Saudela and Brillas, who explained the formation of hydroxyl radicals in the presence of Fe^{2+} ions [53]. In this case, the direct reaction of Fe^{2+} with ozone resulted in the production of hydroxyl radicals:

$$Fe^{2+} + O_3 \rightarrow FeO^{2+} + O_2 \quad \text{(I)}$$

$$FeO^{2+} + H_2O \rightarrow Fe^{3+} + HO^{\bullet} + OH^{-} \quad \text{(II)}$$

At higher concentrations of Fe^{2+}, FeO^{2+} can be oxidised to Fe^{2+}, so that the reactions leading to radical generation take place only at low concentrations of Fe^{2+}:

$$FeO^{2+} + Fe^{2+} + 2H^{+} \rightarrow 2Fe^{3+} + H_2O \quad \text{(III)}$$

During homogeneous catalytic ozonation, an initial complex can be formed between the organic molecule and the metal ion, followed by oxidation of the complex by ozone, which leads to the formation of hydroxyl radicals [52]. Pines et al. proposed that in the ozonation of oxalic acid with Co^{2+}, the first step is the formation of the complex Co^{2+}-oxalate [54]. This is then oxidized by ozone to form Co^{3+}-oxalate, and finally the oxidation of oxalate and the regeneration of Co^{2+} takes place. Beltrán et al. identified four different Co^{2+}-oxalate complexes in the reaction, the main one being $Co(HC_2O_4)_2$, [55]. The mechanism proposed was the following:

$$Co(HC_2O_4)_2 + O_3 \rightarrow Co(HC_2O_4)_2^+ + O_3^{-}\bullet \quad \text{(IV)}$$

$$Co(HC_2O_4)_2^+ \rightarrow Co(HC_2O_4)^+ + 2CO_2 \quad \text{(V)}$$

$$Co(HC_2O_4)^+ + HC_2O_4^- \rightarrow Co(HC_2O_4)_2 \quad \text{(VI)}$$

The reaction of ozone with $Co(HC_2O_4)_2$ was taken to account for the removal of the organic pollutant. Similar reactions were proposed using iron catalysts in the degradation of oxalic acid [56].

Concerning heterogeneous ozonation, the activity of solid catalysts may be due to any of several mechanisms:

I. Adsorption of organics on the solid surface with reaction with oxidized surface sites or adsorbed oxidant species.

II. Reaction of non-adsorbed organics from the bulk with oxidized surface sites or surface-adsorbed oxidants.

III. Reaction of organics adsorbed on the surface of the catalysts that react with the ozone of hydroxyl radicals from the bulk.

IV. The oxidation reaction takes place in the bulk, the activity of the catalyst being based on the enhanced generation of oxidant species through the catalytic decomposition of ozone.

With regard to the formation of oxidized surface sites, several possibilities exist. Legube and Vel Leitner proposed a mechanism for the ozonation on supported metals in which ozone oxidizes the surface of the reduced metal catalyst, thereby generating hydroxyl radicals [57]. Organic molecules, also adsorbed, are supposed to react with oxidized sites by an electron transfer reaction to yield back the metal in reduced form, the mechanism being a particular case of a Langmuir-Hinshelwood interaction.

The decomposition of ozone may take place on the Lewis sites of metal oxides such as Al_2O_3, TiO_2 or ZrO_2 or on non-dissociated hydroxyl groups on the surface of metal oxides, whether supported or not. Alternatively, the decomposition of ozone on activated carbons takes place on basic centres of the catalyst [52].

For a solid to disclose any catalytic activity, the adsorption of ozone, the organic molecule or both must take place on its surface. Langmuir-Hinshelwood mechanisms are based on the simultaneous adsorption of ozone and the organic compound with the formation of products at catalyst surface. In Eley-Rideal mechanisms only one reagent is adsorbed, the other reacting from the bulk and without any previous interaction with the catalyst surface. However, it is very difficult to prove that the adsorption of ozone on solid surfaces plays a role in the catalytic process carried out in aqueous solution. Acid adsorption centres reveal a high affinity towards water, a Lewis base present in high concentration. In basic medium, the presence of hydroxide anion, a strong Lewis base, makes the competitive adsorption of organics even harder. Furthermore, most published papers record rather low adsorption of organic molecules [58]. As a result, ozone decomposition on the surface of the catalysts is usually cited as a factor determining the activity of the catalyst. This is also due to the frequently observed high capacity of such catalytic systems to generate hydroxyl radicals [52].

Several physical and chemical properties determine the catalytic activity such as surface area, density, pore volume, porosity and pore size distribution as well as mechanical strength, purity, and chemical stability. Many of these are variables determining the presence of active surface sites [50]. Also, there are several factors that affect the heterogeneous catalytic ozonation process. The most important are temperature and pH, which significantly affect ozone solubility and stability in water. The ozone decomposition constant is strongly pH dependant and increases with an increase of pH [19]. pH also influences the surface properties of metal oxides, particularly their charge, which has a direct effect on their adsorption capacity towards organic molecules [50].

The most widely used catalysts in heterogeneous catalytic ozonation are supported or unsupported metal oxides, metal on supports and activated carbon. What follows is a brief summary of the most outstanding results covering these three families of catalyst.

The primary parameter determining the catalytic properties of metal oxides in aqueous solution is their acidity. The hydroxyl groups formed on metal surfaces behave as Brönsted acid sites. Lewis acid and Lewis bases are sites located on the metal cation and coordinatively unsaturated oxygen respectively. Both Brönsted and Lewis acid sites determine surface charge and, therefore, the interaction of the catalyst with charged solutes. Ion exchange properties are a consequence of the ability of surface hydroxyl groups to dissociate or to be protonated depending on the pH value of the solution [59]:

$$M–OH + H^+ \leftrightarrows M–OH_2^+ \quad \text{(VII)}$$
$$M\text{-}OH + OH^- \leftrightarrows M\text{-}O^- + H_2O \quad \text{(VIII)}$$

As a function of pH, the surface will bear positive or negative charge, being neutral at a given solution pH known as point of zero charge (pH_{PZC}).

Metal oxides exchange ligands due to the presence of Lewis acid sites on the surface, coordinatively unsaturated metals that bind Lewis bases by displacing water molecules. Moreover, the dissociation of surface hydroxyl groups determines a net positive charge at $pH < pH_{PZC}$, allowing the catalyst to behave as an anion exchanger, and a negative charge at $pH < pH_{PZC}$, at which the surface may exchange anions.

MnO_2 is the most widely studied metal oxide for catalytic ozonation; its efficiency has been reported in many studies [60, 61]. Ma and Graham used MnO_2 formed *in situ* from Mn(II) and proposed a radical-type mechanism for the ozonation of atrazine [62]. Andreozzi et al., studied the ozonation of oxalic acid and assumed the formation of a surface complex followed by a 'one electron' exchange step and the detachment of the reduced surface metal site [63]:

$$=Mn(III)OH_2^+ + C_2O_4^{2-} \leftrightarrows =Mn(III)C_2O_4^- + H_2O \quad \text{(IX)}$$
$$=Mn(III)C_2O_4^- \leftrightarrows =Mn(II) + CO_2^{\bullet -} + CO_2 \quad \text{(X)}$$
$$=Mn(II) \rightarrow =Mn(II)aq \quad \text{(XI)}$$

The adsorbed and/or dissolved ozone can react with the surface $=Mn(III)C_2O_4^-$ complex at a rate at least comparable with that of the intramolecular electron transfer:

$$=Mn(III)C_2O_4^- + O_3 + 2H^+ \rightarrow 2CO_2 + O_2 + =Mn(III)OH_2^+ \quad \text{(XII)}$$

Finally, ozone can also oxidise reduced species =Mn(II)aq and/or =Mn(II):

$$=Mn(II)aq \xrightarrow{O_3} =Mn(III, IV)OH_2^+ \quad \text{(XII)}$$

$$=Mn(II) \xrightarrow[H_2O]{O_3} =Mn(III, IV)OH_2^+ \quad \text{(XIV)}$$

Al_2O_3 is another metal oxide that has been reported as an ozonation catalyst for the removal of organic contaminants in solution. Kasprzyk-Hordem et al. studied the ozonation of natural organic matter (NOM) on alumina and assumed that the adsorption of NOM on the surface played a role in the catalytic process [64]. Ozone was supposed to attack adsorbed NOM from the bulk because the presence of high concentrations of NOM and oxalic acid — compounds with a high affinity towards alumina — was thought to prevent the adsorption of ozone. The oxidative reactions between molecular ozone and adsorbed NOM should take place mainly at the solid–liquid interface.

Ernst et al. suggested that dissolved ozone adsorbs first on the catalyst's surface, while the adsorption of the organic substances seems to inhibit the catalytic effect [65]. Once that the ozone is adsorbed, it decomposes rapidly due to the presence of hydroxyl surface groups.

Although titania is mainly used in photocatalysis, it has also been proposed as an active catalyst in the ozonation of organic molecules such as nitrobenzene [66]. Beltrán et al. proposed a Langmuir-Hinshelwood mechanism in which ozone adsorbs and decomposes on certain catalyst sites (S) at the TiO_2, yielding oxidizing sites that subsequently react with adsorbed oxalate [67]:

$$O_3 + S \leftrightarrows O{=}O{-}O{-}S \quad \text{(XV)}$$
$$O{=}O{-}O{-}S \rightarrow O{-}S + O_2 \quad \text{(XVI)}$$
$$B + S \leftrightarrows B{-}S \quad \text{(XVII)}$$
$$O{-}S + B{-}S \leftrightarrows 2CO_2 + H_2O + 2S \quad \text{(XVIII)}$$

Rosal et al. studied the degradation of clofibric acid by means of catalytic ozonation on titania and suggested that even if the catalytic surface plays a significant role in the production of hydroxyl radicals, the interaction of surface sites and organics is probably limited [23, 26].

Several other metal oxides such as ZnO, SnO_2, NiO, CuO and CeO_2 were also studied as catalysts for the ozonation process. However, the most promising catalyst, apart from those previously mentioned, is goethite (FeOOH). Zhang and Ma suggested that catalytic ozonation on goethite proceeds via a radical pathway in which unchanged surface hydroxyl groups of the catalyst induce the ozone decomposition to generate hydroxyl radicals [68].

Metal oxides such as TiO_2, Fe_2O_3, MnO_2, immobilised on a variety of supports including silicagel, clay, Al_2O_3 or TiO_2, are effective catalysts for the ozonation of aqueous organic compounds. Beltrán et al. studied the degradation of oxalic acid in water with TiO_2/Al_2O_3 and proposed that the process rate could be described by considering an Eley-Rideal mechanism in which adsorbed oxalic acid reacted directly with non-adsorbed ozone [69]. The authors claimed that the catalyst used did not promote the decomposition of ozone and, therefore, did not produce any active oxygen adsorbed species. Other authors, however, reported an enhanced decomposition of dissolved ozone in the presence of TiO_2 [70].

Yang et al. studied the interaction of ozone with mesoporous alumina-supported manganese oxide and assessed the presence of Lewis and Brönsted sites in the catalyst by means of Fourier transform infrared (FTIR) spectroscopy and in situ attenuated total reflection FTIR (ATR-FTIR) spectroscopy [58]. Their results revealed surface hydroxyl groups from adsorbed water, which were caused by the interaction of the catalyst with ozone. The introduction of MnO_x enhanced the formation and activation of new surface hydroxyl groups. On the other hand, Yang observed no significant adsorption of the pharmaceuticals phenazone, ibuprofen, diphenhydramine, phenytoin and diclofenac, and suggested that the oxidation reactions occur mainly in the aqueous phase, not on the surface of the catalyst.

Metals on several supports such as ruthenium or copper deposited Cu-Al_2O_3, CeO_2, Ru/CeO_2-TiO_2 or Cu-Al_2O_3 have also been used as ozonation catalysts [71, 72]. Legube et al. proposed two main mechanisms for the catalytic ozonation of organic compounds in aqueous solution on supported metals [57]. In the first, the organic compound would become adsorbed to yield a surface complex oxidized by ozone to give oxidation by-products either desorbed in solution or detached to the bulk. Ozone or hydroxyl radicals would subsequently oxidize desorbed by-products in homogeneous solution. In the second mechanism, a Mars-van Krevelen-like one, the catalyst would become oxidized by ozone originating oxidizing sites that react with adsorbed organics. Organic would be oxidized by an electron-transfer reaction to yield back the catalyst in reduced form.

Nawrocki and Kasprzyk-Hordern concluded that the mechanisms of heterogeneous catalytic ozonation in the presence of supported metals differ from those observed on metal oxides [52]. They argued that no generation of free hydroxyl radicals is observed in the case of heterogeneous process in the presence of metals on supports. Instead, reactions on the catalyst surface or involving complex formation are believed to be responsible for catalytic effects.

That activated carbon improves considerably the removal rate of organic pollutants in individual water processes is widely accepted [73, 74]. Different mechanisms have been proposed to explain the role of activated carbon in ozonation processes, but the results are puzzling. While some reports indicate an increase in radical exposures, such as Beltrán et al. [73], elsewhere the same authors have suggested that activated carbon does not generate hydroxyl radicals [75].

Faria et al. studied the reaction of oxamic and oxalic acids with ozone using activated carbon [75]. These authors alleged that there is evidence that the ozonation of both carboxylic acids occurred through a catalytic mechanism involving surface and bulk reactions. First, activated carbon is supposed to act as an initiator of the decomposition of dissolved ozone yielding free radical species, such as $HO^{\bullet}$:

$$O_3 \xrightarrow{AC} HO^{\bullet} \qquad \text{(XIX)}$$

Another possibility is the adsorption and reaction of ozone molecules on the surface of the activated carbon, yielding surface-bonded radicals:

$O_3 + AC \rightarrow AC - O$ (XX)

where AC-O stands for any oxygen-containing active species on the surface of the activated carbon, including bonded $HO^{\cdot}$ radicals. It is thus possible for oxidation of carboxylic acids to occur on the surface of the activated carbon between the adsorbed reagent (R) and surface radical species in the following stages:

$R + AC \rightarrow AC - R$ (XXI)
$AC - R \rightarrow AC - O \rightarrow P$ (XXII)

These authors concluded that adsorption should play an important role in the catalytic effect of activated carbon during ozonation process, but it is not clear whether the adsorption of ozone or organics is the key process in the reaction.

1.2. Research objectives

- Assessment of the catalytic degradation of several compounds belonging to different chemical classes by determining the rate of removal and mineralization under different ozonation conditions and in reactions performed in a semicontinuous reactor as well as in a continuous fixed-bed reactor.

- Determination of the role of different metal oxide catalysts in the generation of hydroxyl radicals from ozone using single component kinetics and competitive kinetics in different reaction conditions, including the use of real wastewater matrixes.

- Assessment of the effect of the interaction of catalytic surface and organic compounds by determining the extent and rate of adsorption in different conditions and by exploring a possible interaction with the surface that could lead to a preferential kinetic route.

- Determination of the extent of mineralization, characterization of oxidation by-products, and assessment of the toxicity of partially ozonated mixtures towards different organisms and comparing catalytic and non-catalytic processes.

1.3. Thesis Layout

The present thesis is based on articles published prior to the PhD defense. Each article/chapter is a self-standing unit, but they all belong in the same line of research. There follows a brief summary of each chapter:

Chapter 1 – *Introduction* – describes the background of this study, summarizes its research objectives, explains the connections between chapters and finally enumerates the main results achieved.

Chapter 2 – *Catalytic ozonation of naproxen and carbamazepine on titanium dioxide (Applied Catalysis B: Environmental 84 (2008), 48–57)* – describes the study of the aqueous phase catalytic and non-catalytic ozonation of naproxen (a non-steroidal anti-inflammatory drug) and carbamazepine (an antiepileptic agent) in a semicontinuous regime using Degussa P25 TiO_2 catalyst in the pH range 3-7 in pure water.

Chapter 3 – *Ozonation of clofibric acid catalyzed by titanium dioxide (Journal of Hazardous Materials, 169 (2009), 411-418)* – studies the removal of clofibric acid from aqueous solutions in catalytic and non-catalytic catalytic semi-continuous regime with Degussa P25 TiO_2 catalyst. The kinetics is analyzed using second order expressions for the reactions between organics and ozone or hydroxyl radicals.

Chapter 4 – *Identification of intermediates and assessment of ecotoxicity in the oxidation products generated during the ozonation of clofibric acid. (Journal of Hazardous Materials, 172 (2009), 1061-1068)* – determines the occurrence of oxidation by-products and assesses the toxicity of the oxidized mixtures obtained during the catalytic and non-catalytic ozonation of clofibric acid with Degussa P25 TiO_2.

Chapter 5 – *Catalytic ozonation of fenofibric acid over alumina-supported manganese oxide (Journal of Hazardous Materials, 183 (2010), 271-278)* – uses kinetic data to highlight the mechanism by which solid catalysts enhance the rate of ozonation in aqueous solution and determines whether or not the possible adsorption of organics on catalytic surfaces results in a change of ozonation rate constants in pure water and wastewater.

Chapter 6 – *Catalytic ozonation of atrazine and linuron on MnOx/Al_2O_3 and MnO_x/SBA-15 in a fixed bed reactor (Chemical Engineering Journal, in press, d.o.i. 10.1016/j.cej.2010.10.020, published on line 15 October 2010)* – studies a possible interaction organic molecules and catalytic surface that could lead to an energetically favoured pathway, and determines the influence of MnO_x on the increase of hydroxyl radicals produced from ozone, as well as the effect of a greater surface dispersion of the oxide when using SBA as support instead of activated alumina.

1.4. Results summary

- Most organic compounds were degraded in the first few minutes after coming in contact with ozone. The mineralization of reaction mixtures took place in two periods, a rapid ozonation stage being followed by slow mineralization of the more refractory compounds.

- The nanoparticulate catalyst TiO_2 favours the decomposition of ozone under acidic conditions, while at neutral pH it behaved as an inhibitor of ozone decomposition. This result suggested a blocking of acidic surface sites and a parallel increase in the concentration of hydroxide anion. These sites would be responsible for the adsorption of ozone or organics and reached maximum activity under acidic conditions.

- The depletion of clofibric acid was enhanced by the presence of TiO_2, with an increase in the production of hydroxyl radicals; but the second order rate constant for the reaction with hydroxyl radicals yielded values coincident with those for homogeneous ozonation. Both facts suggested that even if the catalytic surface played a role in the production of hydroxyl radicals, the interaction with the surface sites and organics is probably limited.

- The results of the toxicity bioassays showed a significant increase of toxicity during the initial stages of ozonation both for *Vibrio fischeri* and *Daphnia magna*, but particularly for the latter. The products of catalytic runs exhibited considerably lower toxicity.

- For the oxidation reaction of fenofibric acid with Al_2O_3 and MnO_x/Al_2O_3, the indirect ozonation rate constant did not increase with the use of catalysts. This fact suggested again the absence of any surface interaction with fenofibric acid. The same results were obtained with phosphate buffer water and wastewater. Although the indirect ozonation rate constant did not increase, the hydroxyl radical-to-ozone ratio was significantly improved by the use of catalysts in all matrixes.

- In reactions performed in a fixed bed reactor, a manganese oxide catalyst supported in high area mesoporous silica, MnO_x/SBA-15 (1.0 % as MnO_2), considerably increased the rate of production of hydroxyl radicals from ozone over the same active phase on alumina, showing that the dispersion of the catalyst plays an important role in the ozonation process. The absence of any surface interaction with atrazine and linuron was also demonstrated, probably indicating that their adsorption did not take place at all.

1.5. References

[1] Hoigné, J., Bader, A., The role of Hydroxyl radical reaction in ozonation processes in aqueous solutions, Water Res. 10 (1976) 377-386.

[2] Hoigné, J., Bader, H., Ozonation of water: "Oxidation-competition values" of different types of waters used in Switzerland. Ozone Sci. Eng., 1 (1979) 357-372.

[3] Hoigné, J., Bader, Determination of ozone in water by indigo method, Water Res., 15 (1981) 449-456.

[4] Hoigné, J., Bader, H., Rate constants of reactions of ozone with organic and inorganic compounds in water – I Non-dissociating organics compounds, Water Res., 17 (1983) 173-183.

[5] Hoigné, J., Bader, H., Rate constants of reactions of ozone with organic and inorganic compounds in water – II Dissociating organics compounds, Water Res., 17 (1983) 185-194.

[6] Hoigné, J., Bader, H., Haag, W.R., Staehelin, J., Rate constants of reactions of ozone with organic and inorganic compounds in water – III Inorganic compounds and radicals, Water Res., 19 (1985) 993-1004.

[7] Bühler, R.E., Staehelin, J., Hoigné, J., Ozone decomposition in water studied by pulse radiolysis 1. HO_2/O_2^- and HO_3/O_3^- as intermediates (incl. Erratum), J. Phys. Chem., 12 (1984) 2560-2564.

[8] Staehelin, J., Bühler, R.E., Hoigné, J., Ozone decomposition in water studied by pulse radiolysis 2. OH and OH_4 as chain intermediates, J. Phys. Chem., 88 (1984) 5999-6004.

[9] Staehelin, J., Hoigné, J., Decomposition of ozone in water in the presence of organics solutes acting as promoters and inhibitors or radical chain reactions, Environ. Sci. Technol., 19 (1985) 1206-1213.

[10] Tomiyasu, H., Fukutomi, H., Gordon, G., Kinetics and mechanism of ozone decomposition in basic solution, Inorg. Chem., 24 (1985) 2962-2966.

[11] Hunt, N.K., Mariñas, B.J., Kinetics of *Echerichia Coli* inactivation with ozone, Water Res., 31 (1997) 1355-1362.

[12] Driedger, A., Staub,E., Pinkernell, U., Mariñas, B., Köster, W., Gunten, U., Inactivation of *Bacillus subtilis* spores and formation of bromate during ozonation, Water Res., 35 (2001) 2950-2960.

[13] Driedger, A., Rennecker, J.L., Mariñas, B., Sequential inactivation of *Cryptosporidium parvum* oocysts with ozone and free chlorine, Water Res., 34 (2000) 3591-3597.

[14] Wolfe R.L., Stewart, M.H., Scott, K.N., McGuire M.J., Inactivation of *Giardia muris* and indicator organisms seeded in surface water supplies by peroxone and ozone, Environ. Sci. Technol., 23 (1999) 744-745.

[15] Langlais, B., Reckhow, D.A., Brink, D.R., Ozone in water Treatment: Apllications and Engineering, Lewis Publishers, Boca Raton, 1991.

[16] Von Gunten, U., Hoigné, J., Bromate formation during ozonation of bromide-contining Waters: Interaction of ozone and hydroxyl radical reactions, Environ. Sci. Technol., 28 (1994) 1234-1242.

[17] Von Gunten, Bruchet A., Costentin, E., Bromate formation in advanced oxidation processes, J. Am. Water Works Assoc. 88 (6) (1996) 53-65.

[18] Glaze, W.H., Weinberg, H.S., Identification and occurrence of ozonation by-products in drinking waters, AWWA, Denver, 1993.

[19] Beltrán, F.J., Ozone reaction kinetics for water and wastewater systems, Lewis Publishers, Boca Raton, 2004.

[20] Ternes, T.A., Occurrence of drugs in German sewage treatment plants and rivers, Water Res., 32 (1998) 3245-3260.

[21] Petrovic, M., Eljarrat, E., López, M.J., Barceló, D., Endocrine disrupting compounds and other emerging contaminants in the environment: a surrey on new monitoring strategies and occurrence data, Anal. Bioanal. Chem., 378 (2004) 549-562.

[22] Ternes, T.A., Meisenheimer, M., McDowell, D., Sacher, F., Brauch, H.J., Haist-Gulde, B., Preuss, G., Wilme, U., Zulei-Seibert, N., Removal of pharmaceuticals during drinking water treatment, Environ. Sci. Technol., 36 (2002) 3855-3863.

[23] Rosal, R., Gonzalo, M.S., Boltes, K., Letón, P., Vaquero, J.J., García-Calvo, E., Identification of intermediates and assessment of ecotoxicity in the oxidation products generated during the ozonation of clofibric acid, J. Hazard. Mater., 172 (2009) 1061-1068.

[24] Andreozzi, R., Caprio, V., Insola, A., Marotta, R., Advanced oxidation processes (AOP) for water purification and recovery. Catal. Today, 53 (1999) 51-59.

[25] Andreozzi, R., Caprio, V., Insola, A., Marotta, R. Tufano, V., The ozonation of pyruvic acid in aqueous solutions catalyzed by suspended and dissolved manganese, Water Res., 32 (1998) 1492-1496.

[26] Rosal, R., Gonzalo, M.S., Rodríguez, A., García-Calvo, E., Ozonation of clofibric acid catalyzed by titanium dioxide, J. Hazard. Mater., 169 (2009) 411-418.

[27] Beltrán, F.J., Encinar, J.M., González, J.F., Industrial wastewater advanced oxidation. Part 2. Ozone combined with hydrogen peroxide or UV radiation, Water Res., 31 (1997) 2415-2428.

[28] Pi, Y., Schumacher, J., Jekel, M., The use of para-chlorobenzoic acid (pCBA) as an ozone/hydroxyl radical probe compound, Ozone: Sci. Eng., 27 (2005) 431-436.

[29] Elovitz, M.S., von Gunten, U., Hydroxyl radical/ozone ratios during ozonation proceses. I. The R_{ct} cconcept, Ozone: Sci. Eng., 21 (1999) 239-260.

[30] Elovitz, M.S., von Gunten, U., Kaiser, H., Hydroxyl radical/ozone ratios during ozonation proceses. II. The effect of temperature, pH, alkalinity and DOM properties, Ozone: Sci. Eng., 22 (2000) 123-150.

[31] Buffle, M.O., Shumacher, J., Salhi, E., Jekel, M., von Gunen, U., Measurement of the initial phase of ozone decomposition in water and wastewater by means of a continuous quech-flow system: application to disinfection and pharmaceutical oxidation, Water Res., 40 (2006) 1884-1894.

[32] Real, F.J., Aceero, J.L., Benitez, F.J., Roldán, G., Fernández, L.C., Oxidatioon of hydrochlorothiazide by UV radiation, hydroxyl radicals and ozone: kinetics and elimination from water systems, Chem. Eng. J., 160 (2010) 72-78.

[33] Rosal, R., Gonzalo, M.S., Rodríguez, A., García-Calvo, E., Catalytic ozonation of fenofibric acido ver alumnia-supported manganese oxide, J. Hazard. Mater 183 (2010), 271-278.

[34] Rosal, R., Rodríguez, A., Perdigón-Melón, J.A., Petre, A., García-Calvo, E., Gómez, M.J., Agüera, A., Fernández-Alba, A.R., Ocurrence of emerging pollutants in urban wastewater and their removal through biological treatment followed by ozonation, Water Res., 44 (2010) 578-588.

[35] Winkler, M., Lawrence, J.R., Neu, T.R., Selective degradation of ibuprofen and clofibric acid in two model river biofilm systems, Water Res., 35 (2001), 3197-3205.

[36] Andreozzi, R., Marotta, R., Pinto, G., Pollio, A., Carbamazepine in water: persistence in the environment, ozonation treatment and preliminary assessment on algal toxicity, Water Res., 36 (2002), 2869-2877.

[37] Isidori, M., Nardelli, A., Pascarella, L., Rubino, M., Parrella, A., Toxic and genotoxic impact of fibrates and their photoproducts on non-target organisms, Environ. Int., 33 (2007) 635-642.

[38] Halling-Sorensen, B., Nielsen, S.N., Lanzky, P.F., Ingerslev, F., Holten Lützhoft, H.C., Jorgensen, S.E., Ocurrence, fate and effects of pharmaceuticals substances in the environment, Chemosphere 36 (1998) 357-393.

[39] ISO. Water quality – Determination of the inhibitory effect of water samples on the light emission of *Vibrio fischeri* (Luminescent bacteria test). Part 1: Method using freshly prepared bacteria. ISO 11348-1:2007.

[40] ISO. Water quality – Determination of the inhibitory effect of water samples on the light emission of *Vibrio fischeri* (Luminescent bacteria test). Part 2: Method using liquid-dried bacteria. ISO 11348-2:2007.

[41] ISO. Water quality – Determination of the inhibitory effect of water samples on the light emission of *Vibrio fischeri* (Luminescent bacteria test). Part 2: Method using freeze-dried bacteria. ISO 11348-3:2007.

[42] ISO. Water quality – Determination of the inhibition of the mobility of *Daphnia magna Straus* (Cladocera, Crustacea). Acute toxicity test. ISO 6341:1996.

[43] ISO. Water quality – Freshwater algal growth inhibition test with unicellular green algae. ISO 8692:2004.

[44] ISO. Water quality – Determination of the toxic effect of water constituents and waste water on duckweed (*Lemna minor*). Duckweed growth inhibition test. ISO 20079:2005.

[45] ISO. Water quality – Determination of the acute toxicity of wastewater to zefrafish eggs (*Danio rerio*). ISO 15088:2007.

[46] OECD Guideline for Testing of Chemicals 202 – Daphnia sp., Acute Immobilization Test.

[47] OECD Guideline for Testing of Chemicals 201- Freshwater alga and Cyanobacteria, Growth inhibition test.

[48] European Medicines Evaluation Agency (2006) Guideline on the environmental risk assessment of medicinal products for human use, London, Doc. Ref. EMEA/CHMP/SWP/4447/00.

[49] Cleuvers, M., Aquatic ecotoxicity of pharmaceuticals including the assessment of combination effects, Toxicol. Lett., 142 (2003) 185-194.

[50] Rodea-Palomares, I., Petre, A., Boltes, K., Perdigón-Melón, J.A., Leganés, F., Rosal, R., Fernández-Piñas, F., Application of the combination index (CI)-isobologram equation to study the toxicological interactions of lipid regulators in two aquatic bioluminescent organisms, Water Res., 44 (2010) 427-438.

[51] Kasprzyk-Hordern, B., Ziólek, M., Nawrocki, J., Catalytic ozonation and methods of enhancing molecular ozone reactions in water treatment, Appl. Catal. B: Environ., 46 (2003) 639-669.

[52] Nawrocki, J., Kasprzyk-Hordern, B., The efficiency and mechanisms of catalytic ozonation, Appl. Catal. B: Environ., 99 (2010) 27-42.

[53] Sauleda, R., Brillas, E., Mineralization of aniline and 4-chlorophenol acidic solution by ozonation catalyzed with Fe^{2+} and UVA light Appl. Catal. B: Environ., 29 (2001) 135-145.

[54] Pines, D.S., Reckhow, D.A., Effect of dissolved cobalt (II) on the ozonation of oxalic acid, Environ. Sci. Technol., 36 (2002) 4046-4051.

[55] Beltrán, F.J., Rivas, F.J., Montero-de-Espinosa, R., Ozone-Enchanced oxidation of oxalic acid in water with cobalt catalysts. 1. Homogeneous catalytic ozonation, Ind. Eng. Res. 42 (2003) 3210-3217.

[56] Beltrán, F.J., Rivas, F.J., Montero-de-Espinosa, R., Iron type catalysts for the ozonation of oxalic acid in water, Water Res. 39 (2005) 3553-3564.

[57] Legube, B., Karpel Vel Leitner, N., Catalytic ozonation: a promising advanced oxidation technology for water treatment, Catal. Today, 53 (1999) 61-72.

[58] Yang, L., Hu, C., Nie, Y., Qu, J., Catalytic ozonation of selected pharmaceuticals over mesoporous alumina-supported manganese oxide, Environ. Sci. Technol., 43 (2009) 2525-2529.

[59] Nawrocki, J., Rigney, M.P., McCormick, A., Carr, P.W., Chemistry of zirconia and its use in chromatography, J., Chromatogr. A. 657 (1993) 229-282

[60] Xiao, H., Liu, R., Zhao, X., Qu, J., Enchanced degradation of 2,4-dinitrotoluene by ozonation in presence of manganese (II) and oxalic-acid, J. Mol. Catal. A: Chem. 286 (2008) 149-155.

[61] Faria, P.C.C., Monteiro, D.C.M., Órfao, J.J.M., Pereira, M.F.R., Cerium, manganese and cobalt oxides as catalyst for the ozonation of selected organics compounds, Chemosphere 74 (2009) 818-824.

[62] Ma, J., Graham, N. J.D., Degradation of atrazine by manganese-catalysed ozonation: influence of húmic substances, Water Res., 33 (1999) 785-793.

[63] Andreozzi, R., Insola, A., Caprio, V., Marotta, R., Tufano, V., The use of manganese dioxide as a heterogeneous catalyst for oxalic acid ozonation in aqueous solution, Appl. Catal. A: General, 138 (1996) 75-81.

[64] Kasprzyk-Hordern, B., Raczyk-Stanislawiak, U., Swietlik, J., Nawrocki, J., Catalytic ozonation of natural organic matter on alumina, Appl. Catal. B: Environ., 62 (2006) 345-358.

[65] Ernst, M., Lurot, F., Schotter, J-C.H., Catalytic ozonation of refractory organic model compounds in aqueous solution by aluminium oxide, Appl. Catal. B: Environ., 47 (2004) 15-25.

[66] Yang, Y., Ma, J., Qin, Q., Zhai, X., Degradation of nitrobenzene by nano-TiO2 catalyzed ozonation J. Mol. Catal. A: Chem. 267 (2007) 41-48.

[67] Beltrán, F. J., Rivas, F. J., Montero-de-Espinosa, R., Catalytic ozonation of oxalic acid in an aqueous TiO_2 slurry reactor, Appl. Catal. B: Environ., 39 (2002) 221-231.

[68] Zhang, T., Ma, J., Catalytic ozonation of trace nitrobenzene in water with synthetic goethite, J. Mol. Catal. A: Chem., 279 (2008) 82-89.

[69] Beltrán, F. J., Rivas, F.J., Montero-de-Espinosa, R., A TiO_2/Al_2O_3 catalyst to improve the ozonation of oxalic acid in water, Appl. Catal. B: Environ., 47 (2004) 101-109.

[70] Rosal, R., Rodríguez, A., Zerhouni, M., Enhancement of gas-liquid mass transfer during the unsteady-state catalytic decomposition of ozone in water, Appl. Catal. A. General, 305 (2005) 169-175.

[71] Fu, H., Karpel Ven Leitner, N., Legube, B., Cataytic ozonation of chlorinated carboxylic acids with Ru/CeO_2-TiO_2 catalyst in the aqueous system, New J. Chem. 26 (2002) 1662-1666.

[72] Karpel Ven Leitner, N., Fu, H., pH effects on catalytic ozonation of carboxylic acids with metal on metal oxides catalysts, Top. Catal. 33 (2005) 249-256.

[73] Beltrán, F., Pocostales, J.P. Alvarez, P.M., Jaramillo, J., Mechanism and kinetics considerations of TOC removal from the powdered activated carbon ozonation of diclofenac aqueous solutions, J. Hazard. Mater., 169 (2009) 532-538.

[74] Faria, P.C.C., Órfao, J.J.M., Pereira, M.F.R., Ozonation of aniline promoted by activated carbon, Chemosphere 67 (2007) 809-815.

[75] Beltrán, F. J., Rivas, F.J., Alvarez, P.M., Montero-de-Espinosa, R., Kinetics of heterogeneous catalytic ozone decomposition in water on an activated carbon, Ozone: Sci. Eng., 24 (2002) 227-237.

[75] Faria, P.C.C., Órfao, J.J.M., Pereira, M.F.R., Activated carbon catalytic ozonation of oxamic and oxalic acid, Appl. Catal. B: Environ., 79 (2008) 237-243.

CHAPTER 2

CATALYTIC OZONATION OF NAPROXEN AND CARBAMAZEPINE ON TITANIUM DIOXIDE

Applied Catalysis B: Enviromental, 2008

2. Catalytic ozonation of naproxen and carbamazepine on titanium dioxide

Applied Catalysis B: Enviromental, 2008

2.1. Abstract

This study investigates the ozonation of naproxen and carbamazepine during catalytic and non-catalytic semicontinuous oxidation experiments performed at 25ºC and in the range of pH 3-7. The results showed that naproxen and carbamazepine were completely consumed in the first few minutes of reaction. The extent of mineralization during non-catalytic runs reached about 50% and essentially took place during a period covering the first 10-20 min. Catalytic runs were carried out on a commercial catalyst consisting of fumed colloidal TiO_2 particles. The catalyst increased the extent of mineralization by up to 75% of the initial organic carbon. The results showed that the catalyst enhanced mineralization both in acidic and neutral solutions, but the best results were obtained in a slightly acidic media. This effect was probably linked to the adsorption of ozone or reaction intermediates on Lewis acid catalytic sites. The catalyst enhanced the decomposition of ozone in an acid medium, but inhibited it in a neutral solution. This seems to exclude a mechanism based on the surface reaction of ozone with hydroxide ions linked to a negatively charged surface. Once formed, hydroxyl radicals may react with adsorbed organics or migrate to the bulk. The evolution of the total organic carbon measured in samples taken during the run was modelled as a function of the integral ozone exposure. The kinetic regression model considered that the ozonation products from naproxen or carbamazepine consisted of either oxidizable or refractory compounds, where the latter were necessarily produced from the former. The model assumed a second order reaction between organic compounds and ozone. The higher non-catalytic rate constants for the first

mineralization period were 1.048 x 10^{-2} ± 9.3 x 10^{-4} L $mmol^{-1}$ s^{-1} for naproxen and 6.16 x 10^{-3} ± 5.6 x 10^{-4} L $mmol^{-1}$ s^{-1} for carbamazepine, both at pH 7. The corresponding pseudohomogeneous catalytic rate constants were 7.76 x 10^{-3} ± 3.9 x 10^{-4} L $mmol^{-1}$ s^{-1} and 4.25 x 10^{-3} ± 9.7 x 10^{-4} L $mmol^{-1}$ s^{-1} for naproxen and carbamazepine respectively at pH 5 and with a catalyst load of 1 g/L. The evolution of carboxylic acids during reaction revealed that the catalyst avoided the accumulation of oxalate especially in comparison with non-catalytic runs, in which it accounted for up to 30% of the final organic carbon. Specific ultraviolet absorbance at 254 nm was also followed during the run. The products from naproxen reached a high absorbance from the beginning of the ozonation that was maintained throughout the run. For carbamazepine, however, the absorbance rapidly decreased revealing a different chemical structure of reaction products.

Keywords: Pharmaceuticals, Mineralization, Ozonation, Catalysis, Adsorption, Titanium Oxide.

2.2. Introduction

Human and veterinary drugs and their bioactive metabolites are continuously released into the environment and may lead to long-term adverse effects for aquatic and terrestrial organisms [1]. Ternes reported the existence of a number of drug residues in the discharge waters of German Municipal Sewage Treatment Plants as a consequence of their relatively high persistence in biological treatments performed with non-adapted microorganisms [2-3]. Some pharmaceuticals showed resistance even to advanced water treatment systems such as adsorption on granular activated carbon or ozonation, thus proving that there is a risk of exposure through drinking water supplies, especially in water reuse situations [4]. In fact, significant concentrations of these compounds have already been reported in rivers and other surface waters [5]. A combination of high residence-time biological treatment and ozonation seems to be a promising technology to be applied in wastewater treatment plants [6]. To overcome the relatively high-energy intensity of ozonation and the fact that some compounds are relatively refractory to ozonation treatments, several advanced oxidation processes have also been proposed [7, 8]. The homogeneous rate of hydroxyl radicals produced from ozone is strongly enhanced under alkaline conditions in which an important drawback exists in the case of water with

bromide levels higher than 50 μg/L due to the formation of bromate as an oxidation by-product [9]. Bromate formation can be avoided by limiting ozone exposure and by using pH < 7 [10]. Catalytic ozonation can be used to promote ozone decomposition, ozonation reactions or both in acidic conditions, in which the formation of hydroxyl radicals and the rate of mineralization would otherwise be too low. Moreover, the use of a catalyst has been repeatedly proposed to remove carboxylic acids, a class of organic compounds particularly refractory to the oxidation by ozone and produced during the ozonation of complex organic molecules [11, 12].

Supported and unsupported metals and metal oxides are the most commonly tested catalysts for the ozonation of organic compounds in water. Titanium oxide has been repeatedly reported as an active material able to accelerate the ozonation processes of different compounds [12-14]. Its role in the mineralization of low molecular weight carboxylic acids has been reported by Beltrán et al. [15-16] showing conversions forty times higher than that corresponding to non-catalytic homogeneous ozonation. Gracia et al. [17] reported a high activity of TiO_2 supported in alumina in the removal of organic carbon in natural waters by ozone. On the other hand, Cooper and Burch [18] found no significant differences between pure alumina and TiO_2/Al_2O_3 for the ozonation of oxalic acid. Concerning the mechanism of catalytic ozonation, there is still controversy regarding the ability of the catalyst to adsorb the organic substrate, especially on ionizable surfaces. Catalytic ozonation may proceed with the adsorption of ozone, the organic pollutant or both and the process may or may not involve surface equilibrium. It has been demonstrated that dissolved ozone adsorbs and decomposes on many solid surfaces other than activated carbon, the resulting radicals being responsible for indirect oxidation reactions [19]. The proposed mechanisms for heterogeneous ozone decomposition usually extrapolate the results obtained in the gas phase. For example, Dhandapani and Oyama [20] reported that the ozone decomposition on p-type oxides is consistent with the formation of superoxide (O_2^-) or peroxide (O_2^{2-}) species on the surface. Bullanin et al. [21] suggested that ozone dissociates after adsorption on strong Lewis sites yielding a surface oxygen atom, whereas on weaker sites, ozone molecules coordinate via one of the terminal oxygen atoms. Besides the liquid phase reaction of surface-produced radicals, the adsorption of organic molecules on the catalyst surface leads to additional mechanisms: an adsorbed organic compound may react with ozone or radicals from the bulk aqueous phase or with an adsorbed ozone molecule or

the products of surface ozone decomposition [22]. The prevailing mechanism is not clear. Moreover, it has to be taken into consideration that the formation of surface oxidation sites or the adsorption of neutral compounds on oxides is difficult in aqueous solutions due to the competitive adsorption of water molecules. Adsorption is easier for ionizable organic compounds in water if the surface is charged allowing ion exchange. In fact, the surface of metal oxides exhibits ion exchange properties and the hydroxyl groups formed behave as Brönsted acid sites and dissociate depending on the pH of the solution [23]. Finally, a mechanism has been proposed based on the initiation of ozone decomposition by hydroxide ions linked to the negatively charged surface of metal oxide [24].

The aim of this work is the study of the aqueous phase catalytic ozonation of naproxen, a non-steroidal anti-inflammatory drug, and carbamazepine, an antiepileptic agent (Fig. 2.1). These compounds were selected as representative of two different families of drugs the occurrence of which has previously been reported in water and wastewater [2]. The catalytic reactions were performed in a semi-continuous regime using a commercial Degussa P25 TiO_2 catalyst commonly used in photocatalysis and in photocatalytic ozonation [25]. Moreover, the activity of P25 TiO_2 in decomposing dissolved ozone has been previously reported by our group in unsteady absorption-reaction experiments that allowed the determination of reaction constants and activation energies for ozone decomposition and suggested that P25 could be a good choice as an ozonation catalyst for the mineralization of organic pollutants in water [26]. The main characteristics influencing the TiO_2 activity are surface area, crystalline phase, particle size and the aggregate size in suspension [27]. With respect to the last of these, nanosized P25 TiO_2 particles exist in agglomerates in solution as a consequence of Van der Waals attractive forces, which can be affected by hydrolyzation of TiO_2 surface. The hydrolyzation occurs at pH below pH_{PZC} and therefore in acidic conditions so originating repulsive forces between particles [28]. The effect of pH on the size of particle aggregates of TiO_2 has been reported by some authors, but values do not generally agree. Fernández-Ibáñez et al. [29] reported aggregates from 250 to 600 nm in acidic solutions with significant differences among agitation protocols. Yurkadal et al. [30] obtained much larger values from 2.2 to 2.5 μm for pH in the 3-8 range with a low influence of pH but with an important effect of catalyst concentration on the size of agglomerates at least for low concentrations. Gumy et al. reported 370 nm at pH 6 [31]. Whereas agglomeration has been shown to be an important factor for the catalyst's

activity, its measurement is difficult and published data do not agree. An activity decrease could be expected by bringing surface close to neutrality.

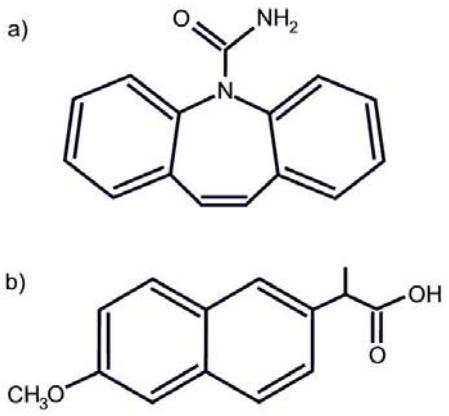

Fig. 2.1. Chemical structures of carbamazepine (a) and naproxen (b).

Concerning the interaction with catalytic surface, the most significant difference between carbamazepine and naproxene was that the former (pK_a = 14.0) was protonated in the whole pH range whereas naproxen (pK_a = 4.60) dissociated, allowing ion exchange on positively charged surfaces. Special attention was paid to the kinetics of mineralization and to the presence of oxalic acid, a common end-product refractory to ozonation. Specific ultraviolet absorbance (SUVA) was also determined as a measure of the aromaticity and the unsaturated character of the products and, therefore, their toxicity potential.

2.3. Experimental

2.3.1. Materials and ozonation procedure

Naproxen and carbamazepine were supplied by Sigma-Aldrich (98% purity). The catalyst used was titanium dioxide P25 Degussa (80/20 anatase-to-rutile ratio). The powder consists of primary particles of about 20 nm forming aggregates of several hundred nanometers that can be removed by filtration using 0.45 μm Teflon filters. The BET specific surface was 50 m^2/g. The point of zero charge (PZC), that is, the pH at which the surface is neutral, was determined by potentiometric titration as described by Halter [32]. The value obtained, pH_{PZC} = 6.6, squared well with similar data published elsewhere [33].

Reaction runs were carried out in a 1 L glass jacketed reactor whose temperature was controlled by a Huber Polystat cc2 thermostatic regulator. The temperature of the liquid inside the reactor was monitored throughout the experiment by means of a Pt100 thermocouple. Ozone was produced by a corona discharge ozonator (Ozomatic, SWO100) fed by oxygen (about 95% purity) produced by an AirSep AS-12 PSA oxygen generation unit. Fig. 2.2 shows details of the experimental set-up.

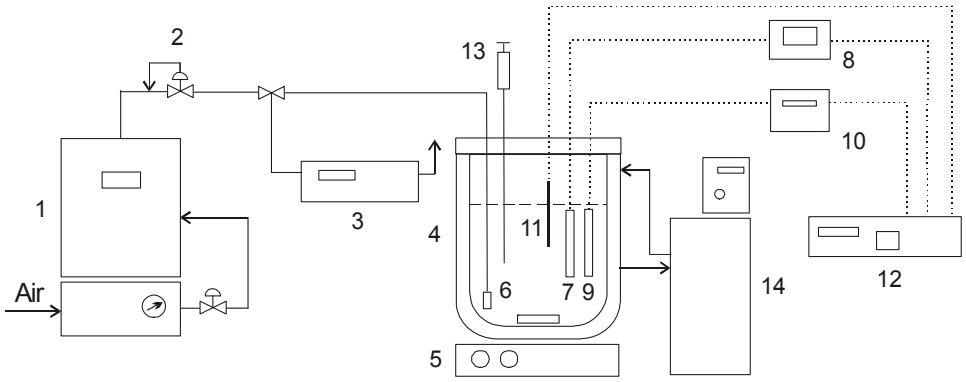

Fig. 2.2. Experimental equipment: 1, ozone generator; 2, flow control; 3, gas-phase UV ozone analyser; 4, reactor; 5, magnetic stirrer; 6, diffuser; 7, ozone amperometric sensor; 8, ozone analyser; 9, pH electrode; 10, pH control unit; 11, thermocouple; 12, data acquisition unit; 13, sampling device; 14, thermostat-cryostat.

The mixture of ozone and oxygen was bubbled into the liquid by means of a porous glass disk with a gas flow of 0.20 Nm^3/h. The reaction vessel was agitated with a magnetic rod at 700 rpm. The ozone decomposition experiments were conducted in a semicontinuous mode using a fixed volume of distilled water containing 15 mg/L of naproxen or carbamazepine (6.51×10^{-5} M and 6.35×10^{-5} M respectively). Catalytic runs were performed at a fixed bulk concentration of 1g/L. During the run, certain samples were withdrawn at prescribed intervals. Ozone was quenched in samples by adding a concentrated solution of sodium thiosulfate or by bubbling nitrogen. In the case of catalytic runs, the catalyst was previously removed by filtration. The experiments were carried out at pH in the 3-7 range, controlled by pumping a diluted sodium hydroxide using a feed-back PID control. The decomposition of ozone tended to acidify the reaction mixture in all cases except for neutral pH during the quick mineralization period that appeared at the beginning of the run. In this case the pH tended to increase and was controlled with the addition of hydrochloric acid. This behaviour was probably due to the reactions between hydroxyl radicals and carbonate and bicarbonate ions produced during the mineralization process

[34]. Fig. 2.3 shows the evolution of dissolved ozone concentration during a representative run performed at 25ºC and pH 3. The relatively large mass transfer volumetric coefficient (k_La = 0.0123 ± 0.0017 s^{-1}) accounts for the rapid increase observed at the beginning of the run. After 120 min, the prescribed reaction time for all runs, the flow of gaseous mixture of ozone and oxygen was stopped and the decay of dissolved ozone was used to supply information on the ozone decomposition reactions due to the organic compounds remaining in the liquid.

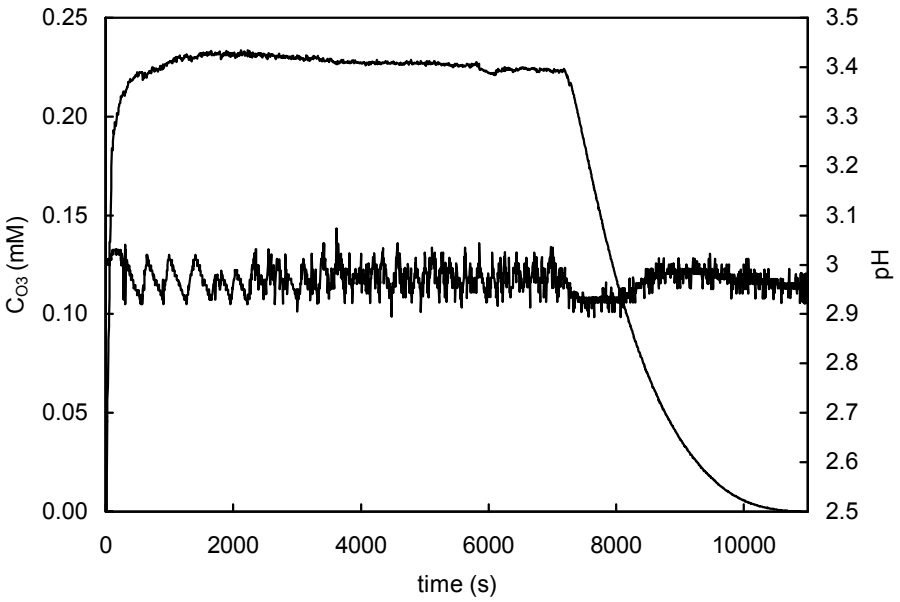

Fig. 2.3. Evolution of pH and concentration of ozone during the non-catalytic ozonation of naproxen at 25ºC. At 7200 s the flow of ozone was stopped.

2.3.2. Analysis

The concentration of ozone in the gas phase was determined with a non-dispersive UV Photometer Anseros Ozomat GM6000 Pro calibrated and tested against a chemical method. The concentration of ozone in the liquid was measured using the Rosemount 499A OZ amperometric analyser equipped with Pt 100 RTD temperature compensation and calibrated against the Indigo Colorimetric Method (SM 4500-O_3 B). The signal was transmitted to a Rosemount 1055 SoluComp II Dual Input Analyser connected to a data acquisition unit. The temperature inside the reactor was monitored with a Pt100 thermocouple and the pH was measured by means of a CRISON electrode connected to a Eutech αlpha-pH100 feed-back control device. The final control element for pH was a LC10AS Shimadzu pump that delivered a solution of hydrochloric acid or sodium hydroxide allowing a control of pH inside ±0.1 units throughout the experiment (Fig. 2.3). The signals from the concentration of dissolved ozone, pH and temperature were monitored and recorded using an Agilent 34970 Data Acquisition Unit connected to a computer.

TOC analyses were carried out by means of a Shimadzu TOC-VCSH total carbon organic analyzer equipped with an ASI-V autosampler. Carboxylic acids were determined using a Dionex DX120 Ion Chromatograph with conductivity detector and an IonPac AS9-HC 4x250mm analytical column (ASRS-Ultra suppressor). The eluent flow was 1.0 mL/min of 9.0 mM Na_2CO_3 and the volume of sample loop was 1 μL. UV absorbance at 254 nm was recorded by means of a Shimadzu SPD-6AV spectrophotometric detector. Specific ultraviolet absorbance ($SUVA_{254}$) was obtained by dividing ultraviolet absorption at 254 nm by the total organic carbon of the sample (TOC) in mg/L. $SUVA_{254}$ is commonly accepted as a measure of the content of humic substances in drinking water, or on the other hand, an indirect measure of the aromaticity and unsaturated character of the organic matter [35]. The analyses of naproxen and carbamazepine were performed by HPLC using a Hewlett Packard 1100 apparatus equipped with a C18 250mm column. The mobile phase was a mixture of acetonitrile and water (70:30) adjusted to pH 2.5 using orthophosphoric acid with an isocratic flow of 1.0 mL/min at room temperature. The UV detection was carried out at 268 nm.

2.4. Results and discussion

The extent of mineralization was tracked by determining the TOC of samples taken during the run. Fig. 2.4 shows the evolution of total organic carbon for selected catalytic and non-catalytic runs. The data show the existence of two mineralization periods. During the first few minutes, a rapid decay of TOC was considerably accelerated by the presence of a catalyst. The second period was essentially independent of pH and corresponded to the mineralization of the less reactive intermediates. In both cases, the parent compounds disappeared during the first few minutes of reaction due, at least, to the direct second order reaction with molecular ozone. The second-order rate constant for the ozonation of carbamazepine determined by Huber et al. [36] at pH 7 and 20ºC was about 3 x 10^5 M^{-1} s^{-1}. Considering that the concentration of ozone in the liquid rapidly reached a plateau value of about 0.23 mM, the half-life time of carbamazepine should be in the order of 10^{-2} s. In practice, small amounts of naproxen and carbamazepine could be detected after the first minute of reaction, a period in which the concentration of dissolved ozone in still low. No data are available for the direct rate constant of naproxen [37] but it always became undetectable after a maximum of three minutes after the beginning of the run, even with dissolved ozone concentrations far from its equilibrium value.

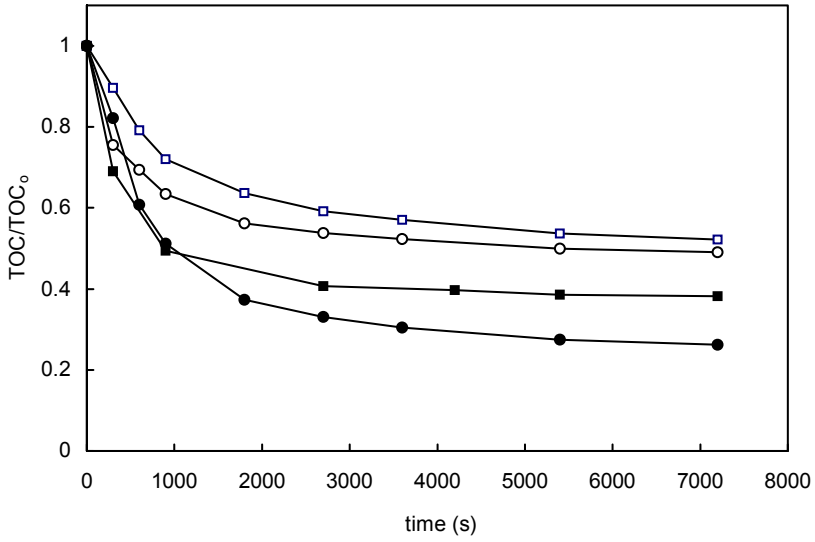

Fig. 2.4. Mineralization of naproxen at pH 5 (■, □) and carbamazepine at pH 5 (●) and pH 7 (○). Gas flow rate 0.20 Nm^3/s, ozone concentration in gas 38-40 g/Nm^3, temperature 25ºC. catalyst 1 g/L of TiO_2 Degussa P25 when used. Empty symbols represent non-catalytic runs.

2.4.1. Non-catalytic ozonation

As indicated previously, the primary reaction of naproxen and carbamazepine with dissolved ozone proceeded at a high rate. Therefore, the compounds analysed as TOC corresponded in any case to ozonation products absent from the initial reaction mixture. In general, the homogeneous rate of reaction of a certain organic compound is the consequence of the second order parallel reactions with dissolved ozone and with hydroxyl radicals:

$$-\frac{d\,c_i}{d\,t} = k_{HO\bullet}\, c_{HO\bullet}\, c_i + k_{O_3}\, c_{O_3}\, c_i \qquad (1)$$

Elovitz and von Gunten introduced a parameter, R_{ct}, that represents the ratio of hydroxyl radicals and ozone at any time during the reaction [38].

$$R_{ct} = \frac{c_{HO\bullet}}{c_{O_3}} \qquad (2)$$

In natural water, it has been shown that R_{ct} is a constant for most of the ozonation process, while during the ozonation of wastewater it behaves as a parameter that characterizes the oxidation process [39]. Combining Eqs. (1) and (2) and integrating the differential equation, the integral ozone exposure becomes the independent variable for the logarithmic decay of the concentration of a given compound:

$$\ln\frac{c_{io}}{c_i} = \left(k_{HO\bullet}\, R_{ct} + k_{O_3}\right)\int c_{O_3}\, dt = k_R \int c_{O_3}\, dt \qquad (3)$$

where k_R is expected to be constant only for a given compound and in conditions at which the ratio R_{ct} does not change. In this work, it was assumed that if the aggregate TOC (in mM or mg/L of organic carbon) is used instead of the concentration of a single compound, a similar kinetic expression could represent the process. In this case, k_R would be expected to decay as a consequence of the formation of more refractory products while ozonation proceeds and the extent of mineralization increases. Figs. 2.5 and 2.6 show experimental data corresponding to the ozonation of naproxen (*NAP,* c_o = 6.51 x 10^{-5} M) and carbamazepine (*CAR,* c_o = 6.35 x 10^{-5} M)

both in several catalytic and non-catalytic runs as a function of the time-integrated concentration of ozone. The results suggest the existence of two mineralization periods that can be modelled by considering that the organic carbon in the reaction products can be sorted into two classes according to its reactivity. The experimental values of TOC could be explained by means of a kinetic model in which a first set of easily oxidizable intermediates (A) yielded a second group of refractory products (B). The results showed that the formation of B from A was not specifically linked to the mineralization of the later and required a specific interconversion constant, k_{Ri}:

$$NAP, CAR \rightarrow A \xrightarrow{k_{R,1}} CO_2 + H_2O \tag{4}$$

$$A \xrightarrow{k_{R,i}} B \tag{5}$$

$$B \xrightarrow{k_{R,2}} CO_2 + H_2O \tag{6}$$

Except for the first few minutes of reaction, the organic carbon measured as TOC always corresponded to the carbon contained in the ozonation products of naproxen and carbamazepine, grouped in A and B, respectively expressed in mM or mg/L as c_A and c_B or as total carbon: $TOC = c_A + c_B$. According to the preceding mechanism, the kinetic expressions for the ozonation of A and B are as follows:

$$-\frac{d c_A}{d t} = k_{R,1} c_{O_3} c_A + k_{R,i} c_{O_3} c_A \tag{7}$$

$$\frac{d c_B}{d t} = k_{R,i} c_{O_3} c_A - k_{R,2} c_{O_3} c_B \tag{8}$$

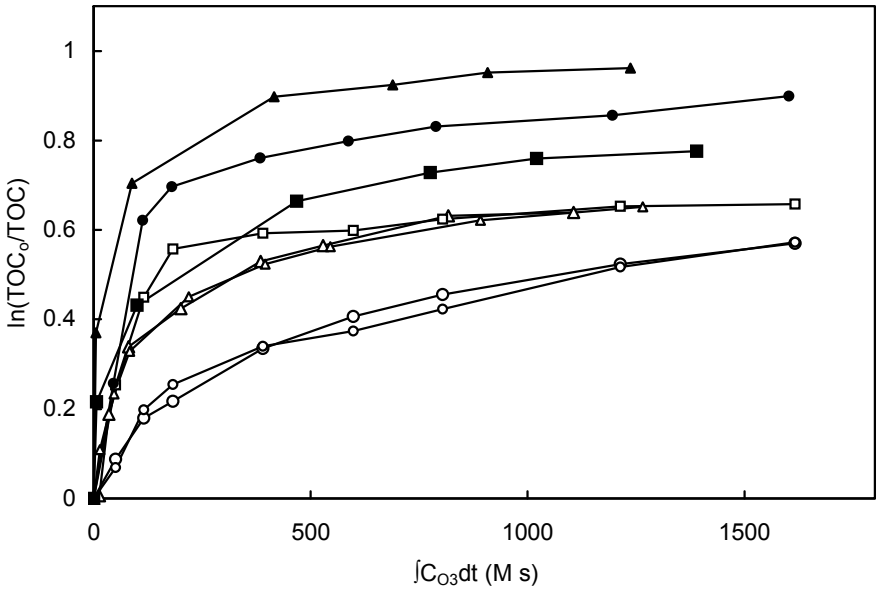

Fig. 2.5. Ozone exposure plot for the mineralization of naproxen at pH 3 (○), 5 (Δ) and 7 (□). Gas flow rate 0.20 Nm^3/s, ozone concentration in gas 38-40 g/Nm^3, temperature 25ºC. Filled symbols represent catalytic runs in the same conditions using 1 g/L of TiO_2 P25. Some runs have been replicated.

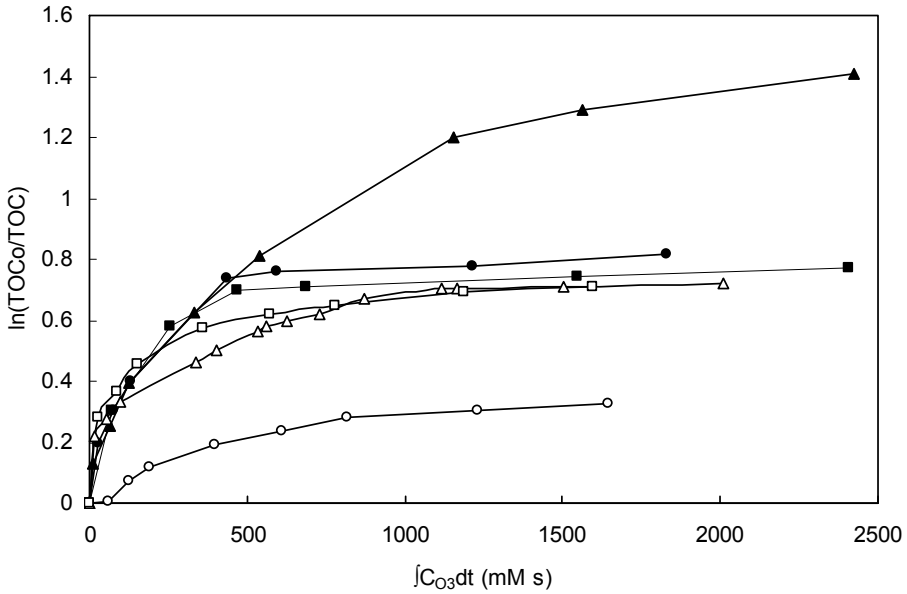

Fig. 2.6. Ozone exposure plot for the mineralization of carbamazepine at pH 3 (○), 5 (Δ) and 7 (□). Gas flow rate 0.20 Nm^3/s, ozone concentration in gas 38-40 g/Nm^3, temperature 25ºC. Filled symbols represent catalytic runs in the same conditions using 1 g/L of TiO_2 P25. Some runs have been replicated.

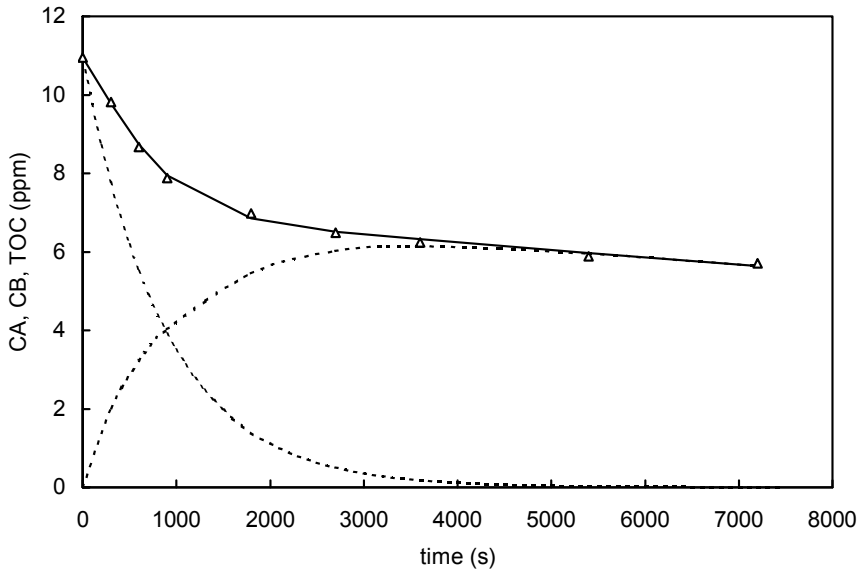

Fig. 2.7. Ozonation of naproxen at pH 5 without catalyst and model predictions for TOC and reaction intermediates A and B. Symbols correspond to experimental data and lines to model results.

Least squares fitting included a fourth order Runge-Kutta routine for the integration of Eqs. (7) and (8). Fig. 2.7 shows the experimental and predicted values of TOC and reaction intermediates for the ozonation of naproxen at pH 5. The calculated rate constants are shown in Table 2.1. The results revealed that increasing the pH of the mixture considerably accelerated the fast mineralization period. This accords well with the well-known role of hydroxide anion in the initiation of ozone decomposition and the subsequent production of hydroxyl radicals. The influence of pH on the interconversion reaction was lower whereas the mineralization of refractory products was slow and practically unaffected. An increasing acidity of oxidation intermediates could explain these differences, as the dissociated forms of weak acids are more reactive towards ozonation reactions.

Table 2.1. Kinetic constants for the mineralization model represented by Eqs. (4-6).

Non-catalytic reactions (L $mmol^{-1}$ s^{-1})			
	k_{R1}	k_{Ri}	k_{R2}
Naproxen			
pH = 3	0.00167	0.0034	1.7×10^{-4}
pH = 5	0.00437	0.0046	1.6×10^{-4}
pH = 7	0.0105	0.0048	1.3×10^{-4}
Carbamazepine			
pH = 3	0.00068	0.0019	2.1×10^{-4}
pH = 5	0.00285	0.0055	1.9×10^{-4}
pH = 7	0.00616	0.0069	1.6×10^{-4}
Catalytic ozonation (L $mmol^{-1}$ s^{-1})			
	k_{Rc1}	k_{Rci}	k_{Rc2}
Naproxen			
pH = 3	0.00587	0.0031	6.2×10^{-5}
pH = 5	0.00776	0.0041	8.1×10^{-5}
pH = 7	0.00458	0.0045	9.1×10^{-5}
Carbamazepine			
pH = 3	0.00277	0.0024	*
pH = 5	0.00425	0.0012	*
pH = 7	0.00271	8.9×10^{-4}	*

* Not significantly different from zero.

Table 2.2 compares the rate of ozone decomposition in distilled water with the same in the reaction mixture at the end of the run (120 min.) for the experimental conditions used in this work. The data were obtained by stopping the gas flow as indicated in Fig. 2.3 and in all cases, a good fitting was obtained by assuming a first order for the kinetics of ozone decomposition. Data showed large differences in the decomposition rate depending on the matrix. In an acidic medium, the reaction products of the ozonation of naproxen and carbamazepine increased the rate of ozone decomposition by up to one order of magnitude with regard to the water matrix. The effect could be attributed to the presence of promoters among

the refractory final products of the ozonation reactions. For increasing pH the difference is lower and, under neutral conditions, the ozonation products even inhibited the decomposition of ozone. The behaviour can be rationalized by taking into consideration the formation of promoters and inhibitors involved in ozone decomposition reactions. For example, formic acid, a radical chain promoter, reached up to 2 mg/L in the products of reaction at pH 3, while at pH 7 was almost undetectable. The inhibition detected at neutral pH might be related to the accumulation of carbonate and bicarbonate ions from the mineralization process. Fig. 2.8 shows the effect of the addition to the reaction mixture of 50 mM of sodium phosphate, a well-known radical scavenger [40]. Solid lines corresponded to the values indicated in Table 2.2 except for $k_{R,1}$, that decreased to about half ($k_{R,1}$ = 0.0015 L $mmol^{-1}$ s^{-1}). This result showed that the main mineralization reactions proceeded via a radical mechanism. The fact that a good fitting was achieved with the same parameter $k_{R,i}$ from Table 2.2 might indicate that interconversion reactions are not stoichometrically linked to the fast mineralization period. In fact, the ratio $k_{R,i}$ /$k_{R,1}$ decreased steadily as pH increased in all cases.

Table 2.2. First-order kinetic constant for the decomposition of ozone in the distilled water matrix and for ozone decay at the end of the ozonation reactions of naproxen and carbamazepine (120 min.). The catalyst load was 1 g/L in catalytic runs.

Non-catalytic decomposition k_d(s^{-1})	pH		
	3	5	7
Distilled water3.07 x 10^{-4}	9.93 x 10^{-4}	8.83 x 10^{-3}	
Naproxen	9.9 x 10^{-4}	1.2 x 10^{-3}	1.8 x 10^{-3}
Carbamazepine2.6 x 10^{-3}	3.2 x 10^{-3}	4.2 x 10^{-3}	
Catalytic decomposition k_{cd}(m^3 kg^{-1} s^{-1})	**pH**		
	3	5	7
Distilled water	4.72 x 10^{-4}	1.45 x 10^{-3}	1.27 x 10^{-3}
Naproxen	9.9 x 10^{-4}	1.04 x 10^{-3}	n.d.
Carbamazepine	9.6 x 10^{-4}	1.10 x 10^{-3}	n.d.

n.d.: not determined.

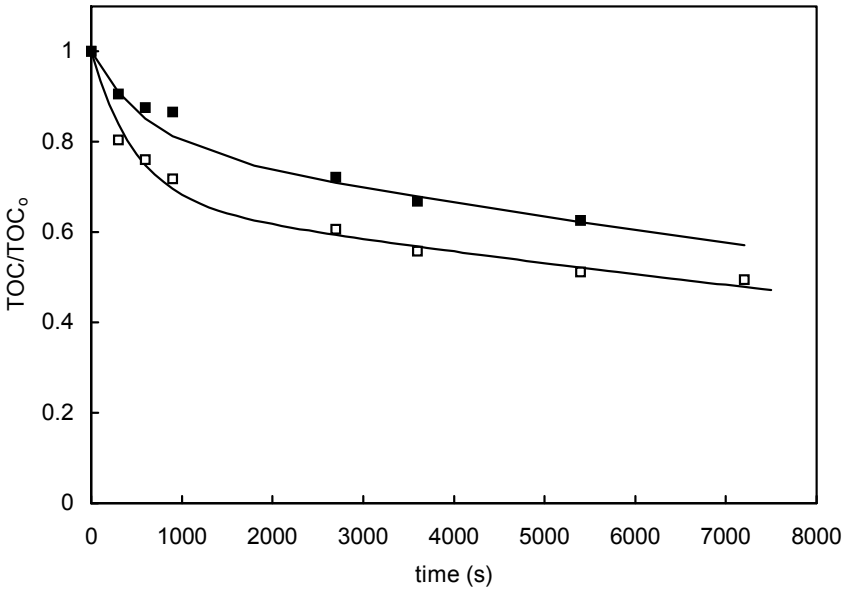

Fig. 2.8. Non-catalytic ozonation of carbamazepine and model predictions for TOC at pH 5 in pure distilled water (□) and with the addition of Na_3PO_4 50 mM (■).

2.4.2. Adsorption of naproxen and carbamazepine on P25 TiO_2

Neutral organic compounds in aqueous solution may adsorb on the surface of metal oxides if the surface is not charged and therefore the pH is near the pH_{PZC} (point of zero charge) of the solid. Otherwise, the coordination layer would prevent any adsorption. Furthermore, it is also necessary that the adsorbate is a Lewis base strong enough to displace adsorbed water molecules. In the case of ionizable substances such as carboxylates the adsorption takes place on positively charged surfaces by exchanging the corresponding counteranion [23]. Fig. 2.9 shows the results for the adsorption of naproxen (pK_a = 4.60) and carbamazepine (pK_a = 14.0) on TiO_2 Degussa P25 (pH_{PZC} = 6.6). The results showed that the adsorption of naproxen is favoured in acidic conditions in which the surface behaves as an anion exchanger. Similar results have been published for other acidic solutes that may be adsorbed by an ion-exchange mechanism [15, 16]. Carbamazepine was protonated in the whole pH range and its adsorption on a neutral or positively charged surface should take place by displacing coordination water in Lewis sites. The extent of adsorption was similar for pH in the 3-7 range. The adsorption kinetics was slow enough to suspect that its rate may play a significant role in the ozonation process. For both drugs, the equilibrium required several hours and the extent of adsorption

reached only 5-15% during the first hour (c_s = 1 g/L). This is in line with several data showing that the adsorption of acid pollutants on metal catalysts supported on alumina is slow, taking from hours to days to reach equilibrium [12, 15].

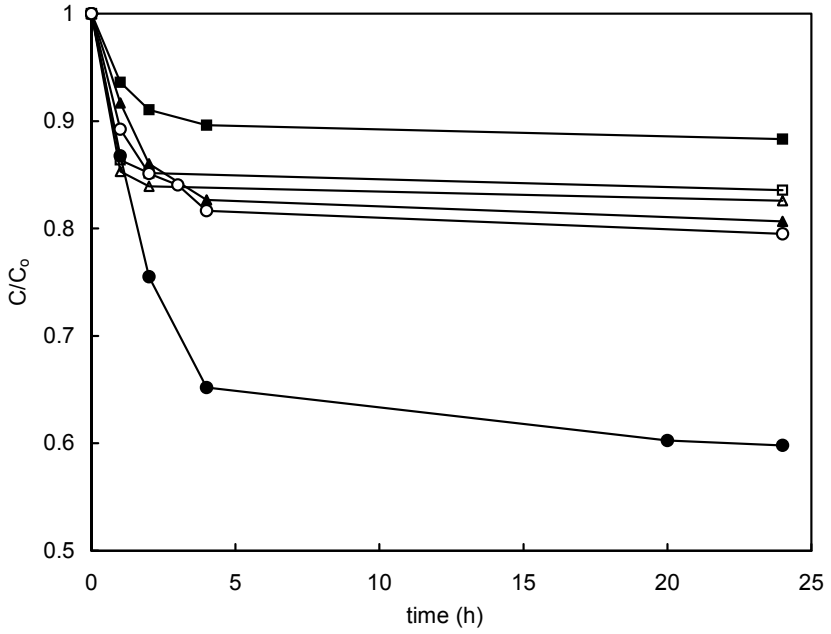

Fig. 2.9. Dimensionless concentration of naproxen at pH 3 (●), 5 (▲) and 7 (■) and carbamazepine at pH 3 (○), 5 (Δ) and 7 (□) corresponding to adsorption experiments on P25 TiO_2 at 25ºC. The initial concentration was 6.35 x 10^{-5} M for carbamazepine and 6.51 x 10^{-5} M for naproxen. Catalyst load 1 g/L.

2.4.3. Ozonation on TiO_2 catalyst

There is still a considerable lack of information regarding the role of metal oxides in the aqueous phase of ozonation reactions, in particular regarding the ozone decomposition reaction. It has been suggested that ozone can be adsorbed on a catalyst surface to yield different oxidizing species [15]. However, the bonding of an adsorbate to a vacant site, must involve the displacement of coordination water prior to adsorption. As indicated earlier, the ion exchange of charged species is much easier. Therefore, with the exception of systems such as those based on activated carbon in which the catalyst behaves merely as a promoter in the decomposition of ozone, the

ozonation mechanism should involve the adsorption or ion exchange of an organic compound on a surface site [41]:

$$A + S \leftrightarrows A\text{-}S \quad (9)$$

where S represents a free active site on the catalyst surface. Once adsorbed, the solute may react with a previously oxidized surface site (Ox-S):

$$O_3 + S \rightarrow Ox - S \quad (10)$$

$$Ox - S + A - S \rightarrow AOx + 2S \quad (11)$$

Alternatively, hydroxyl radicals or any other oxidant such as molecular ozone might react from the bulk with adsorbed organic compounds:

$$HO^{\bullet} + A - S \rightarrow AOx + S \quad (12)$$

The rate of ozonation combines the homogeneous reaction with ozone or hydroxyl radicals and the heterogeneous reaction following any of these mechanisms. The rate expression for a situation in which adsorption equilibrium exists and the adsorbed organic compounds react with hydroxyl radicals from the bulk but do not interact with oxidized sites is as follows:

$$-\frac{dc_A}{dt} = k_{HO^{\bullet}}\, c_{HO^{\bullet}}\, c_A + k_c\, c_s\, c_{HO^{\bullet}} \frac{k_a\, c_A}{k_a\, c_A + k_{-a}} \quad (13)$$

Where k_a and k_d are the adsorption and desorption kinetic constants for the organic compound.

If surface coverage is small, the denominator of Eq. (13) becomes independent on the concentration of adsorbate. Finally, by using the R_{ct} ratio of Elovitz and von Gunten, the concentration of hydroxyl radicals can be expressed as a function of the concentration of dissolved ozone:

$$-\frac{dc_A}{dt} = \left(k_{HO^{\bullet}}\, R_{ct} + k_c\, R_{ct}\, K_a\, c_s\right) c_{O_3}\, c_A \quad (14)$$

The integration of the former expression leads to:

$$\ln \frac{c_{A,o}}{c_A} = \left(k_{HO^\bullet} R_{ct} + k_c R_{ct} K_a c_s \right) \int c_{O_3} \, dt = k_{Rc} \int c_{O_3} \, dt \qquad (15)$$

A Langmuir-Hinshelwood rate expression would represent a situation in which an elementary step occurring on the surface is rate controlling and adsorption equilibrium exists at any time for both oxidant and organics. On the assumption that the equilibrium constant for the oxidation of surface sites is low enough, an integrated expression similar to Eq. (15) can be derived. A surface redox reaction mechanism has sometimes been described by means of a Mars-van Krevelen rate expression. In such case, the rate of catalytic reaction would depend on the rate of the surface oxidation process and on the rate of the organic compound's reaction with the oxidized catalyst. If the catalyst oxidation is slow, the catalytic reaction would be independent of the concentration of oxidant. In contrast, for a high rate of surface oxidation, the reaction rate should be first order in the organic compound. Although relatively common in catalysis, the Mars-van Krevelen rate expression, lacking as it does a solid fundamental background, finally proved to be physically incorrect [42].

The logarithmic decay of the organic carbon was fitted to the linear expression on the ozone integral exposure indicated by Eq. (15) in which the pseudo-homogeneous catalytic kinetic constant is expected to follow a complex dependence probably dominated by the R_{ct} parameter. The evolution of TOC in the catalytic reactions performed in this work is shown in Figs. 2.5 and 2.6 for naproxen and carbamazepine respectively. The trend is similar to that encountered in non-catalytic runs with a rapid initial TOC decay followed by a period in which the rate of mineralization was very low. Therefore, the same model used in non-catalytic runs and based on splitting the organic carbon into two categories according to its rate of mineralization was also used for catalytic ozonations. The interpretation of the apparent kinetic constant, $k_{Rc,}$ depends on the underlying reaction mechanism, but discriminating between rival models was not the objective of this research. With regard to the effect of adsorption of naproxen and carbamazepine on the ozonation process, some experiments were performed in which they were allowed to reach adsorption equilibrium before beginning the run. Results show no significant differences between

ozonation with a 24 h contact time and runs performed with direct addition of the catalyst just before passing ozone.

Another question suggested by the slow adsorption kinetics observed for naproxen and carbamazepine is whether the adsorption kinetics of the intermediate products of ozonation could control the overall reaction rate. The contribution of an adsorption process in parallel with the catalytic reaction would include in the rate expression a term independent of the concentration of oxidant:

$$-\frac{d c_A}{d t} = k_{HO^\bullet} R_{ct} c_{O_3} c_A + k_a c_s c_A \qquad (16)$$

The integration of Eq. (16) leads to an expression in which the logarithmic decrease of the organic compound is not linear in the time-integrated concentration of ozone. The corresponding model can be discriminated from those based on surface equilibrium by using data in which the integral ozone exposure and time are not correlated. Fig 2.10 shows the logarithmic TOC decay for the ozonation of naproxen at pH 7 with a concentration of dissolved ozone ten times lower than the corresponding to the experiment reported in Fig. 2.6. This represented a plateau concentration of about 0.02 mmM (1 mg/L of ozone) instead of 0.22 mM (about 10 mg/L) from the previous run. If the adsorption of reaction intermediates on acid sites were relevant, the plot of the logarithmic decay of TOC as a function of the integral ozone exposure would reflect a deviation from Eq. (15) as indicated by Eq. (16), whose integration yields a contribution to logarithmic TOC reduction linear with time. The result indicated that the mineralization can be explained by a pure catalytic mechanism and that a possible competitive adsorption of reaction products was not important at a neutral pH. For runs performed under acidic conditions, the situation was somewhat different. Fig. 10 shows the result of ozonation of naproxen (pH 3) and carbamazepine (pH 5) in runs in which the ozone flow was stopped at 30 min. From about 40 min to the end of the sampling period (120 min), the concentration of dissolved ozone was not detectable in both runs. The results are compared in Fig. 10 with runs performed with continuous gas flow (filled symbols). Again, if adsorption of reaction intermediates was significant, the plot would show sharp increase after 40 min corresponding to the adsorption of acids produced during ozonation. Results showed, however, a limited increase in dissolved carbon during the part of the runs carried out in the

absence of ozone. This effect, greater at pH 3, was probably linked to the development of Brönsted catalytic sites during ozone decomposition. After ceasing the ozone flow, certain acidic sites could revert with the subsequent desorption of organic compounds to the bulk.

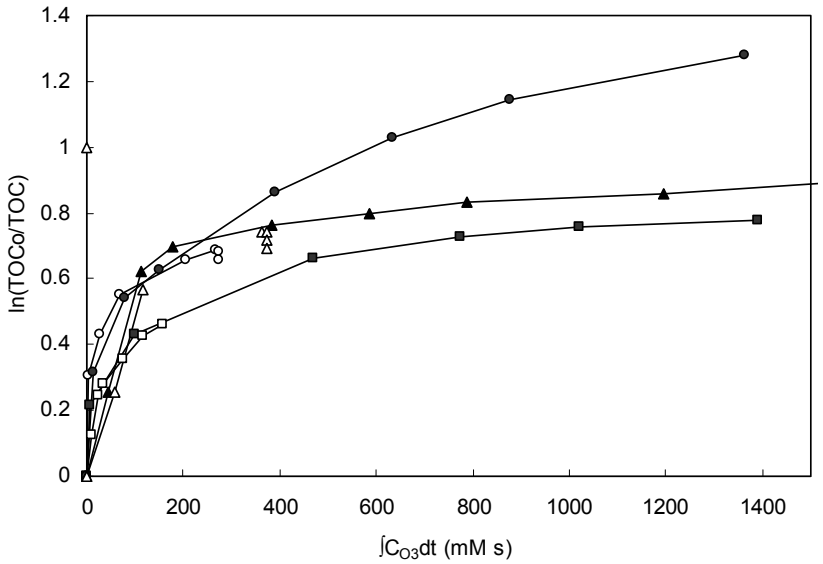

Fig. 2.10. Ozonation of naproxen at pH 7 with marks representing samples for low (□) and high (■) ozone concentration and experiments with ozone stopped-flow for carbamazepine at pH 5 (○) and naproxen at pH 3 (Δ). Filled symbols correspond to runs under constant ozone gas flow.

The kinetic constants estimated by the least squares fitting of experimental data are shown in Table 2.2. Figs. 2.5 and 2.6 show the experimental and theoretical values together with the corresponding results of non-catalytic runs as indicated above. In general, the catalyst accelerated the first mineralization reaction period for the runs carried out in acidic media. At neutral pH the rate of catalytic reaction, k_{Rc1}, decreased to about half the value of the non-catalytic corresponding constant, k_{R1}. Anyway, the catalyst caused a deeper mineralization even at neutral pH because the conversion from oxidizable to refractory compounds (A $\rightarrow$ B) seemed to be inhibited by the catalyst, especially in the case of carbamazepine. The best results for the removal of reaction intermediates were obtained for slightly positive surface charge (pH = 5) suggesting that the adsorption of organics on Lewis sites could be involved in the mechanism of catalytic ozonation. For a higher pH, the lower rate constant could be attributed to the role of

hydroxide ions that, being a strong Lewis base, should inactivate acidic catalyst sites. The results shown in Table 2.2, also indicate that the presence of a catalyst inhibited the decomposition of ozone, lowering the decomposition kinetic constant from $8.83 \times 10^{-3} \pm 4 \times 10^{-5}$ s^{-1} to $1.27 \times 10^{-3} \pm 1 \times 10^{-5}$ s^{-1} for reaction in the distilled water matrix. This result could be due to the role of a catalytic surface in chain termination reactions. The boundaries correspond to 95% confidence intervals. The order of kinetic constants k_{Rc1} was the same as that encountered for the catalytic decomposition of ozone in water, pointing towards a mechanism based on the adsorption of organics and ozone on the same sites. The ratio k_{Rc1}/k_{cd} decreased with increasing pH, following a trend that suggested a greater interaction of the catalytic surface with organic compounds than with molecular ozone. The ratio k_{Rc1}/k_{R1} changed from 3.5-4.0 to less than 0.45 as pH increased from 3 to 7 showing that the mineralization rate was affected more than the ozone decomposition reaction while increasing the concentration of hydroxide. Both observations suggested that the adsorption of organics effectively plays a role in the reaction and that the mineralization is not merely the consequence of an enhanced production of hydroxyl radicals from ozone. The second period of mineralization was characterized by a very reduced rate constant, not significantly different from zero for the ozonation of carbamazepine. The interconversion constant, k_{Rci}, was very similar for catalytic and non-catalytic runs in the case of naproxen, but significantly decreased for carbamazepine as pH increased. This behaviour suggests that the reactions of organic compounds that do not lead to mineralization can exhibit a complex pattern linked to the interaction with a catalytic surface. For homogeneous runs, however, interconversion reactions were favoured by high pH as expected for a hydroxyl-mediated oxidation process.

Fig. 2.11 shows the evolution of the concentration of oxalate measured by ionic chromatography in samples taken at certain intervals during the runs. In the interests of clarity only some representative results are shown. In non-catalytic runs, oxalate steadily increased during the ozonation especially for the higher values of pH that corresponded to the greater mineralization rates. Catalytic runs exhibited a different behaviour and the accumulation of oxalate was only observed at pH 3. In less acidic media and in the presence of a catalyst, the disappearance rate of oxalate increased so that no oxalate was observed in any case at neutral pH. Results showed that, even on a neutral surface, oxalate was oxidized in conditions at which the mineralization was not particularly deep, a behaviour that can be explained

by the higher affinity of organic anions for catalytic sites. Oxalate accounted for as much as 30% of the organic carbon remaining in the reaction mixture in non-catalytic runs and no more than 12% in catalytic runs. Consequently, the use of a catalyst favours not only the reactions leading to oxalate but also the mineralization of oxalate itself, avoiding its accumulation in the reaction mixture. The mineralization of oxalate is not particularly enhanced by a positive surface charge and, therefore, results seem to exclude a mechanism based solely on the ion exchange of oxalate. To support this conclusion, in certain runs the catalyst was washed with an alkaline solution at the end of the reaction, and the extract analyzed by TOC and ionic chromatography in search of adsorbed but not oxidized organic compounds. In all cases, the amount of organic carbon detected was very low showing that a adsorption by anion exchange was not the reason for the disappearance of oxalate. The degree of mineralization was not directly linked to the accumulation of other low molecular weight carboxylic acids. In particular, low levels of acetate and formiate were detected in most runs, but without an accumulation pattern clearly linked to the pH or the evolution of TOC.

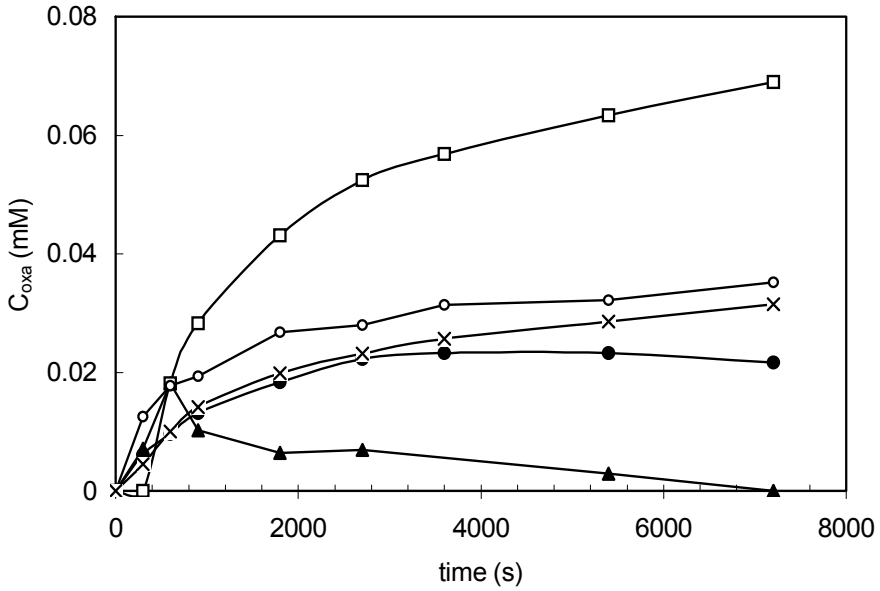

Fig. 2.11. Evolution of the concentration of oxalic acid in several runs. Empty symbols represent non-catalytic ozonation of naproxen ad at pH 3 (○) and 7 (□). Filled symbols correspond to the catalytic ozonation of carbamazepine at pH 3 (●) and 5 (▲). Crosses correspond to catalytic ozonation of naproxen at pH 3.

Figs. 2.12 and 2.13 show the evolution of $SUVA_{254}$ with the integral ozone exposure for the ozonation of naproxen and carbamazepine. The pattern was very different in both cases. During the reaction of carbamazepine the absorbance decreased almost steadily with ozone exposure, but the products of the ozonation of naproxen exhibited a greater absorbance than the parent solution. For runs with a high degree of mineralization, $SUVA_{254}$ showed the highest values. This reflected the formation of aromatic or unsaturated products and their preferential accumulation in the reaction mixture even under relatively deep mineralization conditions and may be favoured by the condensed structure of naproxen. The non-saturated character of the products will probably be linked to an increased toxicity of the reaction mixture even if TOC becomes considerably reduced. The chemical structure of the parent compounds, which is relatively less important for the catalytic ozonation rate, determined the nature of the reaction products and must be taken into account even under strong oxidant conditions.

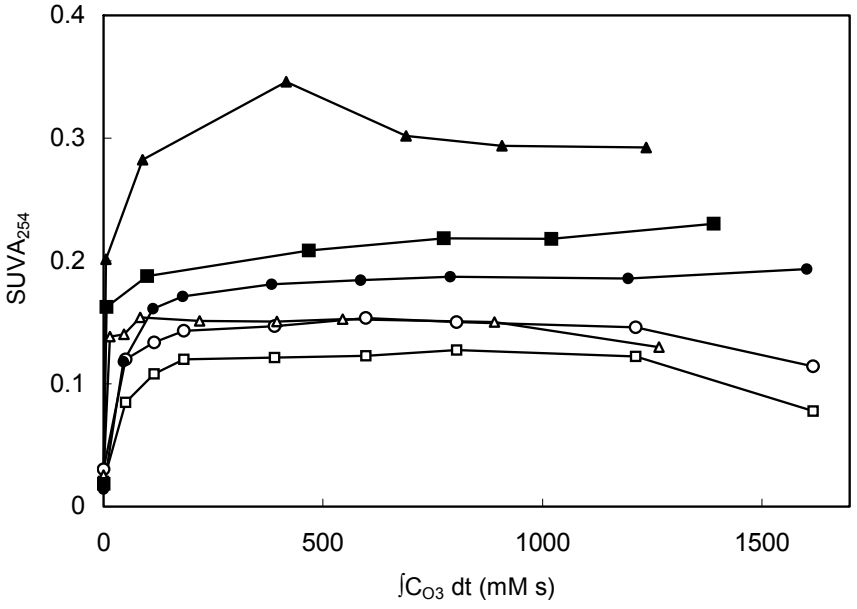

Fig. 2.12. Specific ultraviolet absorption at 254 nm for the ozonation of naproxen at pH 3 (○), 5 (Δ) and 7(□) in the absence of catalyst ant at pH 3 (●), 5 (▲) and 7 (■) using 1 g/L TiO_2.

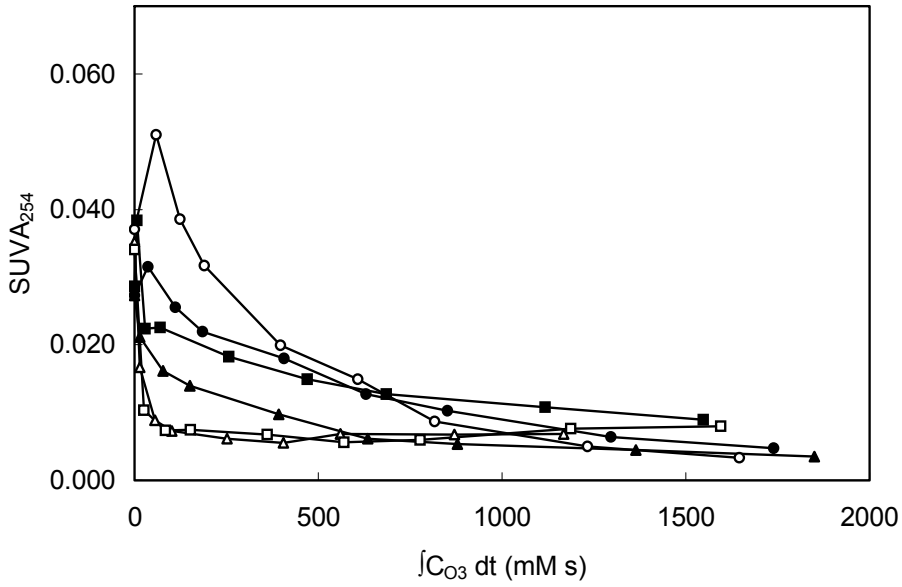

Fig. 2.13. Specific ultraviolet absorption at 254 nm for the ozonation of carbamazepine at pH 3 (○), 5 (Δ) and 7 (□) in the absence of catalyst ant at pH 3 (●), 5 (▲) and 7 (■) using 1 g/L TiO_2.

2.5. Conclusions

The catalytic ozonation of naproxen and carbamazepine in aqueous solution reduced the total organic carbon to about one third of its initial value for reactions carried out at 25ºC with a catalyst load of 1 g/L. Best results, with TOC reduction of 62% for naproxen and 73% for carbamazepine were obtained in slightly acidic conditions with pH 5 and an initial concentration of 15 mg/L. In the same conditions, the non-catalytic ozonation of naproxen and carbamazepine yielded a mineralization degree of only 50% with a maximum reaction rate obtained at neutral pH. Naproxen and carbamazepine reacted during the first few minutes in contact with ozone and, therefore, the organic carbon measured during the run corresponded to ozonation products. Most of the mineralization takes place during the first 10-20 minutes in a rapid ozonation period followed by a slow mineralization of the more refractory compounds. The initial rate of non-catalytic reaction decreased in the presence of sodium phosphate, proving that at least the initial rapid mineralization reactions are an indirect hydroxyl radical-mediated oxidation.

The evolution of the mineralization process was modelled by assuming a different kinetic behaviour for the organic carbon belonging to easily oxidizable substances and to refractory final reaction products. It was also considered that the later were oxidation products from the ozonation of the former. A regression model allowed an estimate of the pseudo-homogenous reaction constants for catalytic and non-catalytic runs. The catalytic rate constant was maximum for pH 5 with a value of $7.76 \times 10^{-3} \pm 3.9 \times 10^{-4}$ L $mmol^{-1}$ s^{-1} for naproxen and $4.25 \times 10^{-3} \pm 9.7 \times 10^{-4}$ L $mmol^{-1}$ s^{-1} for carbamazepine. The results also showed that the catalyst promotes the decomposition of ozone under acidic conditions, while at neutral pH it behaved as an inhibitor of the ozone decomposition in comparison with the homogeneous ozone self-decomposition in pure water. The effect of an increase of pH was greater on the rate constant of the first mineralization period than on the catalytic reaction of ozone decomposition and the rate of mineralization decreased with the increasing concentration of hydroxide. These results suggest that the adsorption of organics or ozone could play a significant role in the reaction and depending on the relative strength or surface interaction. The enhancement of mineralization would not merely be the consequence of a greater surface production of hydroxyl radicals from ozone. The catalyst promotes mineralization especially in slightly acidic conditions, a result that is probably linked to the adsorption of reaction intermediates on acid catalytic sites. The experiments partially carried out in the absence of ozone indicated that the adsorption of intermediates did not play a role in the reduction of dissolved organic carbon during the ozonation reaction. Moreover, the absence of ozone was associated with a desorption of organic compounds probably linked to a decrease in acidic catalyst sites.

The catalyst not only modified the mineralization rate, but also, the composition of the mixture at the end of the process. Oxalate, which accumulates in the reaction mixture from non-catalytic runs, mineralized in catalytic runs particularly in neutral conditions. The amount of oxalate in the products of catalytic experiments accounted for no more than 12% of the organic carbon. Therefore, the catalyst enhanced mineralization reactions of oxalate itself, avoiding its accumulation in the reaction mixture. The reaction products exhibited a markedly different pattern concerning ultraviolet absorption at 254 nm. $SUVA_{254}$ decreased steadily with ozone dosage for the ozonation products of carbamazepine, while they maintained a high value, even greater than the one corresponding to the parent solution, for naproxen. This was linked to the aromatic condensed structure of

naproxen and suggests that toxicity could be higher even after a deep mineralization reaction.

2.6. Notation

c_A c_B	concentration of organic carbon in compounds A and B, mM or mg/L^{-1}
c_i	concentration of a given organic compound, mol L^{-1}
$c_{HO\bullet}$	concentration of hydroxyl radicals, mol L^{-1}
c_{O_3}	concentration of dissolved ozone, mol L^{-1}
c_o	initial concentration, mol L^{-1}
c_s	bulk concentration of solids in the liquid phase, kg_{solids} L^{-1}
k_a	adsorption kinetic constant, L kg_{solids}^{-1} s^{-1}
k_{-a}	desorption kinetic constant, mol kg_{solids}^{-1} s^{-1}
k_c	intrinsic catalytic kinetic constant, L kg_{solids}^{-1} s^{-1}
k_d	kinetic constant of the ozone homogeneous decomposition, s^{-1}
k_{cd}	kinetic constant of the ozone heterogeneous decomposition, L kg_{solids}^{-1} s^{-1}
K_a	adsorption equilibrium constant, L mol^{-1}
$k_{HO\bullet}$, k_{O_3}	second order kinetic constant of homogeneous ozone reactions, L mol^{-1} s^{-1}
k_R	homogeneous kinetic constant defined in Eq. (3), L mol^{-1} s^{-1}
k_{Rc}	pseudo-homogeneous catalytic kinetic constant defined in Eq. (15), L mol^{-1} s^{-1}
R_{ct}	ratio of $c_{HO\bullet}$ to c_{O_3} at a given time during the reaction, dimensionless

2.7. References

[1] Petrovic, M., Eljarrat, E., López, M.J., Barceló, D., Endocrine disrupting compounds and other emerging contaminants in the environment: a survey on new monitoring strategies and occurrence data, Anal. Bioanal. Chem., 378 (2004) 549-562.

[2] Ternes, T.A., Occurrence of drugs in German sewage treatment plants and rivers, Water Res., 32 (1998) 3245-3260.

[3] Ternes, T.A., Meisenheimer, M., McDowell, D., Sacher, F., Brauch, H.J., Haist-Gulde, B., Preuss, G., Wilme, U., Zulei-Seibert, N., Removal of pharmaceuticals during drinking water treatment, Environ., Sci. Technol., 36 (2002) 3855-3863.

[4] Jones, O.A., Lester, J.N., Voulvoulis, N., Pharceuticals: a threat to drinking water?, Trends Biotechnol., 23 (2005) 163-167.

[5] Zuccato, E., Castiglioni, S., Fanelli, R., Identification of the pharmaceuticals for human use contaminating the Italian aquatic environment, J. Hazard. Mater., 122 (2005) 205–209.

[6] Larsen, T.A., Lienert, J., Joss, A., Siegrist, H., How to avoid pharmaceuticals in the aquatic environment, J. Biotechnol., 113 (2004) 295-304.

[7] Vogna, D., Marotta, R., Napolitano, A., Andreozzi, R., d'Ischia, M., Adanced oxidation of the pharmaceutical drug diclofenac with UV/H_2O_2 and ozone, Water Res., 38 (2204) 414-422.

[8] Zwiener, C., Frimmel, F.H., Oxidative treatment of pharmaceuticals in water, Water Res., 34 (2000) 1881-1185.

[9] von Gunten, U., Ozonation of drinking water: part II. Disinfection and by-product formation in presence of bromine, iodide or chlorine, Water Res., 37 (2003) 1469–1487.

[10] Legube, B., Ozonation by-products, in The Handbook of Environmental Chemistry, Vol. 5 Part G, Springer, Berlin, 2003, 95-116.

[11] Andreozzi, R., Marotta, R., Sanchirico, R., Manganese-catalysed ozonation of glyoxalic acid in aqueous solutions, J. Chem. Tech. Biotechnol., 75 (2000) 59-65.

[12] Beltrán, F.J., Rivas, F.J., Montero, R., Mineralization improvement of phenol aqueous solutions through heterogeneous catalytic ozonation, J. Chem. Technol. Biotechnol., 78 (2003) 1225-1333.

[13] Gracia, R., Cortés, S., Sarasa, J., Ormad, P., Ovelleiro, J.L., TiO_2-catalysed ozonation of raw Ebro river water, Water Res., 34 (2000) 1525-1532.

[14] Fu, H., Karpel, N., Legube, B., Catalytic ozonation of chlorinated carboxylic acids with Ru/CeO_2-TiO_2 catalyst in the aqueous system, *New J. Chem.*, 26 (2002) 1662-1666.

[15] Beltrán, F.J., Rivas, F.J., Montero, R., Catalytic ozonation of oxalic acid in an aqueous TiO_2 slurry reactor, Appl. Catal. B: Environ., 39 (2002) 221-231.

[16] Beltrán, F.J., Rivas, F.J., Montero, R., A TiO_2/Al_2O_3 catalyst to improve the ozonation of oxalic acid in water, Appl. Catal. B: Environ., 47 (2004) 101-109.

[17] Gracia R., Cortés S., Sarasa J., Ormad P., Ovelleiro J.L., Heterogeneous catalytic ozonation with supported titanium dioxide in model and natural waters, Ozone Sci. Eng., 22 (2000) 461-471.

[18] Cooper, C., Burch, R., An investigation of catalytic ozonation for the oxidation of halocarbons in drinking water preparation, Water Res., 33 (1999) 3695-3700.

[19] Lin, J., Nakajima, T., Jomoto, T., Hiraiwa, K., Effective catalysts for wet oxidation of formic acid by oxygen and ozone, Ozone Sci. Eng., 21 (1999) 241-247.

[20] Dhandapani, B., Oyama, S.T., Gas phase ozone decomposition catalysts, Appl. Catal. B: Environ., 11 (1997) 129-166.

[21] Bulanin, K.M., Lavalley, J.C., Tsyganenko, A.A., IR spectra of adsorbed ozone. Colloid Surf. A., 101 (1995) 153-158.

[22] Legube, B., Karpel, N., Catalytic ozonation: a promising advanced oxidation tehcnology for water treatment, Catal. Today, 53 (1999) 61-72.

[23] Kasprzyk-Hordern, B., Ziolek, M., Nawrocki, J., Catalytic ozonation and methods of enhancing molecular ozone reactions in water treatment, Appl. Catal. B: Environ., 46 (2003) 639-669.

[24] Ma, J., Graham, N.J.D., Degradation of atrazine by manganese-catalysed ozonation: Influence of humic substances, Water Res., 33 (1999) 785-793.

[25] Agustina, T.E., Ang, H.M., Vareek, V.K., A review of synergistic effect of photocatalysis and ozonation on wastewater treatment, J Photochem. and Photobiol. C: Photochem. Rev., 6 (2005) 264–273.

[26] Rosal, R., Rodríguez, A., Zerhouni, M., Enhancement of gas-liquid mass transfer during the unsteady-state catalytic decomposition of ozone in water, Appl. Catal. A: General, 305 (2006) 169-175.

[27] A. Mills, S. Le Hunte, An overview of semiconductor photocatalysis, J. Photochem. Photobiol. A: Chem. 108 (1997) 1–35.

[28] Hoffmann, M.R., Martin, S.T., Choi, W., Bahnemann, D.W., Environmental applications of semiconductor photocatalysis, Chem. Rev. 95 (1995) 69-96.

[29] Fernández-Ibáñez, P, Malato, S., Nieves, F.J., Relationship between TiO2 particle size and reactor diameter in solar photoreactors efficiency, Catal. Today, 54 (1999) 195–204.

[30] Yurdakal, S., Loddo, V., Bayarri, B., Palmisano, G., Augugliaro, V., Gimenez, J., Palmisano, L., Optical properties of TiO2 suspensions: influence of pH and powder concentration on mean particle size, Ind. Eng. Chem. Res., 46 (2007) 7620-7626.

[31] Gumy, D., Giraldo, S.A., Rengifo, J., Pulgarin, C., Effect of suspended TiO2 physicochemical characteristics on benzene derivatives photocatalytic degradation, Appl. Catal. B: Environ., 78 (2008) 19-29.

[32] Halter, W.E., Surface acidity constants of a-Al2O3 between 25 and 70°C, Geochim. et Cosmochim. Acta, 63 (1999) 3077–3085.

[33] Fernández, P., Nieves, F.J.D.L., Malato, S., Titanium dioxide/electrolyte solution interface: Electron transfer phenomena, J. Colloid Interface Sci., 227 (2000) 510-516.

[34] Beltran, F.J., Ozone Reaction Kinetics for Water and Wastewater Systems, CRC Press LLC, Florida, 2004, pp. 18-19.

[35] Chandrakanth, M.S., Amy, G.L., Effects of NOM source variations and calcium complexation capacity on ozone-induced particle destabilization, Wat. Res. 32 (1998) 115–124.

[36] Huber, M.M., Canonica, S., Park, G.Y., Gunten, U., Oxidation of pharmaceuticals during ozonation and advanced oxidation processes, Environ. Sci. Technol., 37 (2003) 1016-1024.

[37] Ikehata, K., Naghashkar, J., El-Din, M.G., Degradation of aqueous pharmaceuticals by ozonation and advanced ozonation processes, Ozone Sci. Eng., 28 (2006) 353-414.

[38] Elovitz, M.S., von Gunten, U., 1999. Hydroxyl radical/ozone ratios during ozonation processes. I. The R_{ct} concept, Ozone Sci. Eng. 21 (1999) 239–260.

[39] Buffle, M.O., Schumacher, J., Salhi, E., Jekel, M., Gunten, U., Measurement of the initial phase of ozone decomposition in water and wastewater by means of a continuous quench-flow system: application to disinfection and pharmaceutical oxidation, Water. Res., 40 (2006) 1884-1894.

[40] Staehelin, J., Hoigné, J., Decomposition of ozone in water in the presence of organic solutes acting as promoters and inhibitors of radical chain reactions, 19 (1985) 1206-1213.

[41] Sánchez-Polo, M., von Gunten, U., Rivera-Utrilla, J. Efficiency of activated carbon to transform ozone into OH radicals: Influence of operational parameters, Water Res., 39 (2005) 3189–3198.
[42] Vannice, M.A., An analysis of the Mars-van Krevelen rate expression, Catal. Today, 123 (2007) 18-22.

CHAPTER 3

OZONATION OF CLOFIBRIC ACID CATALYZED BY TITANIUM DIOXIDE

Journal of Hazardous Materials, 2009

3. Ozonation of clofibric acid catalyzed by titanium dioxide

Journal of Hazardous Materials, 2009

3.1. Abstract

The removal of clofibric acid from aqueous solution has been investigated in catalytic and non-catalytic semicontinuous ozonation runs. Kinetic data were analyzed using second order expressions for the reaction between organics and ozone or hydroxyl radicals. Catalytic runs used a commercial titanium dioxide catalyst consisting of fumed colloidal particles. The kinetic constant of the non-catalytic ozonation of clofibric acid at pH 3 was 8.16 x 10^{-3} ± 3.4 x 10^{-4} L $mmol^{-1}$ s^{-1}. The extent of mineralization during non-catalytic runs ranged from 50% at pH 7 to 20% at pH 3 in a reaction that essentially took place during the first 10-20 min. The catalyst increased the total extent of mineralization, its effect being more important during the first part of the reaction. The pseudo-homogeneous catalytic rate constant was 2.17 x 10^{-2} L $mmol^{-1}$ s^{-1} at pH 3 and 6.80 x 10^{-1} L $mmol^{-1}$ s^{-1} at pH 5, with up to a three-fold increase with respect to non-catalytic constants using catalyst load of 1 g/L. A set of stopped-flow experiments were designed to elucidate the role of catalyst, whose effect could be due to the adsorption of organics on catalytic sites rather than to the promotion of ozone decomposition. The formation of surface hydroxyl radical from ozone is a more probable route to explain the ozonation of poorly absorbable compounds.

Keywords: Catalytic ozonation; Mineralization; Titanium dioxide; Clofibric acid.

3.2. Introduction

Pharmaceuticals and personal care products (PPCPs) constitute a group of emerging pollutants whose presence in water and wastewater has been well documented [1-4]. It has been recognized that the major source of these pollutants is discharge from Wastewater Treatment Plants (WWTP) with some other minor contributions such as manure disposal and release from the industrial production of pharmaceuticals [5]. The result of constant discharges of these chemicals in the environment may lead to public health problems even though the concentration is low, ranging from micro- to nanograms per liter [6]. In most cases, this represents concentrations far from acute toxicity levels but they are still a cause for concern due to risks associated with genotoxicity, induced pathogen resistance and endocrine disruption [7, 8]. Moreover, many of these substances escape conventional wastewater treatments plants and are already becoming ubiquitous in the environment [9].

This work studies the titanium dioxide catalyzed ozonation of clofibric acid: ethyl 2-(4-chlorophenoxy)-2-methylpropanoate. It is a human metabolite of the active substance clofibrate: ethyl 2-(4-chlorophenoxy)-2-methylpropanoate, a drug used as lipid regulator whose estimated persistence in the environment is over twenty years and which has been detected in lakes even after it fell out of use [10]. Being a polar compound, it also belongs to a class of substances that are not significantly adsorbed in soil and, therefore, can easily spread in surface and groundwater. The presence of this compound in the effluent of WWTP has been repeatedly reported since Ternes measured up to 1.6 μg/L of clofibric acid in the effluent of a German treatment plant [11]. More recently Tauxe-Wuersch et al. [12] also found relatively high concentrations of several hundred nanograms per liter of clofibric acid in Swiss Municipal WWTP and Weigel et al. [13] measured concentrations slightly over 1 ng/L in different samples taken in the North Sea. As for continental surface waters, Boyd et al. [2] reported the detection of clofibric acid in Detroit River water at 103 ng/L at the inlet of a drinking treatment plant. Zuccato et al. [14] reported values of some nanograms per liter in drinking water and Heberer et al., [15, 16] detected clofibric acid in several drinking water samples from the Berlin area at concentrations of up to 270 ng/L that were associated with practices of bank filtration and artificial groundwater enrichment. Recent finds of clofibric acid in environmental water samples in China stresses the fact that its occurrence is part of a global phenomenon [17].

Advanced oxidation processes (AOP) are based on the generation of hydroxyl radicals and other oxidant species in concentrations high enough to allow the oxidation of organic compounds whose chemical stability makes them difficult to degrade otherwise [18]. AOP comprise a family of technologies that differ in the approach used to generate hydroxyl radicals. Photocatalytic methods, Fenton-based systems and the direct use of the oxidants ozone and hydrogen peroxide are complemented by the less developed hydrodynamic and acoustic cavitation, radiolysis and several electrical and electrochemical methods [19, 20]. Moreover, the difficulty of application of certain methods and the relatively low efficiency of others, suggested to combine them in an attempt to treat recalcitrant pollutants in real effluents. Photo-Fenton, sonophotocatalysis, the use of oxidants combined with ultraviolet radiation (H_2O_2/UV and O_3/UV) or ultrasounds have also been considered [21]. Solid catalysts can be used to promote ozonation so that they are suitable for acidic conditions with limited ozone exposure, conditions at which the rate of formation of hydroxyl radicals would be too low. The interest in such working conditions is not only to reduce the cost of ozone generation, but also to limit bromate formation [22]. On the other hand, catalytic ozonation has been proposed to remove carboxylic acids and other refractory oxidation intermediates produced during the ozonation of complex organic molecules [23]. Except for the case of activated carbon, whose role seems to be to promote the decomposition of ozone with the subsequent increase in the production of radicals, the mechanism of catalytic ozonation is still uncertain. In metal oxides, the catalytic reaction is expected to involve the adsorption of organic molecules or ions on surface sites with subsequent oxidation by Eley-Rideal or Langmuir-Hinshelwood interaction with oxidant species. In any case, it should be born in mind that the adsorption of neutral compounds on oxides in aqueous solutions has to overcome the competitive adsorption of water molecules. Adsorption is relatively favoured for ionizable compounds if the surface is charged, this being the reason why metal oxides behave as anion exchangers if the pH of the solution is below the point of zero charge (PZC) of the solid [24].

The aim of this work was to study the catalytic ozonation of clofibric acid in reactions performed in a semi-continuous regime using a commercial titanium dioxide Degussa P25. TiO_2 P25 is a nanosized material commonly used in photocatalysis whose particles tend to agglomerate in solution as a consequence of Van der Waals attractive forces. In acidic conditions the surface hydrolyzes thus originating repulsive forces between particles that

determine the effective size of the aggregates [25]. The role of TiO_2 P25 in promoting ozonation reactions has been already documented [26]. Both the oxidation of clofibric acid and the mineralization of the dissolved organic matter have been studied and fitted to kinetic models as a function of the concentration of dissolved ozone. The interaction of clofibric acid and its ozonation products with the catalyst surface has been specially taken into account in order to separate chemical oxidation from a disappearance due to a physical adsorption.

3.3. Experimental

Clofibric acid was supplied by Sigma-Aldrich (97% purity). Solutions were prepared with high purity water obtained from a Milipore Mili-Q system with a resistivity of at least 18 MΩ cm at 25ºC. pH adjustments were made with analytical grade sodium hydroxide or hydrochloric acid from Merck. The solid used as heterogeneous catalyst was titanium dioxide Degussa P25, a mixture 80/20 of anatase/rutile. The catalyst is a nanometric powder consisting of primary particles of about 20 nm that form aggregates of several hundred nanometers that can be removed by filtration using 0.45 μm Teflon filters. The point of zero charge (PZC) of the catalyst was determined by potentiometric titration as described by Halter [27]. The value obtained, pHPZC 6.6, has been already reported [26] and agrees with similar data published elsewhere [28]. The BET specific surface was 52 ± 2 m^2/g determined by nitrogen adsorption at 77 K.

Ozonation runs were performed in a 1 L glass jacketed reactor connected to a Huber Polystat cc2 thermostatic regulator and agitated by means of a magnetic rod at about 700 rpm. The temperature of the liquid inside the reactor was monitored throughout the experiment by means of a Pt100 RTD sensor whose readings were transferred to an automated data processing system. The mixture of ozone and oxygen was produced by a corona discharge ozonator (Ozomatic, SWO100) fed by an AirSep AS-12 PSA oxygen generation unit. pH was measured by means of an electrode connected to a Eutech αlpha-pH100 feed-back control device. The final control element was a LC10AS Shimadzu pump that delivered a solution of hydrochloric acid allowing pH to be controlled within ± 0.1 throughout the experiment. The concentration of ozone dissolved in the liquid was determined by means of an amperometric analyser Rosemount 499A OZ calibrated against the Indigo Colorimetric Method (SM 4500-O3 B). A

computer stored the signals from the concentration of dissolved ozone, pH and temperature after being captured by means of an Agilent 34970 Data Acquisition Unit. The concentration of ozone in gas phase was determined using a non-dispersive UV Photometer Anseros Ozomat GM6000 Pro. TOC was determined by means of a Shimadzu TOC-VCSH analyzer, carboxylic acids were measured using a Dionex DX120 chromatograph and the analyses of clofibric acid were performed by HPLC using a C18 250 mm column. The mobile phase for the later was a mixture of water containing 4 mL/L of phosphoric acid and 50 mL/L of methanol and acetonitrile (40:60) with an isocratic flow of 1.0 mL/min at room temperature. Detection was carried out at 230 nm. Additional details are given elsewhere [26].

Ozone decomposition experiments were performed in semicontinuous mode using a fixed volume of Mili-Q water containing different amounts of catalyst. The gaseous mixture containing ozone was bubbled into the liquid by means of a porous glass disk with a gas flow of 0.20 Nm^3/h. At a given time, the gas flow was stopped and the evolution of the concentration of dissolved ozone was recorded until its total depletion. In some runs, the flow of ozone was stopped one or more times during the experiment with the purpose of performing experiments in which the exposure to ozone was not correlated with reaction time. In catalytic runs, this procedure also allowed a certain period of contact with the catalyst in the absence of ozone, used to get more insight on the possible adsorption of reaction intermediates.

The ozonation experiments were conducted in a semicontinuous mode using a fixed volume of water containing clofibric acid 25-100 mg/L (116-466 mM). High concentrations compared to that that usually found in wastewater were used in order to provide a high organic load per unit mass of catalyst and to favour the accuracy in analytical determinations. Catalytic runs were performed at a bulk catalyst concentration in the 0.25-1.25 g/L range. During every run, certain samples were withdrawn for analysis at prescribed intervals. Dissolved ozone was removed by bubbling nitrogen immediately after sampling. In catalytic runs, the catalyst was previously removed by filtration by means of Teflon 0.45 μm Millipore filters. The experiments were carried out at pH in the range 3-7 and 25ºC. The decomposition of ozone acidified the reaction mixture in all cases and pH was automatically controlled by pumping a diluted sodium hydroxide as indicated before. The volumetric mass-transfer coefficient had a relatively large value (k_La = 0.0123 ± 0.0017 s^{-1}) and accounted for the rapid increase of dissolved ozone observed at the beginning of each run. The ozone profile

depended on the rate of ozone consuming reactions and usually exhibited a shoulder during the first minutes of reaction after which it reached a plateau value almost constant throughout the run.

3.4. Results and discussion

3.4.1. Ozonation of clofibric acid

The kinetics of a heterogeneous gas-liquid semicontinuous process is governed by the relative rates of absorption and chemical reaction. A characterization of kinetic regimes is given by Hatta number, that represents the maximum rate of chemical reaction relative to the maximum rate of mass transfer. For a second order reaction the Hatta number follows the expression:

$$Ha = \frac{\sqrt{z\, k_R\, C_{A,o}\, D_{O_3}}}{k_L} \qquad (1)$$

where D_{O_3} is the diffusivity of ozone in water (1.77 x 10^{-9} m^2 s^{-1}), k_R is the homogeneous second order rate constant for the depletion of the organic compound, A, whose maximum concentration in the bulk is $C_{A,o}$. The value of the mass transfer coefficient, k_L = 5.5 x 10^{-5} m s^{-1}, was evaluated according to Calderbank and Moo-Young [29]. The stoichiometric coefficient for the reaction between ozone and clofibric acid has been given elsewhere [30]. For the most unfavourable conditions tested in this work, Ha < 0.18, ensuring that the kinetic regime was slow. This finding is consistent with the fact that ozone was detected in solution at any time during runs and allowed the use of the concentrations of ozone and clofibric acid to develop a kinetic model for the reaction taking place in the liquid phase [31]. The homogeneous rate of ozonation of an organic compound is the result of its second order parallel reaction with dissolved ozone and with hydroxyl radicals. A mass balance to a given oxidizable compound in solution yields:

$$-\frac{d\,c_i}{d\,t} = k_{HO^\bullet}\, c_{HO^\bullet}\, c_i + k_{O_3}\, c_{O_3}\, c_i \qquad (2)$$

Elovitz and von Gunten [32] proposed a kinetic model for the ozone-mediated removal of pollutants by using data from integral ozone exposure. According to it, the ozonation process is characterized by a parameter R_{ct} defined as the relationship between the integral exposures to ozone and hydroxyl radical and, derived from it, the ratio between the concentrations themselves:

$$R_{ct} = \frac{C_{HO^{\bullet}}}{C_{O_3}} \tag{3}$$

R_{ct} represents the efficiency of the system in generating hydroxyl radicals from dissolved ozone and allows the estimation of the concentration of hydroxyl radical in water, although it is not necessarily constant throughout an ozonation run [6]. It behaves as an operational parameter that characterizes the oxidation process either in whole or in part [33]. Previous results show that R_{ct} may be considered constant during the part of the ozonation run associated to the depletion of a given type of chemical compounds [6]. By using this concept, the integration of Eq. 2 yields the logarithmic concentration decay ratio as a function of the integral ozone exposure.

$$\ln \frac{c_{io}}{c_i} = \left(k_{HO^{\bullet}} R_{ct} + k_{O_3} \right) \int c_{O_3}\, dt = k_R \int c_{O_3}\, dt \tag{4}$$

The kinetic parameter k_R represents the overall kinetics and may be accurately determined from the information available on the ozone profile, whose concentration was precisely recorded throughout the run with a sampling period of 5 s. Fig 3.1 shows the decay of clofibric acid with time in non-catalytic runs performed at pH 3 and 5. The second order kinetic parameter k_R obtained from experimental data after evaluating the integral ozone exposure by a numerical method, yielded a value of $8.16 \times 10^{-3} \pm 3.4 \times 10^{-4}$ L mmol^{-1} s^{-1} at pH 3 and $1.77 \times 10^{-1} \pm 1.5 \times 10^{-2}$ L mmol^{-1} s^{-1} at pH 5, where the boundaries represent the respective 95% confidence intervals (Table 3.1). At pH 7 the kinetic regime was not slow so that the model outlined before could not be applied. Also shown in Fig.3.1 are the TOC profiles for non-catalytic ozonations performed at pH in the 3-7 range, which exhibit a two-stage pattern already observed before in catalytic and non-catalytic ozonation of other organics [27]. Both TOC decay and the

disappearance of clofibric acid are faster at higher pH values as expected from the higher rate of hydroxyl radical production with increasing pH [34].

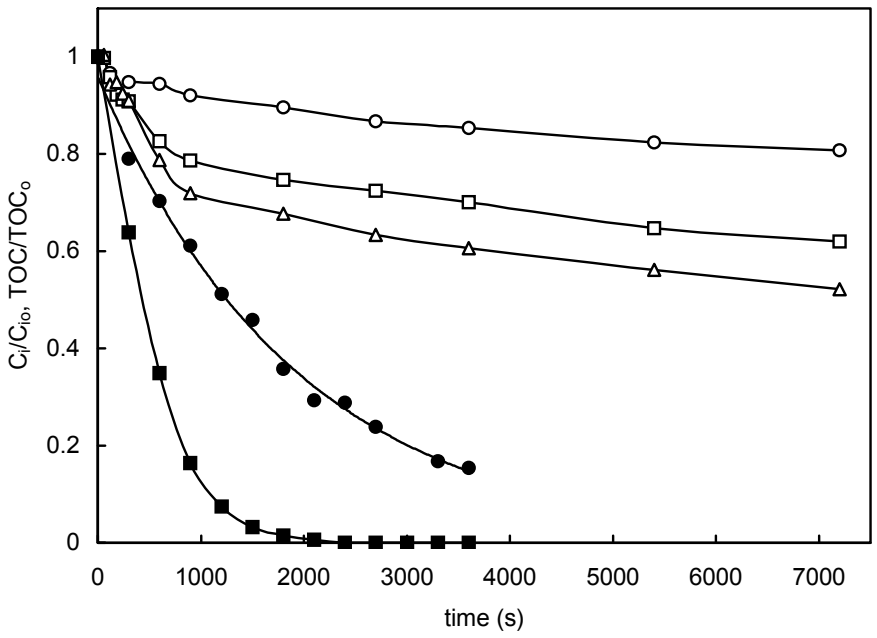

Fig. 3.1. Relative concentration of clofibric acid at pH 3 (●) and 5 (■) and TOC during the non-catalytic ozonation of 50 mg/L of clofibric acid in water at pH 3 (○), 5 (□) and 7 (Δ).

Clofibric acid, whose pK_a is 3.2 [35], dissociates in aqueous solution even under acidic conditions. The results showed that the adsorption of clofibrate was favoured in conditions at which the surface behaves as an anion exchanger [24]. Fig. 3.2 shows the results for the adsorption of clofibric acid at pH 3 and 5 on TiO_2 Degussa P25 (pHPZC = 6.6). The adsorption kinetics was slow and took place essentially during the firsts 2-4 hours, although equilibrium was achieved after a considerably longer period and the extent of adsorption reached only 5-15%. At pH 7 adsorption did not take place in any measurable extension, a result consistent with a negatively charged surface. Similar results have been published for other acidic solutes that may be adsorbed by an ion-exchange mechanism [15, 16].

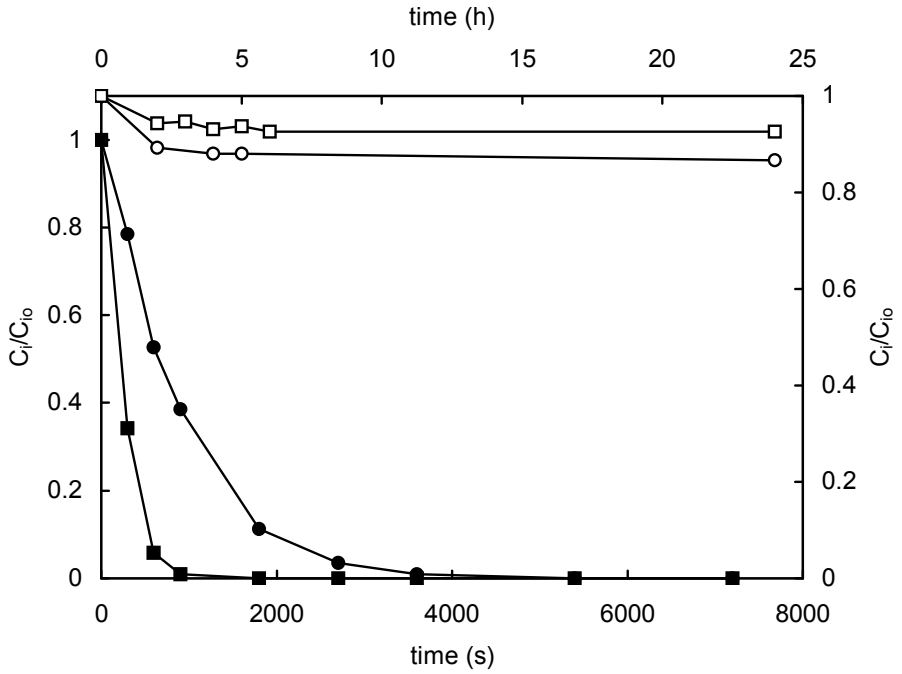

Fig 3.2. Adsorption of clofibric acid at pH 3 (○) and 5 (□) on 1 g/L of TiO_2 (upper scale) and evolution of clofibric acid during catalytic ozonation runs at pH 3 (●) and 5 (■) (lower scale) also using 1 g/L of TiO_2. Initial concentration of clofibric acid: 50 mg/L.

The rate of catalytic ozonation of a certain compound is given by the rate of its homogeneous reaction with ozone or hydroxyl radicals and that of the heterogeneous catalytic reaction. Considering that the reaction between adsorbed species and hydroxyl radicals from the bulk is the limiting process, the rate expression would be:

$$-\frac{dc_i}{dt} = k_{HO^\bullet}\, c_{HO^\bullet}\, c_i + k_c\, c_s\, c_{HO^\bullet}\, \theta \tag{5}$$

where θ is the fraction of surface sites occupied with adsorbate and c_s the bulk concentration of solids. Assuming adsorption equilibrium and including the Rct concept as indicated before, the combined rate becomes:

$$-\frac{dc_i}{dt} = k_{HO^\bullet}\, c_{HO^\bullet}\, c_i + k_c\, c_s\, c_{HO^\bullet}\, \frac{k_a\, c_i}{k_a\, c_i + k_{-a}} \tag{6}$$

in which k_a and k_{-a} are the adsorption and desorption kinetic constants for the organic compound. In the case of small surface coverage $k_a\ c_i << k_{-a}$. and the following equation is obtained in which the adsorption equilibrium constant, K_a (= k_a/k_{-a}) can be included in a group of constants with a linear dependence on catalyst load:

$$-\frac{d\,c_i}{d\,t} = \left(k_{HO^\bullet}\ R_{ct} + k_c\ R_{ct}\ K_a\ c_s\right) c_{O_3}\ c_i \tag{7}$$

The integration of the former equation yields a linear relationship between the logarithmic decay of the concentration of any given compound and the integral exposure to ozone:

$$\ln\frac{c_{i,o}}{c_i} = \left(k_{HO^\bullet}\ R_{ct} + k_c\ R_{ct}\ K_a\ c_s\right) \int c_{O_3}\ dt = k_{Rc} \int c_{O_3}\ dt \tag{8}$$

A Langmuir-Hinshelwood mechanism would lead to the same expression on the assumption that the equilibrium constant for the oxidation of surface sites is low enough [27]. The pseudo-homogeneous kinetic constant k_{Rc} for the ozonation of clofibric acid obtained from the fitting of experimental data to Eq. 8 is shown in Fig. 3.3 for several catalyst loads and for runs performed both at pH 3 and 5. The kinetic constants were linear with the concentration of catalyst, as expected from the previously outlined model. The catalytic constant was $2.17 \times 10^{-2} \pm 5.6 \times 10^{-3}$ L mmol^{-1} s^{-1} (pH 3) and $6.80 \times 10^{-1} \pm 4.1 \times 10^{-2}$ L mmol^{-1} s^{-1} (pH 5) for a catalyst load of 1.0 g/L. It must be noted that this rate constant includes the R_{ct} parameter that was not independently determined in this work. The fact that non-catalytic reaction constants match with the intercepts of catalytic constants extrapolated to zero catalyst load, suggests that the catalyst surface does not play an important role in changing the ratio ozone-to-hydroxyl radicals in solution.

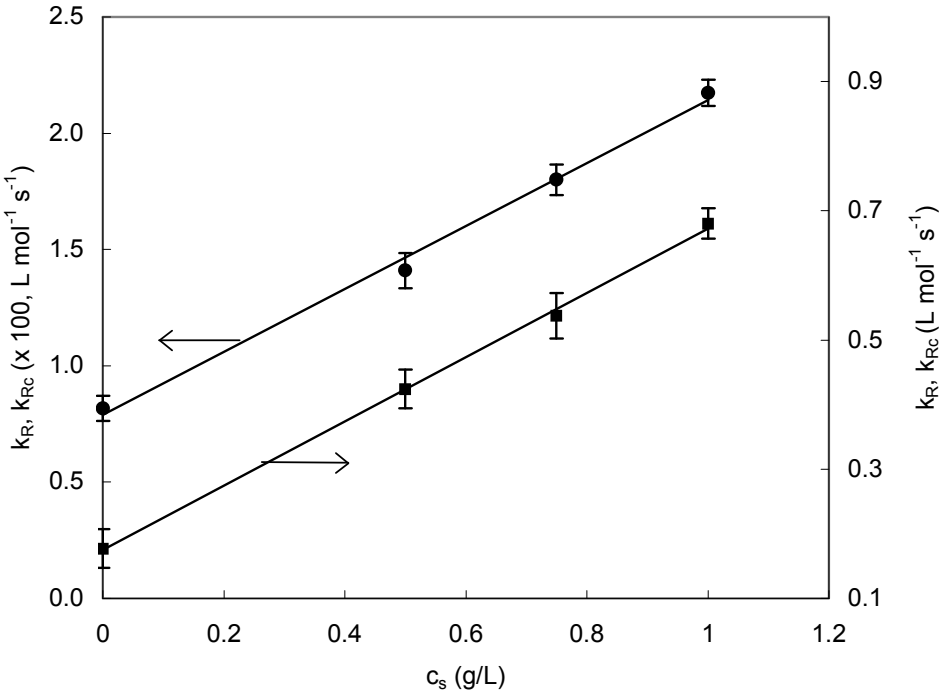

Fig 3.3. Pseudo-homogenous kinetic constant for the ozonation of clofibric acid in catalytic runs as a function of catalyst concentration at pH 3 (●, left scale) and 5 (■, right scale). The error bars represent 95% confidence intervals.

3.4.2. Mineralization kinetics

The mineralization process was followed by determining TOC in samples withdrawn during the runs. The evolution of TOC for representative non-catalytic runs is shown in Fig. 3.1 and for several catalytic experiments at pH 3 and 5 in Fig. 3.4. In all cases, as shown in Fig. 3.4, the logarithmic decrease of the organic carbon was not linear with the time-integrated concentration of ozone. A rapid initial TOC decay was always followed by a much lower rate of mineralization. During all this first ozonation period, there were still measurable amounts of clofibric acid in solution as indicated in Figs. 3.1 and 3.4. Filled squares in Fig. 3.4 represent the concentration of clofibric acid in a run performed at pH 3 with 10 min ozone flow. At this moment, the flow of ozone ceased and the dissolved ozone started to decay. Ozone was still measured in solution for about 20 more min, but the rest of the run, that lasted 120 min, took place in the absence of ozone.

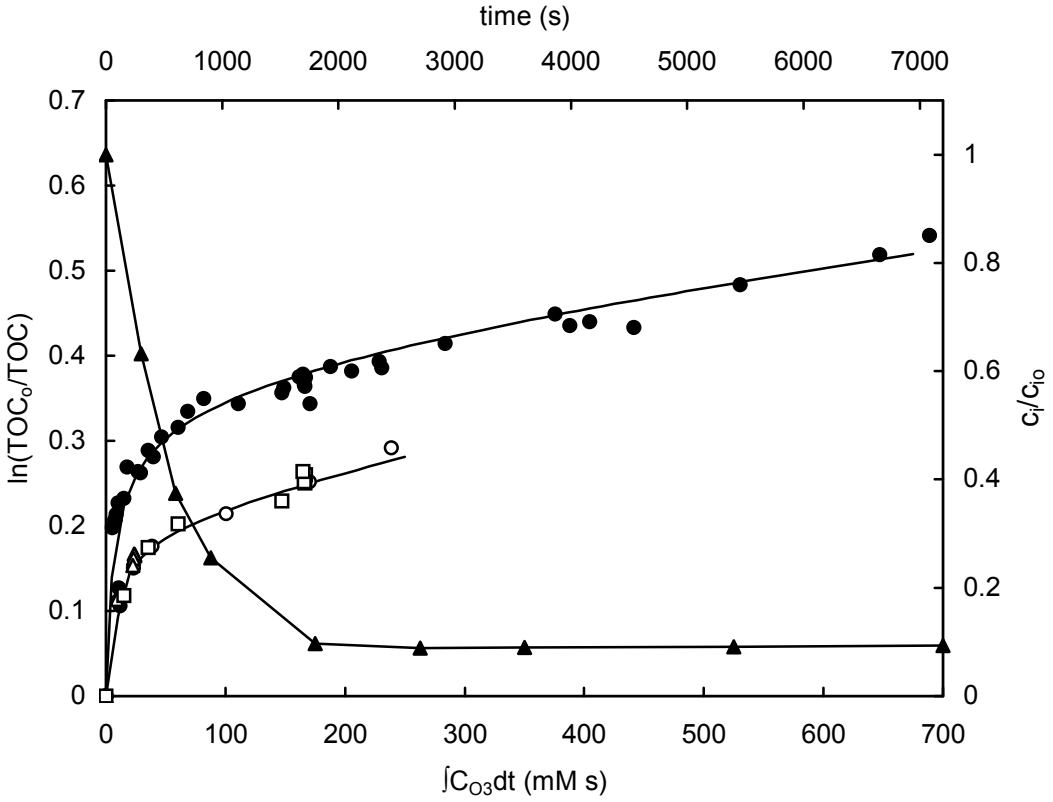

Fig 3.4. Dissolved organic carbon as a function of the integral ozone exposure for catalytic runs performed at pH 5 (●) and at pH 3 (○, □, Δ), where the latter represent runs with stopped flow of ozone. The evolution of clofibric acid at pH 3 is also shown for a run in which the flow of ozone ceased after 10 min (▲, left and upper scales; the TOC for this run corresponded to the empty triangles).

Once ozone was completely depleted, there was still about 4 ppm of clofibric acid, a concentration that did not decrease during the last part of the run. The integral exposure to ozone was limited in this run to 25 mM s (empty triangles) and in the absence of ozone the amount of dissolved carbon (TOC) did not evolve. This results showed that adsorption both of clofibric acid and reaction intermediates was not substantially modified by the absence of ozone under reaction conditions and could not be the reason for the decay of organics in solution. The second and slower mineralization period corresponded to the reaction of the less reactive intermediates, the transition corresponding to the depletion of clofibric acid. The experimental values of TOC were fitted to a kinetic model that considered a first set of easily oxidizable compounds (A) which, on ozonation, yielded a second group of refractory products (B). The kinetics of mineralization did not

match with a simple series A → B → CO_2 + H_2O due to the relatively rapid decay of dissolved carbon during the first part of the runs. This suggested that the formation of intermediates should not be a prerequisite for mineralization and suggested the following model:

$$A \xrightarrow{k_{R1} \text{ or } k_{Rc1}} CO_2 + H_2O$$

$$A \xrightarrow{k_{Ri} \text{ or } k_{Rci}} B$$

$$B \xrightarrow{k_{R2} \text{ or } k_{Rc2}} CO_2 + H_2O$$

Assuming that the reactions considered in the model are ozone-mediated transformations, Eqs. 4 and 8 can be applied for non-catalytic and catalytic runs respectively. The corresponding homogeneous kinetic constants for the three reactions considered have been labelled k_{R1}, k_{Ri} and k_{R2} (k_{Rc1}, k_{Rci} and k_{Rc2} in the case of catalytic runs) for the three individual steps yielding the following kinetic expressions for the ozonation of A and B :

$$-\frac{d c_A}{d t} = k_{R1}\, c_{O_3}\, c_A + k_{Ri}\, c_{O_3}\, c_A \tag{9}$$

$$\frac{d c_B}{d t} = k_{Ri}\, c_{O_3}\, c_A - k_{R2}\, c_{O_3}\, c_B \tag{10}$$

The observed experimental value, TOC, corresponds to $c_A + c_B$ at any time. The calculated profile of *A* essentially corresponded to that of the parent compound clofibric acid, and therefore c_A was considered a directly measurable variable coincident with the concentration of clofibric acid. The modelling by least square fitting included a fourth order Runge-Kutta routine for the integration of Eqs. 9 and 10. Fig. 3.5 shows experimental and predicted values of TOC for the catalytic ozonation of clofibric acid at pH 3(a) and 5(b) with a catalyst load of 1 g/L. In the same figure, the experimental concentration of clofibric acid, which remains detectable up to about 15 min (pH 5) and 50 min (pH 3), is also shown together with the theoretical profiles of c_A and c_B. The fact that clofibric acid can be identified at least as the most significant contribution to the group of oxidizable compounds included in A, indicates that no accumulation of reactive intermediate oxidation products is taking place.

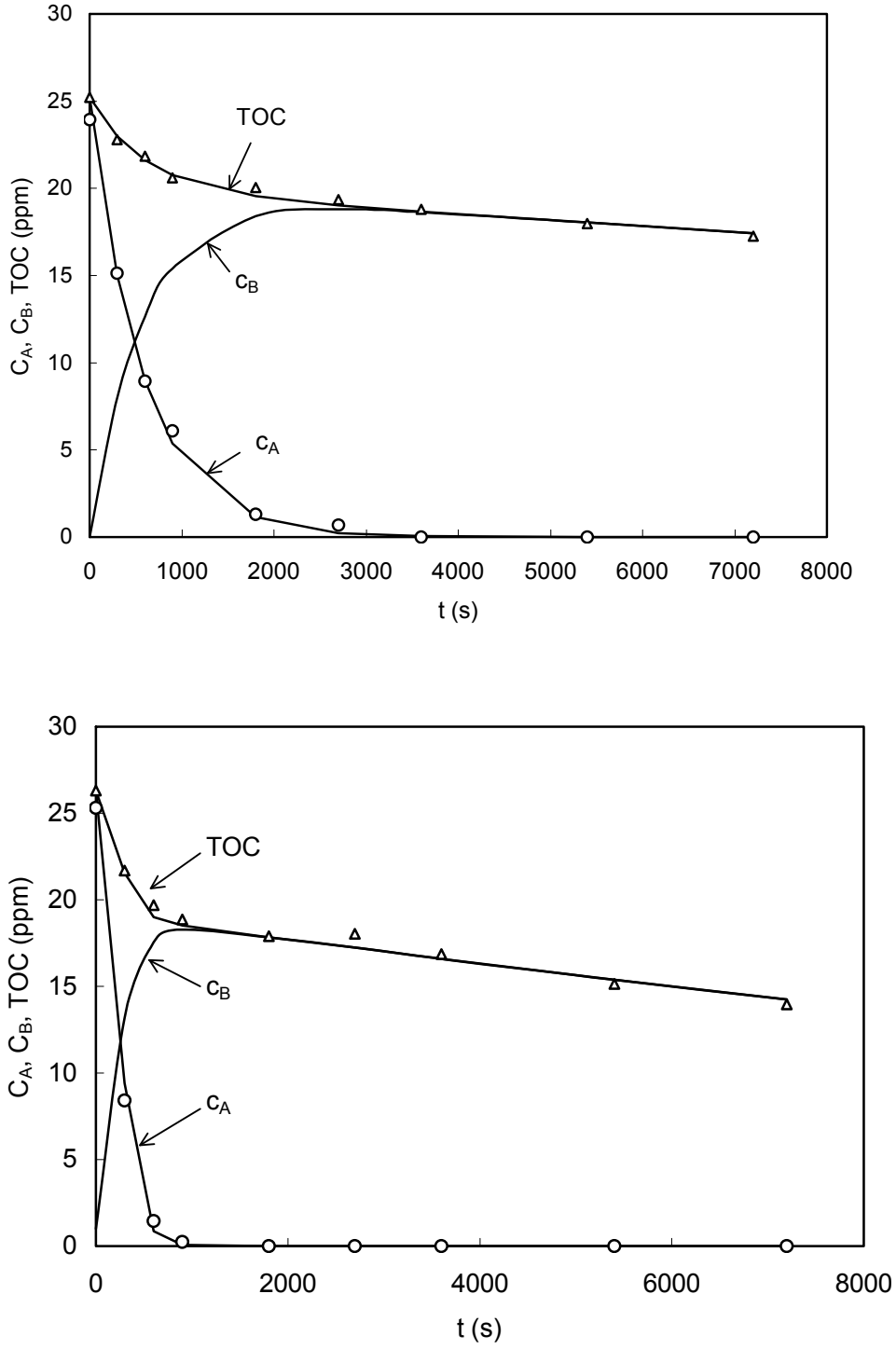

Fig. 3.5. Catalytic ozonation (1 g/L P25) of clofibric acid at pH 3 (a) and 5 (b) and model predictions for clofibric acid (cA), TOC and reaction intermediates (cB). Symbols correspond to experimental data and lines to model results. Empty circles represent the organic carbon in clofibric acid measured in samples.

The calculated rate constants corresponding to the model described by Eqs. 9-10 are shown in Table 3.1 together with their 95% confidence intervals. The fitting achieved confirms that the parameter R_{ct} should not significantly change during the ozonation of the group of compounds that characterize both ozonation periods, namely clofibric acid and acidic oxidation derivatives. The results indicated that an increase of pH accelerated the first mineralization period both in catalytic and non-catalytic runs. This observation is consistent with the role of hydroxide anion in the production of hydroxyl radicals and also agrees with previously published data on the catalytic ozonation of other drugs [27]. The mineralization of the final refractory products was somewhat slower in catalytic runs, but the differences have low statistical significance due to the overlap of their respective confidence intervals. As expected comparing Eqs. 4 and 9, k_{R1} + k_{Ri} was essentially coincident with k_R and the same for the corresponding catalytic runs as shown in Table 3.1.

The role played by the adsorption of clofibric acid in explaining TOC decay is not expected to be important in view of its slow adsorption kinetics as indicated in Fig. 3.2 and the kinetic mineralization data reported in Table 3.1. Moreover, the rate constant of the initial TOC decay in catalytic runs is considerably greater at pH 5 than at pH 3, at which the adsorption of the dissociated form of clofibric acid is more favoured. A related question is whether the adsorption kinetics of the intermediate products formed during ozonation may control the overall reaction rate invalidating the equilibrium-based mechanisms outlined before (Eq. 7). The contribution of an adsorption process in parallel with the catalytic reaction would include a term not dependent on the concentration of oxidant in the rate expression:

$$-\frac{d c_A}{d t} = k_{HO\bullet} R_{ct} c_{O_3} c_A + k_a c_s c_A \qquad (11)$$

Table 3.1. Kinetic constants for the ozonation and mineralization reactions

Ozonation of clofibric acid

	Non-catalytic (k_R, L $mmol^{-1}$ s^{-1})	Catalytic (k_{Rc}, L $mmol^{-1}$ s^{-1}, c_s = 1 g/L)
pH = 3	$8.16 \times 10^{-3} \pm 5.4 \times 10^{-4}$	$2.17 \times 10^{-2} \pm 5.6 \times 10^{-3}$
pH = 5	$1.77 \times 10^{-1} \pm 3.0 \times 10^{-2}$	$6.80 \times 10^{-1} \pm 2.4 \times 10^{-2}$

Mineralization constants for the two-stage mineralization model

Non-catalytic (L $mmol^{-1}$ s^{-1})

	k_{R1}	k_{Ri}	k_{R2}
pH = 3	$1.22 \times 10^{-3} \pm 3.2 \times 10^{-4}$	$7.03 \times 10^{-3} \pm 4.4 \times 10^{-4}$	$5.4 \times 10^{-4} \pm 7 \times 10^{-5}$
pH = 5	$7.43 \times 10^{-3} \pm 8.5 \times 10^{-4}$	$1.59 \times 10^{-1} \pm 2.0 \times 10^{-2}$	$3.5 \times 10^{-4} \pm 6 \times 10^{-5}$

Catalytic (pseudo-homogeneous constant at c_s = 1 g/L, L $mmol^{-1}$ s^{-1})

	k_{Rc1}	k_{Rci}	k_{Rc2}
pH = 3	$4.52 \times 10^{-3} \pm 4.7 \times 10^{-4}$	$1.66 \times 10^{-2} \pm 1.5 \times 10^{-3}$	$4.3 \times 10^{-4} \pm 4 \times 10^{-5}$
pH = 5	$1.68 \times 10^{-2} \pm 1.1 \times 10^{-3}$	$6.49 \times 10^{-1} \pm 2.8 \times 10^{-2}$	$2.9 \times 10^{-4} \pm 7 \times 10^{-5}$

The integration of Eq. 11 gives an expression in which the logarithmic decrease of the organic compound is not linear with the time-integrated concentration of ozone. The situation underlying this model can be discriminated from those models based on surface equilibrium with data in which the integral ozone exposure and reaction time are not correlated. The data shown in Fig 3.4 reflect the logarithmic TOC decay during the ozonation of clofibric acid at pH 5 in four independent runs, in three of which the flow of ozone was stopped several times during the run and for different periods in order to obtain TOC data with different $\int c_{O_3} dt$ in samples taken at the same time intervals. The data are shown together with their theoretical fitting curve obtained from Eqs. 9-10 and indicate that an adsorption-based mechanism like that of Eq. 11 was not governing the observed mineralization kinetics. A different approach leading to the same conclusion is shown in Fig. 3.4, whose data correspond to runs performed at pH 3. In these runs, the ozone flow was stopped after 10, 30 and 120 min in runs represented by triangles, squares and circles respectively. The gas flow was not restored thereafter and ozone remained detectable in solution for about 10 min after stopping gas flow. If the kinetic expression contained a time-dependent term like that in Eq. 11, the TOC decay curve would turn upwards sharply in the part of the run where adsorption of intermediates in the absence of ozone could take place. The same conclusion may be drawn for clofibric acid if it remains in solution from the data shown in Fig. 3.4 that correspond to a run in which the flow of ozone was stopped after 10 min. Fig. 3.6 shows the evolution of mineralization with the time-integrated concentration of ozone in runs performed at pH 3 and 5 while varying the initial concentration of clofibric acid. The fact that the logarithmic TOC decay is not dependent on the initial amount of dissolved carbon supports the assumptions underlying the kinetic expressions based on Eqs. 6-8. It must be noted, however, that the mechanism can not be considered proved as other mechanisms such as a reaction between adsorbed organic compounds and oxidized catalyst sites, are compatible with the same kinetic expressions [36].

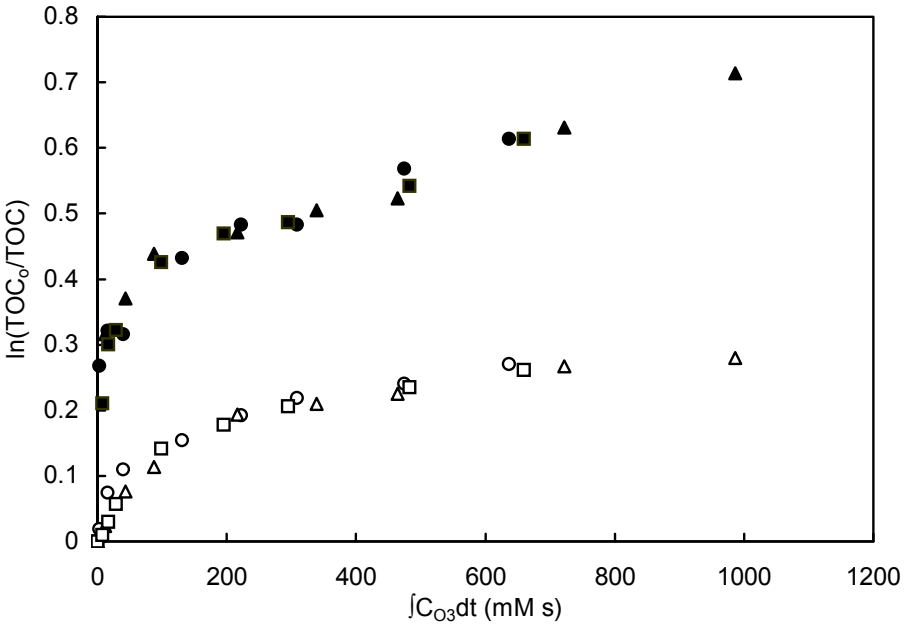

Fig 3.6. Organic carbon as a function of the integral ozone exposure for catalytic runs performed at pH 3 (empty symbols) and pH 5 (filled symbols) and for different initial concentrations of clofibric acid: 25 mg/L (○, ●), 50 mg/L (□, ■), 100 mg/L (Δ, ▲), cs = 1 g/L.

Finally, a series of reactions were also carried out for several concentrations of catalyst in the 0.25-1.25 g/L range at pH 5. The results shown in Fig. 3.7, indicate that kinetic constants k_{R1} and k_{Ri} are linear with the bulk concentration of catalyst. Concerning k_{R2}, it is difficult to draw conclusions due to the high uncertainty associated with this constant. A good fit was obtained using values in the order of 10^{-4} L mmol^{-1} s^{-1}. Fig. 3.7 also shows the first-order decomposition constant of ozone in the presence of TiO_2 P25 as a function of the amount of catalyst in suspension. The increase in the ozone decomposition rate associated to the use of catalyst has a minor importance with a shift from 8.98 x 10^{-4} s^{-1} (non-catalytic run) to 1.01 x 10^{-3} s^{-1} (1.5 g/L).

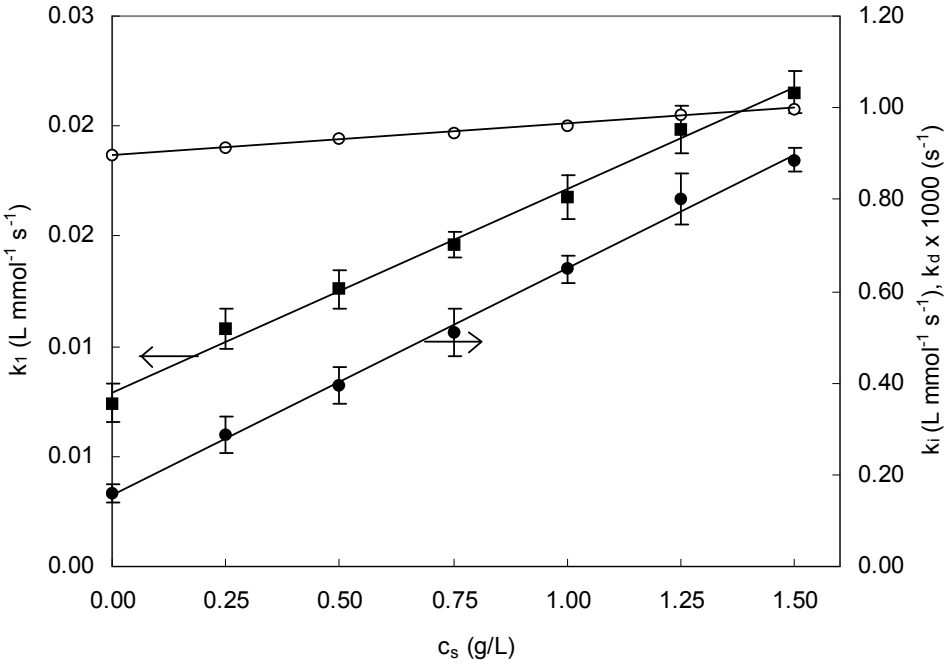

Fig 3.7. Pseudo-homogeneous kinetic constants for the catalytic ozonation of clofibric acid at different catalyst loads: kRc1 (■, left scale) and kRci (●, right scale) and first-order kinetic constant for the catalytic decomposition of ozone, kd (○, right scale).

3.4.3. Ozonation products

Except for the first few minutes, carboxylic acids are the main products of the ozonation of clofibric acid both in catalytic and non-catalytic runs. The three measured carboxylates accounted for over 60% of the organic carbon that remained in solution at the end of runs performed using 1 g/L of catalyst. For the same conditions but in the absence of catalyst, the organic carbon in the form of carboxylates was less than 50% of the total dissolved organic carbon. After 5 min, the amount of organic carbon attributed to carboxylates was 50% and 40% for catalytic and non-catalytic ozonation respectively at pH 5. At pH 3, the difference between catalytic and non-catalytic runs was greater, with 60% and 40% respectively of the organic carbon in the form of carboxylates. The concentration of oxalate, a well-known final product of the ozonation of organic compounds, tend to increase steadily during the runs, particularly at higher pH. The concentration of acetate showed a different profile in runs performed at pH 5, in which a rapid accumulation is followed by a slower decay as shown in Fig. 3.8.

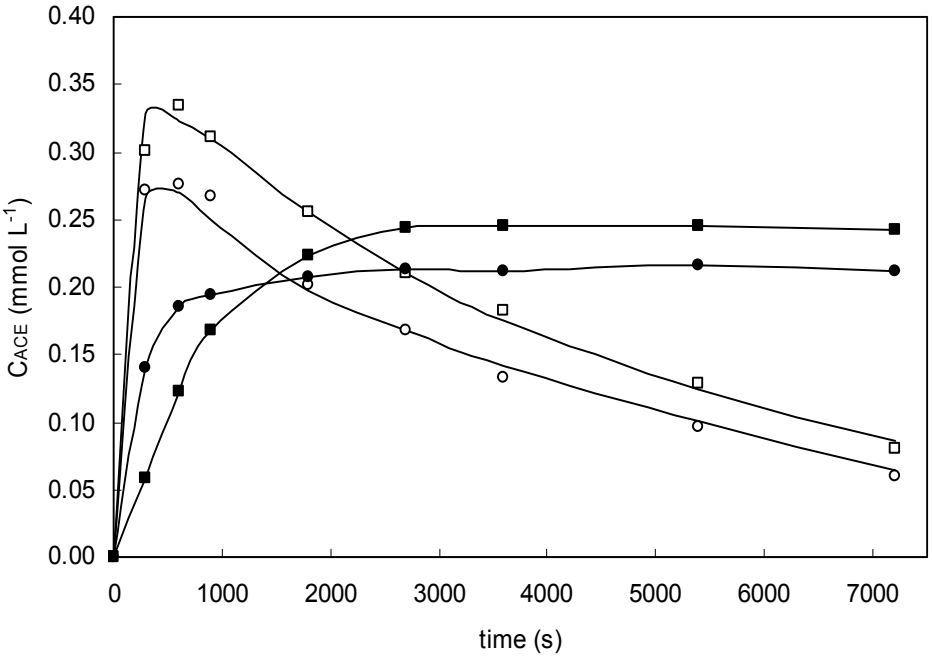

Fig 3.8. Evolution of acetate during the catalytic ozonation of 50 mg/L of clofibric acid at pH 3 (●, ■) and pH 5 (○, □). Circles: non-catalytic, squares: runs using 1 g/L of P25.

The rapid formation of acetate from clofibric acid was probably a consequence of the oxidation of 2-hydroxyisobutiric acid from the parent compound or other ring-opening products. If it could be assumed that all the acetate is produced from clofibric acid, the following kinetic expression applies:

$$\frac{d c_{ACE}}{d t} = k_A c_{O_3} c_A - k_{ACE} c_{O_3} c_{ACE} \tag{12}$$

where k_A and k_{ACE} are the second order constants for the ozonation of clofibric acid (c_A) and acetic acid (c_{ACE}). They include both direct and indirect ozonation and correspond to Eqs. 4 and 8, although in the case of catalytic reactions, the subscript "R" has been dropped for clarity. The values of k_A were not coincident with k_R or k_{Rc} from Table 3.1. For example, for a catalyst load of 1 g/L at pH 5, the fitting of experimental data to Eq. 12 led to a rate constant k_A = 0.36 L $mmol^{-1}$ s^{-1}, almost half of the pseudo-homogeneous rate constant listed in Table 3.1. This result suggest that a

significant fraction of the observed acetic acid is produced from relatively stable reaction intermediates. Even in the absence of reliable data from c_A, accurate values of k_{ACE} can be obtained from the concentration profile of acetic acid. The reason is that during most of the run the kinetic evolution of acetic acid corresponds to a second order consumption dominated by the second term of the right hand of Eq. 12.

The rate constant for the ozonation of acetate, k_{ACE}, was $1.57 \times 10^{-3} \pm 2.6 \times 10^{-4}$ L mmol-1 s-1 for non-catalytic ozonation and $2.09 \times 10^{-3} \pm 1.3 \times 10^{-4}$ L $mmol^{-1}$ s^{-1} when using 1 g/L of P25 catalyst. By contrast, at pH 3 the rate of disappearance of acetate was very low and rate constants could not be determined. The results for representative runs as shown in Fig. 3.8. The data from experiments in which the flow of ozone was stopped before the end of the run, show an almost constant concentration of carboxylates during the period that took place in the absence of ozone. These data indicate that the concentration of carboxylates in solution was not appreciably affected by a parallel adsorption or desorption process either due to anion exchange or induced by changes in catalytic surface associated to the presence of dissolved ozone. The results exclude a reaction mechanism based on a modified oxidized surface reacting with organics from the bulk.

For all reaction conditions studied in this work, the rate of accumulation of oxalic acid was always positive and showed no decay after 120 min, the prescribed reaction time in all cases. The reactions leading to oxalate were predominant during the last part of the ozonation runs. Where a previous work [26] determined that the catalyst favours not only the reactions leading to carboxylates but also the mineralization of carboxylates, in this work this effect has not been clearly observed, probably hindered by a large concentration of organic substrate. In any case, for the larger reaction times, the individual concentration of organic acids was not far different in catalytic and non-catalytic runs, while the former exhibited a greater TOC decay.

3.5. Conclusions

Clofibric acid can be completely removed by catalytic ozonation in less than 60 min at pH 3 and less than 10 min at pH 5 in runs performed at 25ºC with a bulk catalyst concentration of 1 g/L. With an initial concentration of clofibric acid of 50 mg/L and using a concentration of dissolved ozone lower than 0.10 mM, non-catalytic ozonation at pH 3 only reached a conversion of 85% in one hour with an integral ozone exposure of 1500 mM s. The use of 1 g/L of TiO_2 allowed a complete ozonation in the same time using with ozone exposure of 400 mM s. The data of ozone and clofibric acid concentration collected during the runs were fitted to a second order kinetic expression in which the oxidant was assumed to be either ozone or hydroxyl radicals produced from ozone. The kinetic constant of the non-catalytic ozonation of clofibric acid was $8.16 \times 10^{-3} \pm 3.4 \times 10^{-4}$ L mmol^{-1} s^{-1} at pH 3 and $1.77 \times 10_{-1} \pm 1.5 \times 10^{-2}$ L mmol^{-1} s^{-1} at pH 5. Catalytic runs, performed on a Degussa P25 titanium dioxide catalyst, linearly enhanced the rate of ozonation of clofibric acid. It has also been proved that the disappearance of clofibric acid was not a consequence of its adsorption on the catalyst surface. The mechanism involved in the reaction is probably a interaction of bulk oxidants or oxidized surface sites with adsorbed organics.

The evolution of total organic carbon in samples taken during the run was modelled as a function of the integral ozone exposure. It was considered that clofibric acid yielded carboxylic acids and other compounds more difficult to oxidize among which, several simple carboxylic acids were identified. The extent of mineralization during non-catalytic runs ranged from 50% at pH 7 to 20% at pH 3, the reaction taking place essentially during the first 10-20 min. The catalyst decreased TOC in solution with an additional mineralization of 5-10% with respect to non-catalytic ozonation runs at pH in the 3-5 range. The most important consequence of the use of TiO_2 P25 was to enhance the first mineralization period with pseudo-homogeneous rate constants of 4.52×10^{-3} L mmol^{-1} s^{-1} at pH 3 and 1.68×10^{-2} L mmol^{-1} s^{-1} at pH 5, up to three times over the corresponding non-catalytic constants for a catalyst load of 1 g/L. The catalyst led to a higher rate of carboxylate formation during the first period of the run in which the oxidation of clofibric acid is taking place. The ozonation of acetate is also accelerated by the presence of catalyst, with a kinetic constant changing from 1.57×10^{-3}, when no catalyst is used, to 2.09×10^{-3} L mmol^{-1} s^{-1} for 1 g/L of P25.

Stopped-flow experiments showed that the disappearance from solution of clofibric acid and its reaction intermediates was not a consequence of a slow adsorption process on the surface of the solid. It was also shown that the catalyst only moderately enhanced the decomposition of ozone with decomposition rate constants linearly increasing catalyst load. The results might suggest that the adsorption and subsequent reaction of organics on catalyst sites is responsible for the enhancement of ozonation rate observed in catalytic runs. The low extent of organics adsorption, could support a mechanism based on surface ozone decomposition even though the enhancement of ozone decomposition due to the catalyst is not high.

3.6. Nomenclature

c_A c_B	concentration of organic carbon in compounds A and B, mol L^{-1}
c_{ACE}	concentration of acetate, mol L^{-1}
c_i	concentration of a given organic compound, mol L^{-1}
$c_{HO\bullet}$	concentration of hydroxyl radicals, mol L^{-1}
c_{O_3}	concentration of dissolved ozone, mol L^{-1}
c_o	initial concentration, mol L^{-1}
c_s	bulk concentration of solids in the liquid phase, kgsolids L^{-1}
D_{O_3}	diffusivity of ozone in water, m^2 s^{-1}
k_a	adsorption kinetic constant, L kgsolids^{-1} s^{-1}
k_{-a}	desorption kinetic constant, mol kgsolids^{-1} s^{-1}
k_c	intrinsic catalytic kinetic constant, L^2 kg^{-1} $mmol^{-1}$ s^{-1}
k_d	pseudo-homogeneous kinetic constant of ozone decomposition, s^{-1}
K_a	adsorption equilibrium constant, L mol^{-1}
$k_{HO\bullet}$, k_{O_3}	second order kinetic constant of homogeneous ozone reactions, L mol^{-1} s^{-1}
k_R	homogeneous kinetic constant defined in Eq. 4, L mol^{-1} s^{-1}
k_{Rc}	pseudo-homogeneous kinetic constant defined in Eq. 8, L mol^{-1} s^{-1}
k_L	liquid-phase mass individual mass transfer coefficient, m s^{-1}
k_A, k_{ACE}	kinetic constants defined in Eq. 12, L mol^{-1} s^{-1}
R_{ct}	ratio of $c_{HO\bullet}$ to c_{O_3} at any time, dimensionless
z	stoichiometric coefficient

3.7. References

[1] K. Kümmerer, Drugs in the environment: emission of drugs, diagnostic aids and disinfectants into wastewater by hospitals in relation to other sources – a review. Chemosphere, 45 (2001) 957-969.

[2] G.R. Boyd, H. Reemtsma, D.A Grimm, S. Mitrac, Pharmaceuticals and personal care products (PPCPs) in surface and treated waters of Louisiana, USA and Ontario, Canada, Sci. Total Environ., 311 (2003) 135–149.

[3] M. Petrovic, E. Eljarrat, M.J. López, D. Barceló, Endocrine disrupting compounds and other emerging contaminants in the environment: a survey on new monitoring strategies and occurrence data, Anal. Bioanal. Chem., 378 (2004) 549-562.

[4] F. Gagné, C. Blaise, C. André, Occurrence of pharmaceutical products in a municipal effluent and toxicity to rainbow trout (Oncorhynchus mykiss) hepatocytes. Ecotoxicol. Environ. Saf., 64 (2006) 329-336.

[5] T. Heberer, K. Reddersen, A. Mechlinski, From municipal sewage to drinking water: fate and removal of pharmaceutical residues in the aquatic environment in urban areas, Water Sci. Technol., 46 (2002) 81-88.

[6] R. Rosal, A. Rodríguez, J.A. Perdigón-Melón, M. Mezcua, A. Agüera, M.D. Hernando, P. Letón, E. García-Calvo, A.R. Fernández-Alba, Removal of pharmaceuticals and kinetics of mineralization by O3/H2O2 in a biotreated municipal wastewater, Water Res., 42 (2008) 3719-3728.

[7] E.R. Cooper, T.C. Siewicki, K. Phillips, Preliminary risk assessment database and risk ranking of pharmaceuticals in the environment, Sci. Total Envion., 398 (2008) 26-33.

[8] B. Halling-Sørensen, S.N. Nielsen, P.F. Lanzky, F. Ingerslev, H.C.H. Lützhoft, S.E. Jorgensen, Occurrence, fate and effects of pharmaceutical substances in the environment - A review, Chemosphere, 36 (1998) 357-394.

[9] M. Carballa, F. Omil, J.M. Lema, M. Llompart, C. García-Jares, I. Rodríguez, M. Gómez, T.A. Ternes, Behaviour of pharmaceutical and cosmetic products in a sewage treatment plant, Water Res., 38 (2004) 2918-2926.

[10] H.R. Buser, M.D. Müller, N. Theobald, Occurrence of the pharmaceutical drug clofibric acid and the herbicide Mecoprop in various Swiss Lakes and in the North Sea, Environ. Sci. Technol., 32 (1998) 188–192.

[11] T.A. Ternes, Occurrence of drugs in German sewage treatment plants and rivers. Water Res., 32 (1998) 3245–60.

[12] A. Tauxe-Wuersch, L.F. Alencastro, D. Grandjean, J. Tarradellas, Occurrence of several acidic drugs in sewage treatment plants in Switzerland and risk assessment, Water Res., 39 (2005) 1761-1772.

[13] S. Weigel, J. Kuhlmann, H. Hühnerfuss, Drugs and personal care products as ubiquitous pollutants: occurrence and distribution of clofibric acid, caffeine and DEET in the North Sea, Sci. Total Environ., 295 (2002) 131-141.

[14] E. Zuccato, D. Calamari, R. Natangelo, R. Fanelli, Presence of therapeutic drugs in the environment, Lancet, 355 (2000) 1789-1790.

[15] Th. Heberer, H.J. Stan, Vorkommen von polaren organischen Kontaminanten im Berliner Trinkwasser. Vom Wasser, 86 (1996) 19–31.

[16] Th. Heberer, H.J. Stan, Determination of clofibric acid and N-(phenylsulfonyl)-sarcosine in sewage, river and drinking Water, Int. J. Environ. Anal. Chem. 67 (1997) 113-124.

[17] X. Peng, Y. Yu, C. Tang, J. Tan, Q. Huang, Z. Wang, Occurrence of steroid estrogens, endocrine-disrupting phenols, and acid pharmaceutical residues in urban riverine water of the Pearl River Delta, South China, Sci. Total Environ., 397 (2008) 158–166.

[18] R. Andreozzi, V. Caprio, A. Insola, R. Marotta, Advanced oxidation processes (AOP) for water purification and recovery, Catal. Today, 53 (1999) 51–59.

[18] K. Rajeshwar J.G. Ibañez G.M. Swain, Electrochemistry and environment. J. Appl. Electrochem., 24 (1994) 1077-1091.

[20] P.R. Gogate, A.B. Pandit, A review of imperative technologies for wastewater treatment I: oxidation technologies at ambient conditions, Adv. Environ. Res., 8 (2004) 501–551.

[21] P.R. Gogate, A.B. Pandit, A review of imperative technologies for wastewater treatment II: hybrid methods, Adv. Environ. Res., 8 (2004) 553–597.

[22] B. Legube, B., Formation of ozonation by-products, in: A. Nikolau (Ed.), The Handbook of Environmental Chemistry, Vol. 5 Part G, Haloforms and Related Compounds in Drinking Water, Springer, Berlin, 2003, pp. 95-116.

[23] F.J. Beltrán, F.J. Rivas, R. Montero, Mineralization improvement of phenol aqueous solutions through heterogeneous catalytic ozonation, J. Chem. Technol. Biotechnol., 78 (2003) 1225-1333.

[24] B. Kasprzyk-Hordern, M. Ziolek, J. Nawrocki, J., Catalytic ozonation and methods of enhancing molecular ozone reactions in water treatment, Appl. Catal. B: Environ., 46 (2003) 639-669.

[25] M.R. Hoffmann, S.T. Martin, W. Choi, D.W. Bahnemann, Environmental applications of semiconductor photocatalysis, Chem. Rev. 95 (1995) 69-96.

[26] R. Rosal, A. Rodríguez, M.S. Gonzalo, E. García-Calvo, Catalytic ozonation of naproxen and carbamazepine on titanium dioxide, Appl. Catal. B: Environ., 84 (2008) 48-57.

[27] W.E. Halter, Surface acidity constants of a-Al2O3 between 25 and 70°C, Geochim. et Cosmochim. Acta, 63 (1999) 3077–3085.

[28] P. Fernández, F.J.D.L. Nieves, S. Malato, Titanium dioxide/electrolyte solution interface: Electron transfer phenomena, J. Colloid Interface Sci., 227 (2000) 510-516.

[29] P.H. Calderbank, M.B. Moo-Young, The continuous phase heat and mass transfer properties of dispersions, Chem. Eng. Sci., 16 (1961) 39-54.

[30] F.J. Beltrán, 2004. Ozone reaction kinetics for water and wastewater systems. CRC, Boca Raton, p 59.

[31] R. Andreozzi, V. Caprio, R. Marotta, A. Radovnikovic, Ozonation and H2O2/UV treatment of clofibric acid in water: a kinetic investigation, J. Hazard. Mater., B103 (2003) 233-246.

[32] M.S. Elovitz, U. von Gunten, 1999. Hydroxyl radical/ozone ratios during ozonation processes. I. The Rct concept, Ozone Sci. Eng. 21 (1999) 239–260.

[33] M.O. Buffle, J. Schumacher, E. Salhi, M. Jekel, U von Gunten, Measurement of the initial phase of ozone decomposition in water and wastewater by means of a continuous quench flow system: application to disinfection and pharmaceutical oxidation, Water. Res., 40 (2006) 1884-1894.

[34] J. Hoigné, Chemistry of aqueous ozone and transformation of pollutants by ozone and advanced oxidation processes, in: J. Hrubec (Ed.), The Handbook of Environmental Chemistry, Vol. 5, Part C, Quality and Treatment of Drinking Water II, Springer, Berlin-Heidelberg, 1998, pp. 83-141.

[35] S.J. Kahn, E. Rorije, Pharmaceutically active compounds in aquifer storage and recovery, in: P.J. Dillon (Ed.), Proceedings of the 4th International Symposium on Artificial Recharge of Groundwater, ISAR-4, A.A. Balkema Publishing, Leiden, the Netherlands, 169–174, 2002.

[36] A. Rodríguez, R. Rosal, J.A. Perdigón, M. Mezcua, A. Agüera, M.D. Hernando, P. Letón, A.R. Fernández-Alba, E. García-Calvo, Ozone-based Technologies in Water and Wastewater Treatment, in Damià Barceló and Mira Petrovic (Eds.) Emerging Contaminants from Industrial and Municipal Waste, The Handbook of Environmental Chemistry: Removal Technologies, Vol. 5.S/2: Water Pollution, Springer-Verlag, Berlin, pp. 127–175, 2008.

CHAPTER 4

IDENTIFICATION OF INTERMEDIATES AND ASSESSMENT OF ECOTOXICITY IN THE OXIDATION PRODUCTS GENERATED DURING THE OZONATION OF CLOFIBRIC ACID

Journal of Hazardous Materials, 2009

4. Identification of intermediates and assessment of ecotoxicity in the oxidation products generated during the ozonation of clofibric acid

Journal of Hazardous Materials, 2009

4.1. Abstract

The degradation of an aqueous solution of clofibric acid was investigated during catalytic and non-catalytic ozonation. The catalyst, TiO_2, enhanced the production of hydroxyl radicals from ozone and raised the fraction or clofibric acid degraded by hydroxyl radicals. The rate constant for the reaction of clofibric acid and hydroxyl radicals was not affected by the presence of the catalyst. The toxicity of the oxidation products obtained during the reaction was assessed by means of *Vibrio fischeri* and *Daphnia magna* tests in order to evaluate the potential formation of toxic by-products. The results showed that the ozonation was enhanced by the presence of TiO_2, the clofibric acid being removed completely after 15 min at pH 5. The evolution of dissolved organic carbon, specific ultraviolet absorption at 254 nm and the concentration of carboxylic acids monitored the degradation process. The formation of 4-chlorophenol, hydroquinone, 4-chlorocatechol, 2-hydroxyisobutyric acid and three non-aromatic compounds identified as a product of the ring opening reaction was assessed by exact mass measurements performed by liquid chromatography coupled to time-of-flight mass spectrometry (LC-TOF-MS). The bioassays showed a significant increase of toxicity during the initial stages of ozonation following a toxicity pattern closely related to the formation of ring-opening by-products.

Keywords: Ozonation; Toxicity; Kinetics, Titanium dioxide; Clofibric acid; D. magna; V. fischeri.

4.2. Introduction

The presence of environmental xenobiotics such as pharmaceuticals and personal care products in surface and groundwaters has become a major cause for concern due to their effects on aquatic life and potential impact on human health. Pharmaceutical compounds such as analgesics, antibiotics, β-blockers or lipid regulators have a widespread distribution in the environment due to their continuous release. Municipal wastewaters are important sources of micropollutant discharges into the environment. In particular, hospitals may constitute a major contributor of disinfectants and biologically-active pharmaceuticals to the bulk wastewater discharges [1, 2]. Ellis also noted the importance of episodic events associated with stormwaters and non-point sources that tend to increase with urbanization [3]. Many drugs pose environmental risks not only because of their acute toxicity, but also the development of pathogen resistance and endocrine disruption [4]. The presence of these compounds in aqueous streams exposes aquatic organisms to multigenerational exposure with a risk of accumulative effects leading to changes that may remain undetected until irreversible damage has been caused [5]. Most drugs are persistent and many have even been designed to resist metabolic degradation. Although some compounds are not persistent, their continuous discharge to the environment ensures that they are often present at measurable levels in receiving waters. Another effect related to the environmental effects of pharmaceuticals is the large variety of metabolites and degradation products they may originate and the complexity of mixtures originated in wastewater.

Clofibric acid is the primary metabolite of clofibrate, a drug used as a lipid regulator which remains in the environment for a long time [6]. Due to its polar character, clofibric acid does not significantly adsorb in soil and can easily spread in surface and groundwater. Its biological effects are not completely understood, but it has been associated with endocrine disruption through interference with cholesterol synthesis [7]. The presence of clofibric acid in WWTP has been reported repeatedly since Ternes measured up to 1.6 μg/L of clofibric acid in the effluent of a German treatment plant [8]. Heberer et al. [9] and Heberer [10] found clofibric acid in drinking water samples from the Berlin area at concentrations of up to 270 ng/L; this was associated with the practices of bank filtration and artificial groundwater enrichment. Zuccato et al. reported values of various nanograms per liter in drinking water in Lombardy, Italy [11] and Weigel et al. measured over 1 ng/L in different samples taken in the North Sea [12]. Boyd et al. reported

over 100 ng/L of clofibric acid in samples taken at the inlet of a drinking water treatment plant [13]. Andreozzi et al. and Tauxe-Wuersch et al. found concentrations of several hundred nanograms per liter of clofibric acid in the effluent of WWTP [14, 15].

Ozonation has been studied with a view to transforming dissolved organic compounds into a more biodegradable form that can eventually be removed by conventional methods [16, 17]. Recently, it has been shown that ozonation may release oxidation intermediates with enhanced toxicity for aquatic life [18, 19]. Dantas et al. monitored the biodegradability and toxicity of a solution of sulfamethoxazole during an ozonation treatment in conditions of moderate Total Organic Carbon (TOC) removal [20]. The results showed a considerable increase in biodegradability accompanied by a rise in acute toxicity during the first thirty minutes of ozonation. This problem can be overcome by advanced oxidation processes. These processes include alkaline ozonation and the combination of ozone and hydrogen peroxide; they involve the generation of hydroxyl radicals, a highly reactive and unselective species, in sufficient amounts to oxidize dissolved organics [21]. A major drawback of AOP is the relatively high cost of reagents and energy, which forces a balance to be struck between the target degree of mineralization and the quality required for the effluent. A toxicity assessment of partially oxidized mixtures would allow optimal low severity ozonation treatments to be designed.

The aim of this study was to assess the toxicity of the oxidation products obtained during the catalytic and non-catalytic ozonation of clofibric acid. The catalytic reactions were performed using a commercial TiO_2 catalyst usually employed in photocatalysis whose ability to decompose dissolved ozone and to improve ozonation reactions has been previously studied elsewhere [22- 24]. The acute toxicity of the intermediates was assessed by means of *Vibrio fischeri* and *Daphnia magna* bioassay tests and results were related to the evolution of TOC, specific ultraviolet absorption at 254 nm ($SUVA_{254}$) and the concentrations of carboxylic acids of low molecular weight. The presence of several reaction intermediates was assessed by LC-TOF-MS.

4.3. Material and methods

4.3.1. Materials

Clofibric acid, atrazine, and tert-butanol (t-BuOH) were high-purity analytical grade reagents supplied by Sigma Aldrich. MiliQ ultrapure water with a resistivity of at least 18 MΩ cm at 25ºC was obtained from a Milipore system. pH adjustments were made with analytical grade sodium hydroxide or hydrochloric acid from Merck. The heterogeneous catalyst used was titanium dioxide Degussa P25, a 80/20 mixture of anatase/rutile. The catalyst is a powder whose primary particles have a size of about 20 nm; that in water forms aggregates of several hundred nanometers. The catalyst's point of zero charge (PZC) was pH_{PZC} 6.6, a result that has been reported elsewhere [23]. The specific BET surface was 52 ± 2 m^2/g as determined by nitrogen adsorption.

4.3.2. Ozonation procedure

The ozonation of clofibric acid was performed in a 1 L glass jacketed reactor whose temperature was controlled by a Huber Polystat cc2 thermostatic regulator and recorded by means of a Pt100 RTD sensor. pH was measured using a Crison 5052 electrode connected to a Eutech αlpha-pH100 feed-back control device that delivered a solution of sodium hydroxide by means of a LC10AS Shimadzu pump. The pH control system allowed pH to be controlled with ± 0.1 units. The experiments were carried out at pH 1, 3 and 5. The mixture of ozone and oxygen was produced by a corona discharge ozonator (Ozomatic, SWO100) fed by an AirSep AS-12 PSA oxygen generation unit; the mixture was bubbled into the liquid by means of a porous glass diffuser. The concentration of ozone in the gas was essentially constant at 27 ± 1 g m^{-3}. Details of the experimental set-up are given elsewhere [23, 24]. Ozonation experiments were conducted during one hour using a concentration of clofibric acid of 25-100 mg/L (116-466 μM), necessary to analyze reaction intermediates and to assess the evolution of toxicity during treatment. t-BuOH, 10 mM, has been added in some runs to suppress the contribution of the radical reaction due to its well-known role of radical scavenger. Atrazine has been added at a concentration of 1 mg/L as reference compound to use competition kinetics to determine rate constants [25]. Although the use of p-chlorobenzoic acid is widespread, we preferred atrazine because, being a weak base, it does not dissociate nor adsorbs significantly on positively charged surfaces (< 3% in one hour at pH

5 for the conditions used in this work). In the samples withdrawn for analysis, dissolved ozone was removed by bubbling nitrogen. In samples taken during catalytic runs, and after removing ozone, the pH was raised to > 8.5 with NaOH and kept under stirring for at least 30 min prior to filtering using 0.45 μm Teflon filters. The reason was to force the desorption of ionised acidic substances by raising pH over the point of zero charge of the surface. The role of anion exchangers played by positively charged surfaces ($pH < pH_{PZC}$, $pH_{PZC} = 6.6$) with dissociated acids has been widely recognised [26]. Comparative runs have also been carried out with the catalyst being immediately filtered from samples.

4.3.3. Toxicity bioassays

Toxicity tests were performed with the photo-luminescent bacteria *Vibrio fischeri* (*V. fischeri*) and the planktonic crustaceans *Daphnia magna* (*D. magna*). During and incubation period of 15 min, the bioassay with *V. fischeri* measures the decrease in bioluminescence induced in the cell metabolism by the presence of a toxic substance and was carried out in accordance with ISO 11348 standard protocol [27]. The bacterial assay used the commercially available Biofix Lumi test (Macherey-Nagel, Germany). The bacterial reagent was supplied freeze-dried (*Vibrio fischeri* NRRL-B 11177) and was reconstituted with a growth medium (NaCl, 2%) and incubated at +3 °C for 5 min before use. Tests were performed at 15 °C and light measurements were taken by an Optocomp luminometer. The effect of toxics was measured as percentage of inhibition with respect to the light emitted under test conditions in the absence of any toxic influence. Acute immobilization tests with *D. magna* were conducted following the standard protocol described in the European Guideline [28]. The *D. magna* bioassay used a commercially available test kit (Daphtoxkit F™ magna, Creasel, Belgium). The dormant eggs were incubated in standard culture medium imitating natural freshwater at 20 ± 1ºC under continuous illumination of 6000 lx in order to induce hatching. Between hatching and test steps, the daphnids were fed with the cyanobacteria *Spirulina* to avoid mortality during tests. The pH of samples was adjusted so that if fell within the tolerance interval of the test organisms [29]. Test plates with *D. magna* neonates were incubated for 48 h in the dark at 20°C. Acute toxicity was assessed by observing the effects of the test compounds on the mobility of *D. magna*. The neonates were considered immobilized if they lay on the bottom of the test plate and did not resume swimming within a period of 15 s. Acute toxicity is expressed in this test as the median effective

concentration (EC_{50}) leading to the immobilization of 50% of the daphnids after the prescribed exposure time. All bioassays were replicated with different ozonation batches.

4.3.4. Analytical methods

The concentration of ozone dissolved in the liquid was continuously monitored using an amperometric Rosemount 499AOZ analyzer equipped with Pt 100 RTD temperature compensation and calibrated against the Indigo Colorimetric Method (SM 4500-O_3 B). The signal from the electrode was transmitted to an Agilent 34970 Data Acquisition Unit by means of a Rosemount 1055 SoluComp II Dual Input Analyser. The Data Acquisition unit digitalized the signals from the concentration of dissolved ozone, pH and temperature with a sampling period of 5 s. The concentration of ozone in gas phase was determined using a non-dispersive UV Photometer Anseros Ozomat GM6000 Pro, tested against a chemical method. Total Organic Carbon (TOC) was determined by means of a Shimadzu TOC-VCSH total carbon organic analyzer equipped with an ASI-V autosampler. COD measurements were performed using the Standard Method 5220D. Carboxylic acids were determined in dissociated form using a Dionex DX120 Ion Chromatograph with a conductivity detector and an IonPac AS9-HC 4 x 250mm analytical column (ASRS-Ultra suppressor). The eluent was 9.0 mM Na_2CO_3 with a flow of 1.0 mL/min and the sample loop volume was 1 μL. Ultraviolet absorbance at 254 nm was recorded by means of a Shimadzu SPD-6AV spectrophotometric detector. Specific ultraviolet absorbance ($SUVA_{254}$) was obtained by calculating the ratio of ultraviolet absorbance at 254 nm while the total organic carbon of the sample in mg/L. $SUVA_{254}$ provided an indirect measure of the aromaticity of the dissolved organic matter and was calculated in accordance with the protocol of the US Environmental Protection Agency [30]. The analyses of clofibric acid and atrazine were performed by HPLC using a Hewlett Packard 1100 apparatus (Agilent Technologies, Palo Alto, USA) equipped with a reversed-phase Zorbax C18 analytical column of 3 mm x 250 mm, 5 μm particle size. The mobile phase was a mixture of water containing 4 mL/L of phosphoric acid and 50 mL/L of methanol and acetonitrile (40:60) with an isocratic flow of 1.0 mL/min at room temperature. The UV detection was carried out at 230 nm. High accuracy mass analyses of the ozonation products were performed using an Agilent 1100 G1354A chromatograph coupled with an Agilent 6210 ESI/MS time-of-flight mass spectrometer (LC-TOF-MS) that used the same column as indicated above. The mobile phase was a mixture of 0.1%

formic acid and 5% Milli-Q water in acetonitrile as mobile phase A and 0.1% formic acid in water as mobile phase B (pH 3.5) at a flow rate of 0.4 mL min^{-1}. A linear gradient progressed from 10% A (initial conditions) to 100% A in 30 min, and then remained steady at 100% A for 5 min. The injection volume was 20 µL. TOF acquisition parameters were used: capillary 4000 V, nebulizer: 340 kPa, drying gas: 10 L min^{-1}, gas temperature 350 °C, skimmer voltage 60V, 4000 V.

4.4. Results and discussion

4.4.1. Ozonation of clofibric acid

In order to ensure a slow gas-liquid kinetic regime, all measurements were made with ozone in solution with at least $1/10^{th}$ of its equilibrium concentration calculated from that of the ozone in the gas phase. These conditions ensure Hatta numbers lower than 0.20 even at pH 5. In contrast, for pH > 6, the kinetic regime was not slow and that the model outlined above can not be applied. The ozonation of a given organic compound, M, is the consequence of second order parallel reactions with dissolved ozone and hydroxyl radicals. The hydroxyl radicals originate from the decomposition of ozone in a reaction initiated by the hydroxyl anion. Following Elovitz and von Gunten [31], a constant ratio of hydroxyl radicals to ozone existed at any time, leading to the following expression:

$$-\frac{dc_M}{dt} = k_{HO^\bullet}\, c_{HO^\bullet}\, c_M + k_{O_3}\, c_{O_3}\, c_M = \left(k_{HO^\bullet}\, R_{ct}\, c_{O_3} + k_{O_3}\, c_{O_3}\right) c_M = k_R\, c_{O_3}\, c_M \quad (1)$$

The presence of 0.1 mM t-BuOH, a substance acting as radical scavenger, eliminates the contribution of the radical reaction and, therefore, the direct ozonation constant k_{O_3} can be derived from the integrated form of Eq. 1:

$$-\ln\left(\frac{c_{M,o}}{c_M}\right) = k_{O_3} \int c_{O_3}\, dt \quad (2)$$

Runs performed at different pH values and, therefore, with a different degree of dissociation of clofibric acid (pK_a = 3.2), allowed the calculation of the direct ozonation constant for the protonated (pH 1) and dissociated form (pH 5). Fig. 4.1 shows the experimental values of the logarithmic

decay of the concentration of clofibric acid as a function of the integral ozone exposure. The results evidenced an increase of the rate constant from 3.5 ± 0.5 M^{-1} s^{-1} at pH 1 to 14.3 ± 1.6 M^{-1} s^{-1} at pH 5, the last corresponding to the deprotonated form. Direct ozonation rate constants typically depend on speciation. This result agrees with observations reporting that deprotonated species react faster with the electrophilic ozone molecule [32].

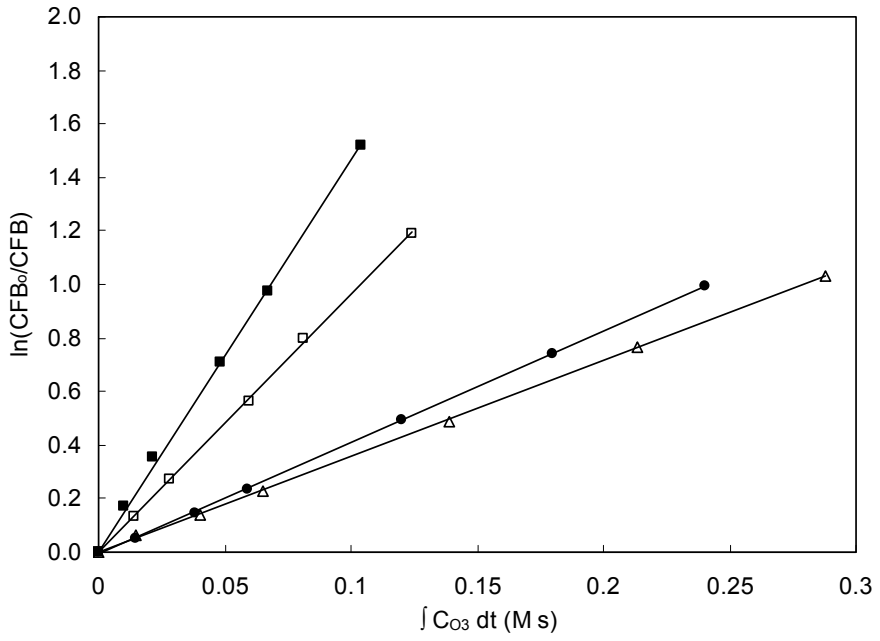

Fig. 4.1. Logarithmic decay of clofibric acid as a function of the integral ozone exposure during non-catalytic ozonation runs in the presence on t-BuOH 10 mM at pH 1 (Δ) and 5 (□). Filled symbols correspond to catalytic ozonation at pH 3 (●) and 5 (■) using 1 g/L of P25 TiO_2.

A competition kinetics method using atrazine as reference compound, R, was used to determine the rate constant for the reaction with hydroxyl radicals. Eq. 1 can be applied for both compounds yielding the following expression:

$$\ln\left(\frac{c_{M,o}}{c_M}\right) = \frac{k_{R(M)}}{k_{R(R)}} \ln\left(\frac{c_{R,o}}{c_R}\right) = \frac{k_{R(M)}}{k_{O_3(R)} + R_{ct}\, k_{OH(R)}} \ln\left(\frac{c_{R,o}}{c_R}\right) \qquad (3)$$

The fitting of experimental data to Eq. 3 was performed using the apparent rate constants for clofibric acid, $k_{R,}$, previously evaluated at pH 3 (8.16 M^{-1} s^{-1}) and 5 (177 M^{-1} s^{-1}) with the same catalyst load [24] and the values reported in the literature for the rate constants of atrazine ozonation, k_{O_3} = 4 M^{-1} s^{-1} and k_{OH} = 2.7 x 10^{-9} M^{-1} s^{-1} [33]. R_{ct} values of 2.9 x 10^{-8} (pH 5) and 7.5 x 10^{-10} (pH 3) have been derived. The rate constant for the reaction of clofibric acid with hydroxyl radical, $k_{OH,}$ can be calculated from the integrated form of Eq. 1 yielding 5.5 x 10^{9} ± 8 x 10^{8} M^{-1} s^{-1}. Huber et al. [34] and Packer et al. [35] published second order rate constants for the reaction of O_3 (< 20 M^{-1} s^{-1}) and HO· (4.7 x 10^{9} M^{-1} s^{-1}) with clofibric acid at pH 7. Razawi et al. [36] recently reported a value of 6.98 x 10^{9} ± 1.2 x 10^{8} M^{-1} s^{-1} for the bimolecular reaction rate constants with HO·. All these values are in good agreement with those reported here. These figures also show that at pH 5, 90% of the oxidation of clofibric acid takes place by reaction with hydroxyl radicals, while at pH 3 only half of clofibric acid reacted through a direct ozonation route.

Catalytic ozonation has been shown to follow the same kinetic expression by making simple assumptions such as the adsorption equilibrium of organic compounds and reaction with hydroxyl radicals from the bulk [37]. In a previous work, we reported pseudo-homogeneous rate constants at pH 3 (21.7 M^{-1} s^{-1}) and 5 (680 M^{-1} s^{-1}) for a bulk catalyst concentration of 1 g/L [24]. Using these data and with the same procedure described before, we obtained R_{ct} values of 4.5 x 10^{-9} (pH 3) and 1.2 x 10^{-7} (pH 5). They represent about a four to six-time increase respectively in the efficiency of the production of hydroxyl radicals from ozone. Using k_{O_3} determined in catalytic runs performed in the presence of t-BuOH, 4.2 M^{-1} s^{-1} at pH 3 and 14 M^{-1} s^{-1} at pH 5, it was also possible to derive the rate constant for the reaction with hydroxyl radical by means of Eq. 1. These values were 4.0 x 10^{-9} (pH 3) and 5.7 x 10^{-9} (pH 5), both essentially coincident with the same rate constant obtained in the absence of catalyst. These results suggest that the catalyst surface plays a significant role in the production of hydroxyl radicals but the interaction between solid surface and organics seems to be limited. At least, the kinetic data obtained in this work did not reveal a significant change in $k_{OH.}$ as a consequence of such interaction.

4.4.2. Efficiency of mineralization

The mineralization of reaction intermediates was monitored by simultaneously determining TOC and COD in samples taken during the experiments. The decay of TOC was relatively rapid during the first part of the runs. Thereafter, it took place a second period marked by a much lower rate of mineralization and in which we measured important amounts of simple carboxylic acids. The catalyst, TiO_2 P25, increased the rate of TOC decay during the first period, in which still persisted a certain amount of unreacted clofibric acid, with almost no effect on the final part of the run. The evolution of TOC has been extensively treated in a previous work [24]. We determined the dissolved organic carbon in the form of clofibric, oxalic (OXA), acetic (ACE), and formic (FOR) acids, in all samples collected during the runs. The organic carbon belonging to non-quantified compounds was defined as:

$$TOC_{oc} = TOC - TOC_{CFB} - TOC_{OXA} - TOC_{ACE} - TOC_{FOR} \quad (4)$$

The relative amount of TOC_{oc} in catalytic and non-catalytic runs performed at pH 3 and 5 is shown in Fig. 4.2. Non-catalytic reactions clearly produced a higher amount of intermediates other than carboxylic acids, at least during the first part of the ozonation. The effect of the introduction of catalyst can also be computed by using the mean oxidation number of carbon (MOC). The increment of this parameter, ΔMOC, is expressed as follows in molar units [25]:

$$\Delta MOC = 4\left(\frac{COD_o}{TOC_o} - \frac{COD}{TOC}\right) \quad (5)$$

Also plotted in Fig. 4.2 are the values of ΔMOC for representative samples. The graph shows a steady increase in the oxidation number of carbon associated with the formation of oxidized derivatives but without reaching a stationary state in terms of the carbon oxidation number after one hour. Another parameter used to reflect the mineralization efficiency of an oxidation system is the partial oxidation efficiency, E, defined in Eq. 6 with units expressed in mg/L [38]:

$$E = \left(\frac{COD_o}{TOC_o} - \frac{COD}{TOC} \right) \left(\frac{TOC}{COD_o - COD} \right) \quad (6)$$

E represents the percentage of COD still not mineralized at a given time. In the catalytic runs performed in this study, E reached an almost constant value with a mineralization fraction that approached 65% after 20-30 minutes. In all cases the degree of mineralization obtained was not particularly high and was consistent with the accumulation of partially oxidized intermediates in the reaction mixture.

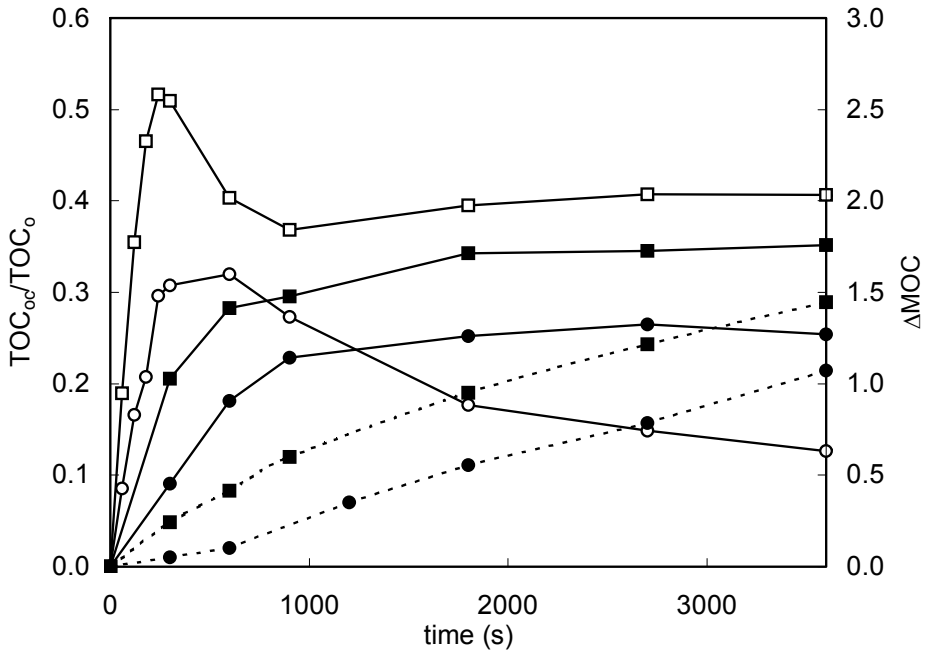

Fig. 4.2. Relative amount of organic carbon in non-quantified compounds at pH 3 (circles) and 5 (squares) during catalytic (filled symbols and solid lines) and non-catalytic (empty symbols). Also MOC (dashed lines and right scale) for catalytic runs at pH 3 (●) and 5 (■)

4.4.3. Identification of oxidation intermediates

The two main simple carboxylic acids detected by ionic chromatography were acetic and oxalic acids. Oxalic acid was the only oxidation product that accumulated in all runs irrespective of pH. As indicated in Fig. 4.3, its concentration increased with the severity of treatment, reaching about 15% of the remaining dissolved carbon. Jointly, oxalic and acetic acid accounted for over one-third of the total organic carbon at the end of catalytic and non-catalytic runs. Both a pH increase and the addition of catalyst improved the formation of simple carboxylic acids up to a certain point; beyond that point their rate of mineralization was greater than that of their formation, mostly due to the mineralization of acetic acid [24].

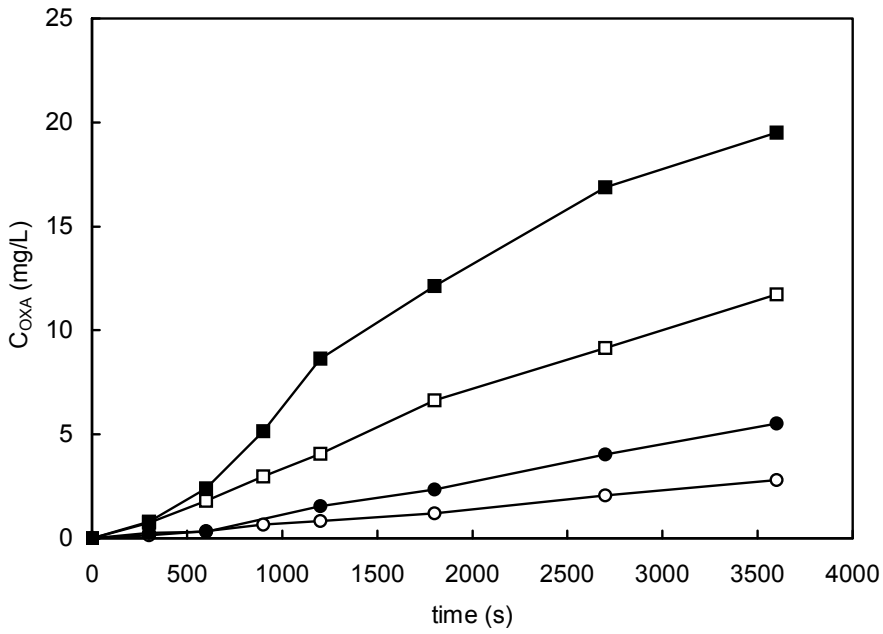

Fig. 4.3. Concentration of oxalic acids in runs at pH 3 (circles) and 5 (squares) during catalytic (filled) and non-catalytic (empty) runs. Initial concentration of clofibric acid: 100 mg/L.

The identification of more complex oxidation by-products was performed by LC-TOF-MS carried out on reaction samples collected during non-catalytic runs performed with the highest concentration of clofibric acid. The measurements allowed elemental compositions to be proposed with precision for the molecular ions of the compounds detected as well as for their characteristic fragments and sodium adducts. The high resolution of TOF instruments yields accurate mass measurements and permits elemental compositions to be proposed for the fragment ions of the detected compounds. As indicated in Table 4.1, errors were below 10 ppm except for 4-chlorophenol detected in negative mode, a compound also detected in positive mode with less error. Although this information does not provide full certainty with regard to chemical structures, a structure assignment was proposed based on these measurements and on the chemistry of ozone reactions. Some of the intermediates detected coincided with those reported elsewhere. Sirés et al. [39] studied the oxidation of clofibric acid using Fenton systems and proposed a reaction scheme in which clofibric acid is first oxidized to 4-chlorophenol by the breaking of the C(1)-O bond, thus also yielding 2-hydroxyisobutiric acid. Further hydroxyl attack on C4 position of 4-chlorophenol yields hydroquinone, whereas the attack on C(2) position leads to 4-chlorocatechol. The formation of 4-chlorocatechol from 4-chlorophenol may take place as a result of a direct ozone attack or by the selective attack of hydroxyl radical on the *ortho*-position of 4-chlorophenol [40]. Doll and Frimmel [41] investigated the catalytic photodegradation products of clofibric acid and proposed the same pathway together with a parallel dechlorination reaction which supposedly yields 2-(4-hydroxyphenoxy)-isobutyric acid. This reaction was not detected in the present study. 4-chlorophenol, 4-chlorocatechol and hydroquinone were detected in most samples tested but in very low amounts and, therefore, they have not been quantified. A fragment ion with *m/z* 103.0391 was also detected in EI negative mode with signals decreasing with time and intensity of treatment. The signal was attributed to the empirical formula [$C_4H_7O_3^-$] corresponding to 2-hydroxyisobutyric acid, also detected by Doll and Frimmel [41]. These results suggest that the breaking of the C(1)-O bond to yield 4-chlorophenol, characteristic of HO· attack, is a minor degradation route in ozonation in acidic conditions. The corresponding reaction scheme in shown in Fig. 4a. The relatively large amount of acetic acid detected during the runs was possible the outcome of the oxidation of 2-hydroxyisobutiric acid.

Table 4.1. Mass measurements obtained by LC-TOF-MS for clofibric acid and its identified ozonation products. Compound numbers refer to Fig.4. 4.

No.	Name	Molecular Formula	Detected ion	Ionization mode	Experimental mass (*m/z*)	Calculated mass (*m/z*)
1	clofibric acid	$C_{10}H_{11}ClO_3$	$(C_{10}H_9ClO_3)^+$	negative	213.0312	213.0317
2	4-chlorophenol	C_6H_5ClO	$(C_6H_4ClO)^-$	negative	126.9971	126.9951
		C_6H_5ClO	$(C_6H_6ClO)^+$	positive	129.0098	129.0107
3	2-hydroxyisobutyric acid	$C_4H_8O_3$	$(C_4H_7O_3)^-$	negative	103.0391	103.0395
4	hydroquinone	$C_6H_6O_2$	$(C_6H_5O_2)^-$	negative	109.0284	109.0290
5	4-chlorocatechol	$C_6H_5ClO_2$	$(C_6H_4ClO_2)^-$	negative	142.9913	142.9900
6	P6	$C_9H_{10}O_8$	$(C_9H_9O_8)^-$	negative	245.0292	245.0297
7	P7	$C_8H_{10}O_6$	$(C_8H_{10}O_6Na)^+$	positive	225.0371	225.0375
8	P8	$C_7H_8O_7$	$(C_7H_9O_7)^+$	positive	205.0359	205.0348

The three other oxidation products, identified as P6, P7 and P8 in Table 4.1, were assumed to correspond to the ring-cleavage of clofibric acid though a normal ozonation mechanism. The ion fragment at *m/z* 245.0292 ($C_9H_9O_8^-$, -2.04 ppm error) was assigned to the neutral empirical formula $C_9H_{10}O_8$, an oxidation and dechlorination product from a ring opened structure still preserving the methylpropionic group from clofibric acid. The extracted ion chromatogram (XIC) at *m/z* 245.029 clearly shows four isomers with the same exact mass; these were assumed to be the products of the ozonation of different positions in the aromatic ring. A probable reaction pathway leading to four isomers has been depicted in Fig. 4.4b with an initial ozone attack on C2-C3 and C4-C5 bonds. The proposed pathway starts with the ring-opening by ozone cycloaddition and includes a double HO· addition to the double bond followed by the oxidation and decarboxylation of the α-keto acid. This sequence leads to four isomers, the Z-E forms of the structures labelled as 6 in Fig. 4.4b. Compound 6 may undergo further decarboxylation to yield 7, whose proposed structure was confirmed by the presence of the corresponding sodium adduct *m/z* 225 ($C_8H_{10}O_6Na^+$, -1.78 ppm error). By following an oxidative sequence such as that indicated in Fig. 4c, 7 could generate 8. Compound 8 showed a nominal mass *m/z* 204 ($C_7H_8O_7$, 5.36 ppm) and its oxidation products should be 2-hydroxyisobutyric and oxalic acids, thus completing the oxidative chain. It is worth noting that prior to this study, none of these three ring-opening products from the ozonation of clofibric acid had been previously reported.

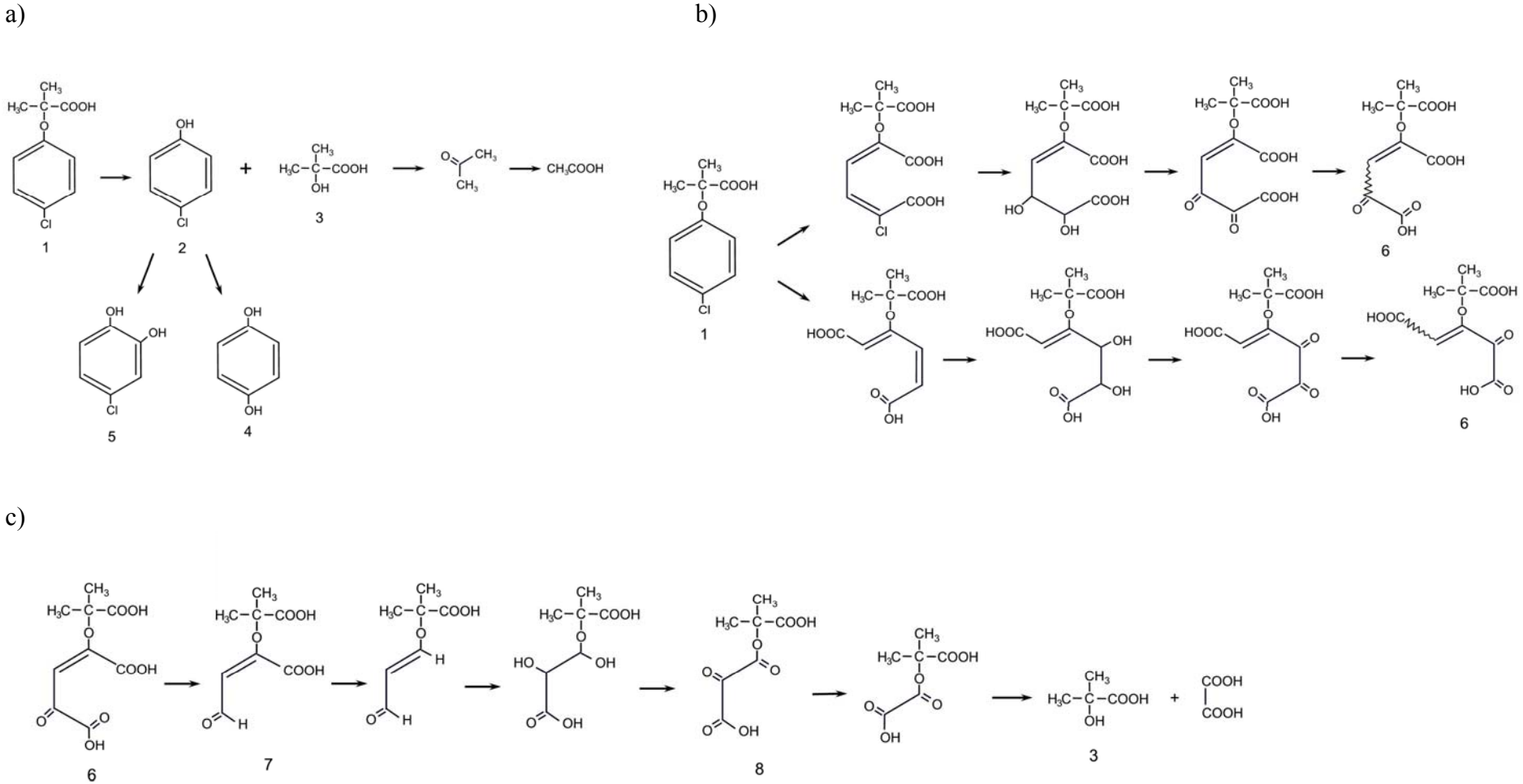

Fig. 4.4. Suggested reaction scheme for the ozonation of clofibric acid

4.4.4. Toxicity of ozonated samples

The evolution of $SUVA_{254}$ with reaction time is shown in Fig. 4.5. The pattern was similar in all cases, with a maximum reached during the first few minutes that was more pronounced at higher pH. The catalyst always reduced the absorbance during the first part of the run, even though for runs at pH 3, $SUVA_{254}$ reached higher maximum values for intermediate reaction times in the presence of catalyst. These data seem to reflect shifts in the absorbance of aromatic derivatives of clofibric acid which tended to accumulate in the reaction mixture at pH 3 probably as a consequence of the greater interaction of the positively charged catalyst with clofibric acid. UV-absorbing compounds like 4-chlorophenol and other probable products not detected in this work are supposed to be responsible for the $SUVA_{254}$ peak at the beginning of the run. The non-saturated character of these reaction products was expected to be linked to an increase in the toxicity of the reaction mixture even if TOC diminished considerably. A certain similarity between $SUVA_{254}$ profiles and the relative TOC in non-quantified compounds, especially for non-catalytic runs, also supported this assumption.

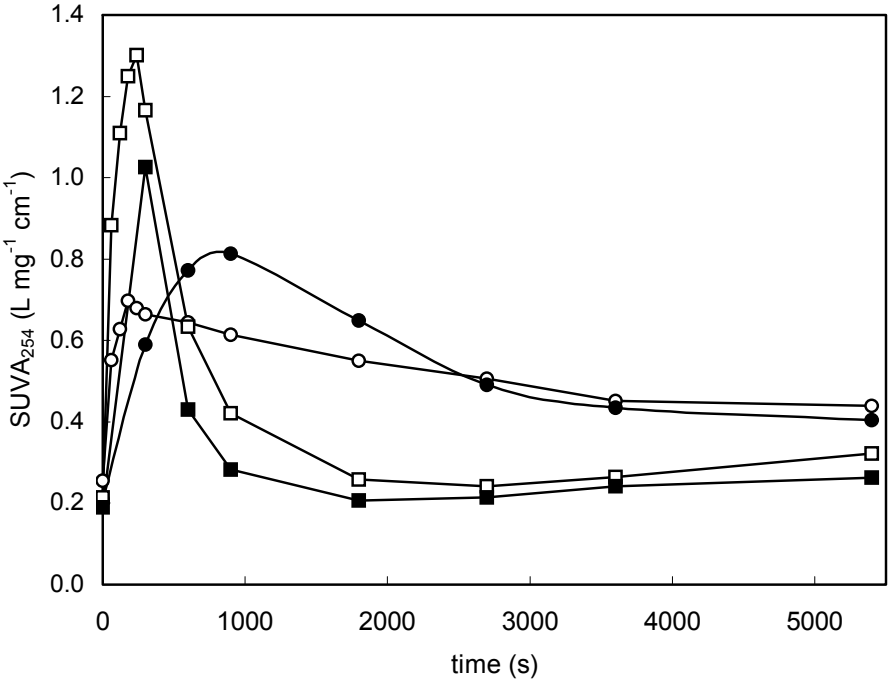

Fig. 4.5. Specific ultraviolet absorption at 254 nm ($SUVA_{254}$) for the ozonation of clofibric acid at pH 3 (○) and 5(□) in the absence of catalyst and at pH 3 (●) and 5 (■) using 1 g/L of TiO_2 as catalyst.

The toxicity of reaction mixtures consisting of partially oxidized reaction intermediates was assessed on *V. fischeri* and acute *D. magna*. The inhibition observed in *V. fischeri* bioassay of an untreated solution of 100 mg/L of clofibric acid in ultrapure water was 21% for a contact time of 15 min, consistent with the EC_{50} value obtained in this work, namely, 258 ± 34 mg/L. The toxicity obtained was considerably lower than that obtained by Ferrari et al. for a 30 min Microtox assay with a reported EC_{50} value of 91.8 mg/L [42]. The experimental value of EC_{50} for clofibric acid in 48 h *D. magna* toxicity test was 91 ± 9 mg/L, in good agreement with data presented by Henschel et al. who reported 89 mg/L [43].

The results of toxicity bioassays of samples taken during the runs at different reaction times area shown in Figs. 4.6 and 4.7 and represent the average of two replicate runs. The results obtained at pH 5 (Fig. 4.7) follow a pattern similar to the $SUVA_{254}$ profile represented in Fig. 4.5 with a significant increase of toxicity during the initial stages of ozonation. This phenomenon is particularly marked for *D. magna* tests, which reached near 100% immobilization during the first 5-10 min. This period of increased toxicity lasted considerably longer than the maximum observed in $SUVA_{254}$. As indicated below, the discrepancy with the $SUVA_{254}$ profile could be attributed to the accumulation of reaction products from the breaking of the aromatic ring. These compounds may account for a substantial part of the relatively high amount of dissolved carbon, up to 40% of the initial TOC that remained in solution after one hour in the form of compounds different from the three simple carboxylic acids that were accurately monitored in this work.

a)

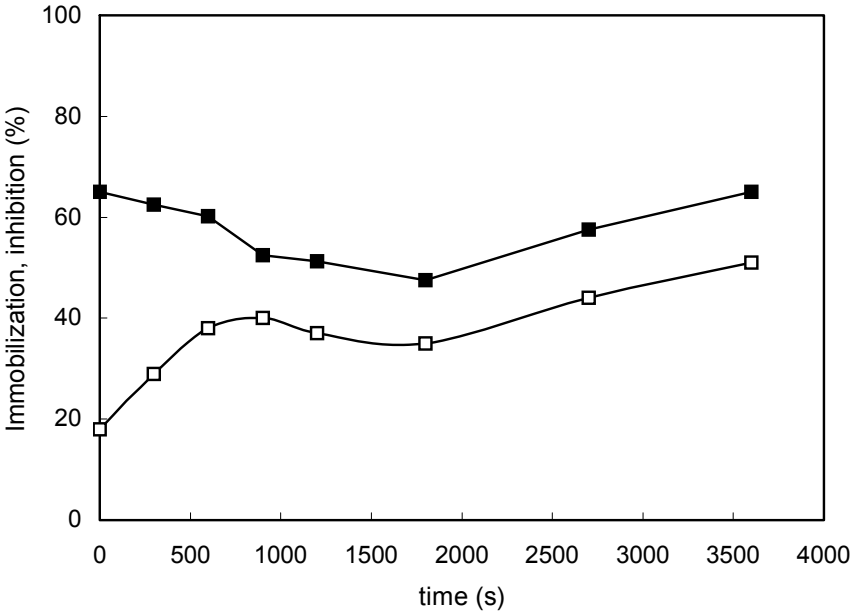

b)

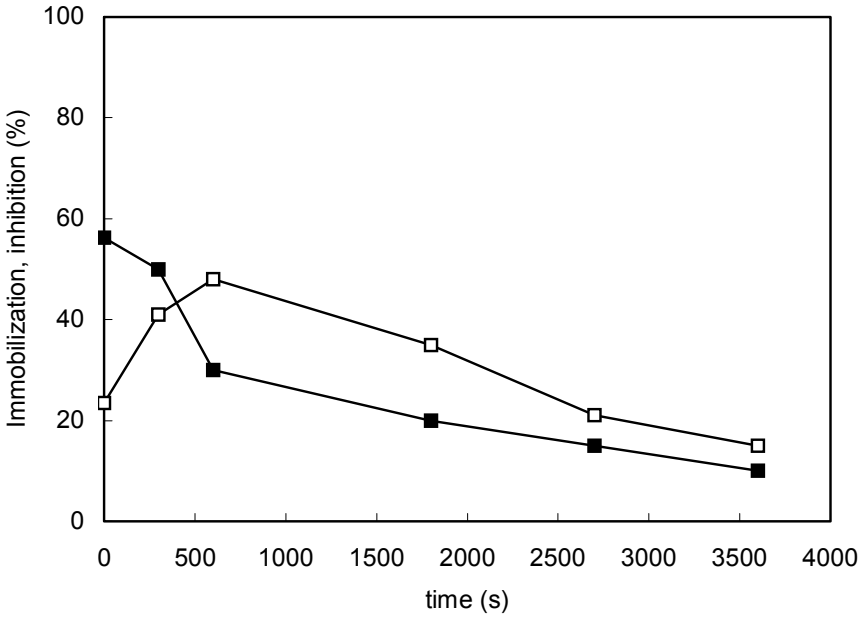

Fig. 4.6. Toxicity assessed by inhibition of *V. fischeri* (□) and immobilization of *D. magna* (■) in the reaction mixture from the ozonation of 100 mg/L of clofibric acid in non-catalytic (a) and catalytic (b) runs at pH 3. The catalyst used was 1 g/L of TiO_2.

a)

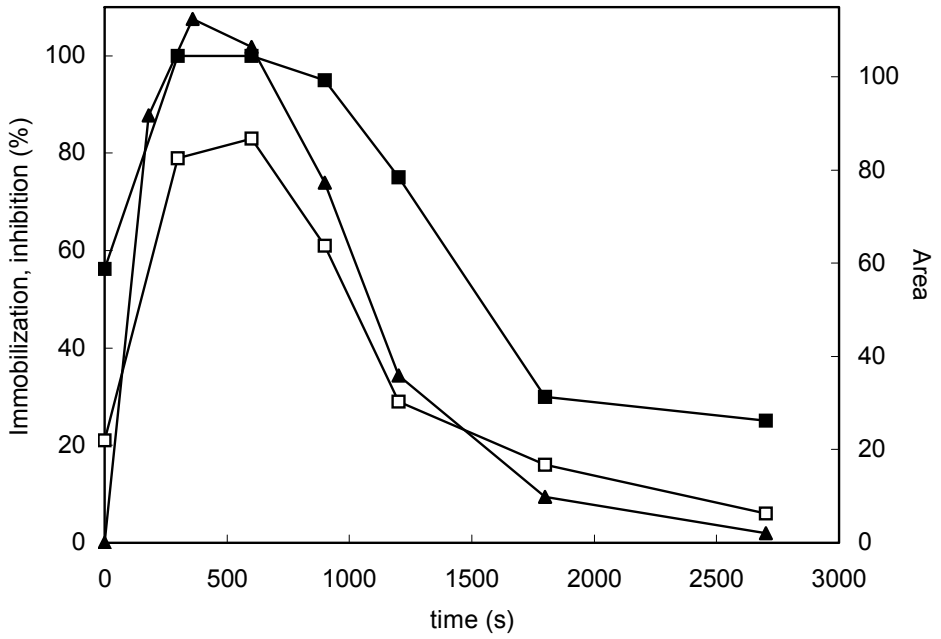

b)

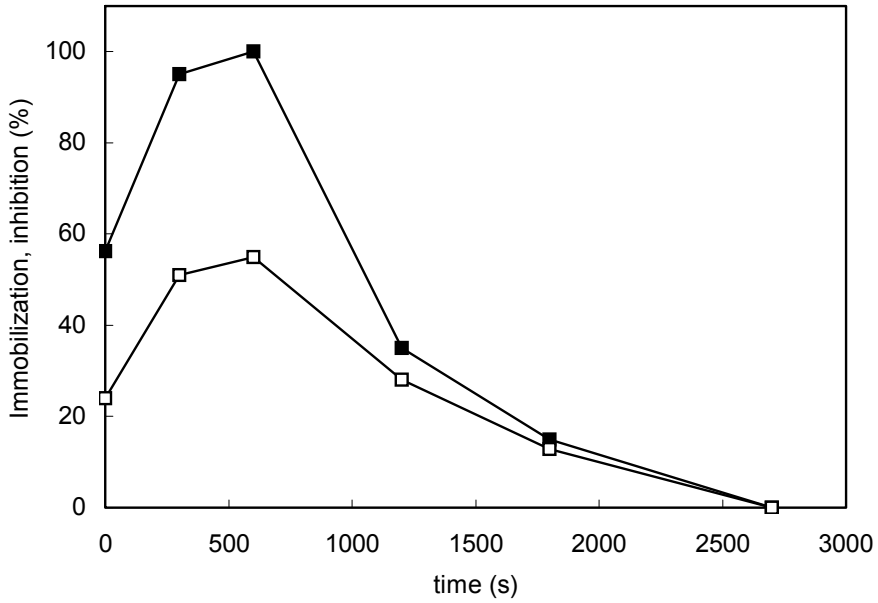

Fig. 4.7. Toxicity assessed by inhibition of *V. fischeri* (□) and immobilization of *D. magna* (■) in the reaction mixture from the ozonation of 100 mg/L of clofibric acid in non-catalytic (a) and catalytic (b) runs at pH 5. In Fig. 7a the area corresponding to compounds 6, 7 and 8 in Table 1 is also shown in arbitrary units (▲, right scale). The catalyst used was 1 g/L of TiO_2.

A toxicity increase in treated samples due to the formation of by-products that can cause greater toxicity than the parent compound has been previously observed [44]. Closely related to this work, Shang et al. [18] reported a toxicity increase during the early stages of the ozonation of chlorophenols that was attributed to the formation of chlorocatechols, chloromuconic acids and other hydroxylated or chlorinated compounds. In the present study, the identified oxidation products with higher toxicity were hydroquinone and 4-chlorophenol with EC_{50} values one order of magnitude lower for *V. fischeri* than for *D. magna*. Reported EC_{50} for *V. fischeri* (15 min) are 1.2 mg/L for 4.chlorophenol [44] and 0.041 mg/L for hydroquinone [45]. As for *D. magna* (48 h), the corresponding figures are 12.8 mg/L [46] and 0.15 mg/L [47]. In the present study the observed toxicity was in general higher for *D. magna* than for *V. fischeri*, suggesting a major effect associated with the ring-opening products rather than the aforementioned aromatic compounds. In support of this hypothesis, the sum of chromatographic areas from peaks corresponding to compounds 6, 7 and 8, closely following the experimental toxicity pattern, are shown in Fig. 4.7a.

The significantly different evolution of toxicity observed at pH 3 with respect to pH 5 is probably due to the lower rate of accumulation on oxidized intermediates. Low molecular weight carboxylic acids might also play a role in the significantly lower immobilization of *D. magna* during the first part of ozonations at pH 3. These compounds were preferentially produced during the first part of runs performed at pH 5 and were markedly more toxic for *D. magna* than for *V. fischeri* [45, 48]. As for formic acid, at pH 5, its concentration showed a maximum of about 20 mg/L after 15 min of ozonation, whereas it accumulated continuously at pH 3 with little difference between catalytic and non-catalytic runs.

The considerably lower toxicity observed in catalytic runs indicates that the catalyst reduces the accumulation of oxidation intermediates in the mixture. As shown before, the catalyst enhanced the ozonation of clofibric acid, which suggests that the same mechanism could operate with acidic intermediates, particularly acidic compounds from the ring opening of clofibric acid. The interaction of a catalyst with organic molecules in aqueous solution is governed by the pH of the medium and the point of zero charge (PZC) of the solid, which is the pH at which the surface is neutral. The adsorption of neutral compounds on oxides in aqueous solutions is hindered by the competitive adsorption of

water molecules, but the adsorption of dissociated acidic compounds is relatively favoured as the surface is positively charge below pH_{PZC} and may behave as anion exchanger [32]. Clofibric acid and other compounds dissociated in considerable amounts at pH 3-5 can adsorb on TiO_2.

The aromatic intermediates formed in the ozonation of clofibric acid were not dissociated in the operational conditions established in the present study as the pK_a of hydroquinone is 10.35 and that of 4-chlorophenol 9.38. The results of *D. magna* immobilization, particularly low at pH 3, might be explained on the basis of the interaction of the catalyst with acidic substances generated during the run. The aromatic compounds, not affected by the presence of catalyst are more toxic for *V. fischeri*, and would be perceived selectively by this bioassay.

4.5. Conclusions

The rate constant for the homogeneous direct ozonation of clofibric acid increased from 3.5 ± 0.5 M^{-1} s^{-1} at pH 1 to 14.3 ± 1.6 M^{-1} s^{-1} at pH 5 due to the speciation of the acid. The rate constant for the reaction of hydroxyl radicals and clofibric acid was calculated using the competitive method of kinetic analysis yielding 5.5 x 10^9 ± 8 x 10^8 M^{-1} s^{-1}. At pH 3, 50% of the oxidation of clofibric acid takes place by reaction with hydroxyl radicals, a figure that increases to 90% at pH 5. The depletion of clofibric acid during ozonation was considerably enhanced by the presence of titanium dioxide with at least a four-time increase in the efficiency of the production of hydroxyl radicals from ozone. The catalyst raised the fraction or clofibric acid degraded by hydroxyl radicals to 85% (pH 3) and 98% (pH 5). The estimation of the rate constant for the reaction of clofibric acid with hydroxyl radicals in catalytic reactions yielded values essentially coincident with homogeneous ozonation. Both facts suggest that even if the catalytic surface plays a significant role in the production of hydroxyl radicals, the interaction of surface sites and organics is probably limited.

A simultaneous increase in the mean oxidation number of carbon was observed with ΔMOC of up to 1.5 at pH 5 for a one-hour treatment in conditions of about 30% mineralization. The reaction produced simple carboxylic acids as end-products but only oxalic acid tended to accumulate in the reaction mixture in reflection of its more refractory character under the non-alkaline ozonation conditions used in the present study. In all cases, a significant 20-40% of the

dissolved organic carbon was in the form of reaction intermediates which differed from the simple carboxylic acids that represented the final reaction step before mineralization.

The identification of oxidation by-products was performed by LC-TOF-MS and a structure assignation was proposed for those whose exact mass could be clearly assessed. Minor amounts of 4-chlorophenol, hydroquinone and 4-chlorocatechol were detected and are probably associated with the maximum for $SUVA_{254}$ observed during the first part of the ozonation runs. These intermediates were assumed to be the product of breaking the C(1)-O bond, the corresponding hydroxyl radical attack constituting the primary reaction which led in turn to the depletion of clofibric acid. Accordingly, 2-hydroxyisobutyric acid was also detected throughout the run in amounts that decreased with reaction time. Three more compounds, whose occurrence had not been reported previously, were identified by accurate mass measurements. Tentative structures were proposed for these products that correspond to the ring-cleavage of clofibric acid though a normal ozonation mechanism followed by a sequence of oxidation and decarboxylation reactions. The results showed that this group of compounds retained the methylpropionic group from clofibric acid and at least one of them ($C_9H_{10}O_8$) was a mixture of four isomers that accumulated in relatively large amounts during reaction.

The results of toxicity bioassays on samples taken during the runs showed a significant increase of toxicity during the initial stages of ozonation both for *V. fischeri* and *D. magna* tests, but particularly for the latter. The accumulation of ring-opened acidic structures from clofibric acid was the most likely origin of the increased toxicity of treated samples. The products of catalytic runs exhibited considerably lower toxicity. There was a particular fall in the immobilization of *D. magna* at pH 3, a result that was thought to reflect the interaction of the positively charged catalyst surface with the dissociated acidic intermediates generated during the run.

4.6. References

[1] F. Gagné, C. Blaise, C. André. Occurrence of pharmaceutical products in a municipal effluent and toxicity to rainbow trout (Oncorhynchus mykiss) hepatocytes. Ecotoxicol Environ Saf, 64 (2006) 329–336.

[2] R. Rosal, A. Rodríguez, J.A. Perdigón-Melón, M. Mezcua, A. Agüera, M.D. Hernando, P. Letón, E. García-Calvo, A.R. Fernández-Alba. Removal of pharmaceuticals and kinetics of mineralization by O_3/H_2O_2 in a biotreated municipal wastewater. Water Res, 42 (2008) 3719–3728.

[3] J.B. Ellis. Pharmaceutical and personal care products (PPCPs) in urban receiving waters. Environ Pollut, 144 (2006) 184–189.

[4] B. Halling-Sørensen, B.N. Nielsen, P.F. Lanzky, F. Ingerslev, H.C.H. Lützhoft, S.E. Jorgensen. Occurrence, fate and effects of pharmaceutical substances in the environment, a review. Chemosphere, 36 (1998) 357–394.

[5] C.G. Daughton, T.A. Ternes. Pharmaceuticals and Personal Care Products in the Environment: Agents of Subtle Change? Environ Health Perspect, 107 (1999) 907–938.

[6] H.R. Buser, M.D. Müller. Occurrence of the pharmaceutical drug clofibric acid and the herbicide Mecoprop in various Swiss Lakes and in the North Sea. Environ Sci Technol, 32 (1998) 188–192.

[7] P. Pfluger, D.R. Dietrich. Pharmaceuticals in the environment— an overview and principle considerations, in Kümmerer, K. (Ed.), Pharmaceuticals in the Environment, Springer Verlag, Heidelberg, 2001, pp. 11–17.

[8] T.A. Ternes. Occurrence of drugs in German sewage treatment plants and rivers. Water Res, 32 (1998) 3245–60.

[9] T. Heberer, H.J. Stan. Determination of clofibric acid and N-(phenylsulfonyl)-sarcosine in sewage, river and drinking Water. Int J Environ Anal Chem, 67 (1997) 113–124.

[10] T. Heberer. Occurrence, fate, and removal of pharmaceutical residues in the aquatic environment: a review of recent research data. Toxicol. Lett., 131 (2002) 5–17.

[11] E. Zuccato, D. Calamari, R. Natangelo, R. Fanelli. Presence of therapeutic drugs in the environment. Lancet, 355 (2000) 1789–1790.

[12] S. Weigel, J. Kuhlmann, H. Hühnerfuss. Drugs and personal care products as ubiquitous pollutants: occurrence and distribution of clofibric acid,

caffeine and DEET in the North Sea. Sci Total Environ, 295 (2002) 131–141.

[13] G.R. Boyd, H. Reemtsma, D.A. Grimm, S. Mitrac. Pharmaceuticals and personal care products (PPCPs) in surface and treated waters of Louisiana, USA and Ontario, Canada. Sci Total Environ, 311 (2003) 135–149.

[14] R. Andreozzi, M. Raffaele, P. Nicklas. Pharmaceuticals in STP effluents and their solar photodegradation in aquatic environment. Chemosphere, 50 (2001) 50 1319–1330.

[15] A. Tauxe-Wuersch, L.F. de Alencastro, D. Grandjean, J. Tarradellas. Occurrence of several acidic drugs in sewage treatment plants in Switzerland and risk assessment. Water Res, 39 (2005) 1761–1772.

[16] S. Baig, P.A. Liechti. Ozone treatment for biorefractory COD removal, Water Sci Technol, 43 (2001) 197–204.

[17] S. Contreras, M. Rodríguez, F.A. Momani, C. Sans, S. Espulgas. Contribution of the ozonation pre-treatment to the biodegradation of aqueous solutions of 2,4-dichlorophenol. Water Res, 37 (2003) 3164–3171.

[18] N.C. Shang, Y.H. Yu, H.W. Ma, C.H. Chang, M.L. Liou. Toxicity measurements in aqueous solution during ozonation of mono-chlorophenols. J Environ Manage, 78 (2006) 216–222.

[19] R.F. Dantas, M. Canterino, R. Marotta, C. Sans, S. Esplugas, R. Andreozzi. Bezafibrate removal by means of ozonation: Primary intermediates, kinetics, and toxicity assessment. Water Res, 41 (2007) 2525–2532.

[20] R.F. Dantas, S. Contreras, C. Sans, S. Esplugas. Sulfamethoxazole abatement by means of ozonation. J Hazard Mater, 150 (2008) 790–794.

[21] S. Esplugas, J. Giménez, S. Contreras, E. Pascual, M. Rodríguez. Comparison of different advanced oxidation processes for phenol degradation. Water Res, 36 (2002) 1034–1042.

[22] R. Rosal, A. Rodríguez, M. Zerhouni. Enhancement of gas-liquid mass transfer during the unsteady-state catalytic decomposition of ozone in water, Appl Catal A: General, 305 (2005) 169-175.

[23] R. Rosal, A. Rodríguez, M.S. Gonzalo, E. García-Calvo. Catalytic ozonation of naproxen and carbamazepine on titanium dioxide. Appl Catal B: Environ, 84 (2008) 48–57.

[24] R. Rosal, M.S. Gonzalo, A. Rodríguez, E. García-Calvo. Ozonation of clofibric acid catalyzed by titanium dioxide. J Hazard Mater, doi:10.1016/j.jhazmat.2009.03.111.

[25] F.J. Beltran. Ozone Reaction Kinetics for Water and Wastewater Systems. CRC Press LLC, Florida, 2004, pp. 124-125.

[26] B. Kasprzyk-Hordern, M. Ziolek, J. Nawrocki. Catalytic ozonation and methods of enhancing molecular ozone reactions in water treatment, Appl Catal B: Environ, 46 (2003) 639-669.

[27] ISO 11348-2, Water Quality – Determination of the inhibitory effect of water samples on the light emission of *Vibrio fischeri* (Luminescent bacteria test) - Part 2: Method using liquid-dried bacteria, Geneva, Switzerland, 2007.

[28] Commission of the European Communities. Methods for determination of ecotoxicity, Annex V, C.2, Daphnia, acute toxicity to Daphnia, L. 383A, EEC Directive 92/69/EEC, 1992, p. 172-178.

[29] J.I. Seco, C. Fernández-Pereira, J. Vale. A study of the leachate toxicity of metal-containing solid wastes using *Daphnia magna*. Ecotox Environ Saf, 56 (2003) 339–350.

[30] Environmental Protection Agency, EPA. Determination of total organic carbon and specific UV absorbance at 254 nm in source water and drinking water, Method 415.3, EPA Document #EPA/600/R-05/055, 2005.

[31] M.S. Elovitz, U. von Gunten. Hydroxyl radical/ozone ratios during ozonation processes. I. The R_{ct} concept. Ozone Sci Eng, 21 (1999) 239–260.

[32] M.M. Huber, S. Canonica, G.Y. Park, U. von Gunten, Oxidation of pharmaceuticals during ozonation and advanced oxidation processes, Environ Sci Technol, 37 (2003) 1016-1024.

[33] J.L. Acero, K. Stemmler, U. von Gunte, Degradation kinetics of atrazine and its degradation products with ozone and OH radicals: a predictive tool for drinking water treatment, Environ Sci Technol, 34 (2000) 591-597.

[34] M.N. Huber, A. Gobel, A. Joss, N. Hermann, D. Loffler, C.S. McArdell, A. Ried, H. Siegrist, T.A. Ternes, U. von Gunten. Oxidation of pharmaceuticals during ozonation of municipal wastewater effluents: A pilot study. Environ Sci Technol, 39 (2005) 4290-4299.

[35] J.L. Packer, J.J. Wermer, L.E. Douglas, K. McNeil, W.A. Arnold, Photochemical fate of pharmaceuticals in the environment: naproxen, diclofenac, clofibric acid, and ibuprofen, Aquat Sci, 65 (2003) 342-351.

[36] B. Razavi, W. Song, W.J. Cooper, J. Greaves, J. Jeong, Free-Radical-Induced Oxidative and Reductive Degradation of Fibrate Pharmaceuticals: Kinetic Studies and Degradation Mechanisms, J Phys Chem A, 113 (2009) 1287–1294.

[37] A. Rodríguez, R. Rosal, J.A. Perdigón, M. Mezcua, A. Agüera, M.D. Hernando, P. Letón A.R. Fernández-Alba, E. García-Calvo. Ozone-based Technologies in Water and Wastewater Treatment, in Damià Barceló and Mira Petrovic (Eds.) Emerging Contaminants from Industrial and Municipal Waste, The Handbook of Environmental Chemistry: Removal Technologies, Vol. 5.S/2: Water Pollution, Springer-Verlag, Berlín, 2008, pp. 127–175.

[38] M. Carbajo, F.J. Beltrán, O. Gimeno, B. Acero, F.J. Rivas. Ozonation of phenolic wastewaters in the presence of a perovskite type catalyst. Appl Catal B: Environ, 74 (2007) 203–210.

[39] I.. Sirés, F. Centellas, J.A. Garrido, R.M. Rodríguez, C. Arias, P. Cabor, E. Brillas. Mineralization of clofibric acid by electrochemical advanced oxidation processes using a boron-doped diamond anode and Fe^{2+} and UVA light as catalysts. Appl Catal B: Environ, 72 (2007) 373–381.

[40] R. Sauleda, E. Brillas. Mineralization of aniline and 4-chlorophenol in acidic solution by ozonation catalyzed with Fe^{2+} and UVA light. Appl Catal B: Environ, 29(2001) 135–145.

[41] T.E. Doll, F.H. Frimmel. Kinetic study of the photocatalytic degradation of carbamazepine, clofibric acid, iomeprol and iopromide assisted by different TiO_2 materials – determination of intermediates and reaction pathways. Water Res, 8 (2004) 955–964.

[42] B. Ferrari, N. Paxeus, R. Giudice, A. Pollio, J. Garrica, J. Ecotoxicological impact of pharmaceuticals found in treated wastewaters: study of carbamazepine, clofibric acid, and diclofenac. Ecotox Environ Saf, 55 (2003) 359–370.

[43] K.P. Henschel, A. Wenzel, M. Diedrich, A. Fliedner. Environmental Hazard Assessment of Pharmaceuticals. Regul Toxicol Pharm, 25(1997) 220–225.

[44] R. Zona. Detoxification of aqueous chlorophenol solutions by ionizing radiation. Water Res, 33 (1999) 1314–1319.

[45] A. Santos, P. Yustos, A. Quintanilla, F. García-Ochoa, J.A. Casas, J.J. Rodríguez. Evolution of toxicity upon wet catalytic oxidation of phenol, Environ Sci Technol, 38 (2004) 133–138.

[46] M. Trapido, A. Hirvonen, Y. Veressinina, J. Hentunen, R. Munter. Ozonation, Ozone/UV and UV/H_2O_2 Degradation of Chlorophenols, Ozone Sci Eng, 1997; 19(1): 75–96.

[47] R. Guerra. Ecotoxicological and chemical evaluation of phenolic compounds in industrial effluents. Chemosphere, 44 (2001) 1737–1747.

[48] K. Vershueren K. Handbook of Environmental Data on Organic Chemicals, Van Nostrand Reinhold, New York, 1983.

CHAPTER 5

CATALYTIC OZONATION OF FENOFIBRIC ACID OVER ALUMINA-SUPPORTED MANGANESE OXIDE

Journal of Hazardous Materials, 2010

5. Catalytic ozonation of fenofibric acid over alumina-supported manganese oxide

Journal of Hazardous Materials, 2010

5.1. Abstract

The catalytic ozonation of fenofibric acid was studied using activated alumina and alumina-supported manganese oxide in a semicontinuous reactor. The rate constants at 20ºC for the non-catalytic reaction of fenofibric acid with ozone and hydroxyl radicals were 3.43 ± 0.20 M^{-1} s^{-1} and (6.55 ± 0.33) x 10^9 M^{-1} s^{-1}, respectively. The kinetic constant for the catalytic reaction between fenofibric acid and hydroxyl radicals did not differ significantly from that of homogeneous ozonation, either using Al_2O_3 or MnO_x/Al_2O_3. The results showed a considerable increase in the generation of hydroxyl radicals due to the use of catalysts even in the case of catalytic runs performed using a real wastewater matrix. Both catalysts promoted the decomposition of ozone in homogeneous phase, but the higher production of hydroxyl radicals corresponded to the catalyst with more activity in terms of ozone decomposition. We did not find evidence of the catalysts having any effect on rate constants, which suggests that the reaction may not involve the adsorption of organics on catalyst surface.

Keywords: Heterogeneous catalytic ozonation; Manganese oxide; Fenofibric acid; Adsorption; Hydroxyl radicals

5.2. Introduction

Fenofibrate is a drug prescribed worldwide to reduce plasma triglycerides, which is metabolized through the hydrolytic cleavage of carboxyl ester moiety resulting in 2-[4-(4-Chlorobenzoyl)phenoxy]-2-methylpropanoic acid, usually referred to as fenofibric acid. The presence of fenofibric acid has been repeatedly reported. Stump et al. found concentrations of up to 500 ng/L in the influent of several Brazilian WWTP [1]. In Europe, Ternes et al. reported 130 ng/L of fenofibric acid in the effluent of a German WWTP [2]. Acero et al. found 180 ng/L in a secondary effluent from a municipal WWTP located in Móstoles, Madrid, Spain [3]. Rodríguez et al. [4] and Rosal et al., [5] reported 165 ng/L and 129 ng/L respectively of fenofibric acid in the effluent of a WWTP located in Madrid.

The high toxicity of fenofibric acid for several aquatic microorganisms has recently been assessed [6]. The release of complex mixtures of such biologically active chemicals severely jeopardises the reuse of treated wastewater, a reasonable solution to achieve a sustainable water cycle management [7]. The removal of organic compounds in wastewater can be performed by means of advanced oxidation processes that are those in which hydroxyl radicals represent the primary oxidant species [8]. Among them, heterogeneous catalytic ozonation has received attention due to the simplicity of catalyst recovery. It is also a choice to limit the formation of oxidation intermediates [9, 10]. Alumina and alumina supported metal oxides exhibit a high activity for the gas phase ozone-assisted oxidation of volatile pollutants [11]. In aqueous phase, Yang et al. showed that the removal of dissolved organics is significantly enhanced by the presence of mesoporous alumina-supported manganese oxide [12]. The mechanism for heterogeneous catalytic ozonation involve the adsorption of ozone or its decomposition at specific sites on the surface. The main discrepancy between models consists in whether or not the chemisorption of the organic compound takes place. The adsorption of dissolved neutral compounds on metal oxides is limited due to the competitive adsorption of water molecules, but ionizable organics may adsorb if the surface is charged and allows ion exchange. This is the case of metal oxides, which behave as anion (cation) exchangers if the pH of the solution is below (above) the point of zero charge of the surface [13]. Although it is generally true that the extent of adsorption considerably decreases under the unfavourable

electrostatic conditions that take place on charged surfaces, it has been pointed out that small but significant adsorption may occur even in this case through surface complexation reactions [14].

The objective of the present study was to use kinetic data to highlight the mechanism by which solid catalysts enhance the rate of ozonation in aqueous solution and to determine whether or not the possible adsorption of organics on catalytic surfaces results in a change of rate constants. To this end, we performed kinetic experiments either in pure water and wastewater and studied the extent to which the catalysts increased the concentration of hydroxyl radicals derived from ozone.

5.3. Experimental section

5.3.1 Materials

Atrazine and *tert*-butyl alcohol (*t-BuOH*) supplied by Sigma-Aldrich were high-purity analytical grade reagents. Fenofibric acid was produced as indicated elsewhere [6]. MiliQ ultrapure water with a resistivity of at least 18 MΩ cm at 25ºC was obtained from a Milipore system. The catalysts used in this study were alumina (γ-Al_2O_3) and alumina-supported manganese oxide (MnO_x/Al_2O_3). γ-Al_2O_3 was purchased from Sigma-Aldrich and used as received. Its surface area was 155 m^2 g^{-1}, determined by nitrogen adsorption, and its average particle size was 100 μm. The MnO_x/Al_2O_3 catalyst was prepared by incipient wetness impregnation dried γ-Al_2O_3 using an aqueous solution of $Mn(CH_3COO)_2{\cdot}4H_2O$ (Sigma-Aldrich). The catalyst was subsequently dried in air at 423 K and calcined at 773 K for 3 hours. The catalyst was washed twice in PBW to avoid further leaching of manganese. The amount of manganese used corresponded to a 10% wt. of MnO_2. The BET surface area was 119 m^2/g. The isoelectric point (IEP) of the catalysts was obtained by measuring the ζ-potential in aqueous solutions at 25ºC after adjusting ionic strength to 10^{-3} M with NaCl. The values obtained for IEP were 8.2 for γ-Al_2O_3 and 7.3 for MnO_x/Al_2O_3 as prepared, which fell to 3.0 for MnO_x/Al_2O_3 after contact with bubbling ozone in aqueous slurry for 30 min.

Wastewater was collected from the secondary clarifier of a WWTP located in Colmenar Viejo (Madrid). The plant operates with a conventional activated sludge treatment, has a capacity of 53000 equivalent inhabitants and was designed to treat a maximum volume of wastewater of 8000 m^3/day. The main characteristics of treated wastewater are shown in Table 5.1.

Table 1. Main wastewater parameters

pH	8.2
Total Suspended Solids (mg/L)	13
Conductivity (μS/cm)	624
COD (mg/L)	83
TOC (mg/L)	14.3
PO_4-P (mg/L)	0.15
Anions and cations (mg/L)	
Fluoride	0.1
Chloride	133.1
Nitrite	0.3
Nitrate	8.2
Sulfate	67.2
Carbonate	2.8
Bicarbonate	114.8
Sodium	116.4
Potassium	19.2
Ammonium	11.9
Magnesium	7.1
Calcium	27.4

5.3.2. Ozonation procedure

The ozonation runs were performed in a 1 L glass jacketed reactor whose temperature was controlled at 20ºC using a thermostatic regulator. For experiments with spiked wastewater and non-buffered pure water, pH was controlled at 6.5 within ± 0.1 units by means of a feed-back control device that delivered a solution of sodium hydroxide though a LC10AS Shimadzu pump. The rest of the runs were performed in solutions adjusted to pH 6.5 using a 0.1 M phosphate buffered water (PBW). Ozone was produced by a

corona discharge and continuously bubbled throughout the run with a gas flow of 0.20 Nm^3/h. Further details are given elsewhere [15].

The experiments using fenofibric acid in pure water were conducted with a concentration of fenofibric acid in the 5-15 mg/L range (16-47 mM) and, in certain runs, *t-BuOH* at 5 mg/L (67 μM), 74 mg/L (1.0 mM) and 741 mg/L (10 mM), in order to inhibit or suppress the contribution of the radical reaction. Atrazine was added at a concentration of up to 2 mg/L as reference compound [16]. In the samples withdrawn for analysis, dissolved ozone was removed either by the addition of sodium thiosulfate or by bubbling nitrogen at a flow-rate of about 0.2 Nm^3/h. For the later, we could check that the concentration of ozone fell below 3% in less than 30 s.

For the experiments with spiked wastewater, the prescribed amount of fenofibric acid was dissolved in raw wastewater whose pH was previously adjusted to 6.5 with HCl. In these runs fenofibric acid and atrazine were dissolved in wastewater previously ozonated until ozone appeared in solution. The reason for this procedure was to avoid interferences due to the presence of organic compounds that react rapidly with ozone [17].

In all catalytic runs, the catalyst was pre-oxidized prior to the addition of organics for 15 min with the same ozone flow as that used for ozonation runs. In samples taken from catalytic runs, pH was raised to > 8.5 with NaOH and stirred continuously for at least 30 min prior to filtering using 0.22 μm Millex-GV PVDF Millipore filters. The aim of this procedure was to avoid the loss of organics adsorbed on the catalyst surface by displacing them with a strong base. Certain ozone decomposition experiments were also performed by stopping the gas flow at a given moment using a procedure described elsewhere [18].

5.3.3. Analyses

The concentration of ozone dissolved in the aqueous phase was monitored with an amperometric Rosemount 499AOZ analyzer periodically calibrated using the Indigo Colorimetric Method (SM 4500-O3 B). A Data Acquisition unit digitalized the signals from the concentration of dissolved ozone, pH and temperature with a sampling period of 1 s. The concentration of ozone in gas phase was determined using an Anseros Ozomat GM6000 Pro

photometer calibrated against potassium iodide. Total Organic Carbon (TOC) was determined by means of a Shimadzu TOC-VCSH total carbon organic analyzer equipped with an ASI-V autosampler. The BET specific surface was determined by nitrogen adsorption at 77 K using a SA 3100 Beckman Coulter Analyzer. Anions were determined using a Metrohm 861 Advance Compact IC with suppressed conductivity detector and a Metrosep A Supp 7-250 analytical colum with 36 mM Na_2CO_3 as eluent with a flow of 0.8 mL/min. Cations were quantified by means of a Metrosep C3 column using 5.0 mM HNO_3 as eluent with a flow of 1 mL/min. The analyses of fenofibric acid and atrazine were performed by HPLC using a Hewlett Packard 1200 Series apparatus (Agilent Technologies, Palo Alto, USA) equipped with a reversed phase Kromasil 5u 100A C18 analytical column. UV detection was carried out at 280 nm (fenofibric acid) and 228 nm (atrazine). To allow statistical analysis to be performed, runs were replicated and all HPLC determinations were carried out in quintuplicate.

5.4. Results and discussion

The kinetics of a gas–liquid ozonation process depends on the relative rates of physical absorption and chemical reaction. The kinetic regime is determined by the Hatta number, which represents the maximum rate of chemical reaction relative to the maximum rate of mass transfer. For a second order reaction, the Hatta number is:

$$Ha = \frac{\sqrt{\nu\, k_R\, c_A\, D_{O_3}}}{k_L} \qquad (1)$$

in which k_R is the second order homogeneous rate constant based on the depletion of the organic compound, D_{O_3} the diffusivity of ozone in water (1.77×10^{-9} m^2 s^{-1}) and c_A the concentration of substance to be oxidized. An estimation of the mass transfer coefficient, k_L = 5.5 × 10^{-5} m s^{-1}, was obtained according to Calderbank and Moo-Young [19]. Using initial concentrations, c_{Ao} as those corresponding to the most unfavourable conditions, we found that all results reported in what follows corresponded to slow kinetic regime (Ha < 0.4). This was confirmed by a criterion based on appearance of ozone in solution that was explained in a previous work [5]. The upper boundary for the stoichiometric coefficient was estimated by

relating the moles of ozone transferred to the liquid phase to the amount of fenofibric acid oxidized at a given time:

$$\nu < \frac{k_L a\, c^*_{O_3}\, t - k_L a \int_o^t c_{O_3}\, dt}{c_A - c_{Ao}} \qquad (2)$$

The volumetric mass transfer coefficient, k_La, was determined in transient runs with pure water and $c^*_{O_3}$ is the equilibrium concentration of ozone in the liquid calculated from Henry's law. Details are given elsewhere [20]. This procedure yielded a value of $\nu \sim 2$. In addition to catalytic ozonation runs, the adsorption of fenofibric acid on the catalyst surface was assessed. Fenofibric acid, whose pK_a is 2.9, dissociates in aqueous solution even under acidic conditions. The adsorption of dissociated acids is favoured when the surface can behave as an anion exchanger, but is hindered by the presence of dissolved salts. After 24 h in contact with Al_2O_3 and MnO_x/Al_2O_3, the amount adsorbed was near 10% (initial concentration 15 mg/L, amount of catalyst 1 g/L) in pure water but fell below statistical significance in PBW and wastewater. Particularly, the amount adsorbed was not significantly different from zero in any case after one hour. Other studies have reported the lack of adsorption of organics on various catalysts including supported manganese oxide at several pH values [10]. It should be noted that the isoelectric point of manganese oxides is strongly dependent on its oxidation state and crystallographic form. Manganese oxide supported catalysts exist as multivalent oxidation states that under heat treatments proceed from MnO_2, to Mn_2O_3 and Mn_3O_4 [21]. Mn_2O_3 is the form with the highest IEP, in the 7.6-9.0 range, which probably dominates the MnO_x/Al_2O_3 catalyst prior to contact with ozone [22]. The fact that IEP in aqueous slurry in the presence of ozone fell to 3.0, a value typical for tetrahedrally coordinated Mn^{4+}, is consistent with the assumption that MnO_2 was the main species in manganese oxide catalysts in contact with ozone. The oxidation of MnO_x/Al_2O_3 catalysts by ozone to their higher oxidation state has been observed in gas phase [23].

5.4.1. Non-catalytic ozonation

Fenofibric acid's depletion rate is the consequence of its second order parallel reaction with dissolved ozone and with hydroxyl radicals:

$$r_{FFA}^h = k_{O_3}^h \, c_{FFA} \, c_{O_3} + k_{HO\bullet}^h \, c_{FFA} \, c_{HO\bullet} \tag{3}$$

According to the hypothesis proposed by Elovitz and von Gunten, the ozonation process is characterized by a parameter defined as the relationship between the ratio of the concentration of hydroxyl radicals and ozone that represents the efficiency of the system in generating hydroxyl radicals [24].

$$r_{FFA}^h = \left(k_{O_3}^h + k_{HO\bullet}^h R_{ct}^h \right) c_{FFA} \, c_{O_3} \tag{4}$$

A mass balance to fenofibric acid in the reactor leads to a differential equation, $r_{FFA}^h = -\dfrac{d\, c_{FFA}}{dt}$, that can be readily integrated assuming that R_{ct}^h the ratio of $c_{HO\bullet}$ to c_{O_3} in homogeneous conditions, is constant throughout the run:

$$\ln\left(\frac{c_{FFA(o)}}{c_{FFA(t)}} \right) = \left(k_{O_3}^h + k_{HO\bullet}^h \, R_{ct}^h \right) \int_o^t c_{O_3} \, dt = k_R^h \int_o^t c_{O_3} \, dt \tag{5}$$

The data represented in Fig. 5.1, corresponding to runs performed in PBW in the presence of *t-BuOH* 10 mM as hydroxyl radical scavenger, allowed $k_{O_3}^h$ to be calculated for fenofibric acid, yielding 3.43 ± 0.20 M^{-1} s^{-1}, a relatively low constant for the direct ozonation reaction. The linear relationship of the logarithmic concentration decay with integral ozone exposure indicates a constant value for R_{ct}^h. In the same figure, we represented the data for atrazine, also in 10 mM *t-BuOH*, with a direct ozonation constant of 7.43 ± 0.11 M^{-1} s^{-1}, a result in good agreement with the value previously given by von Gunten [25]. As usual, boundaries represent 95% confidence intervals.

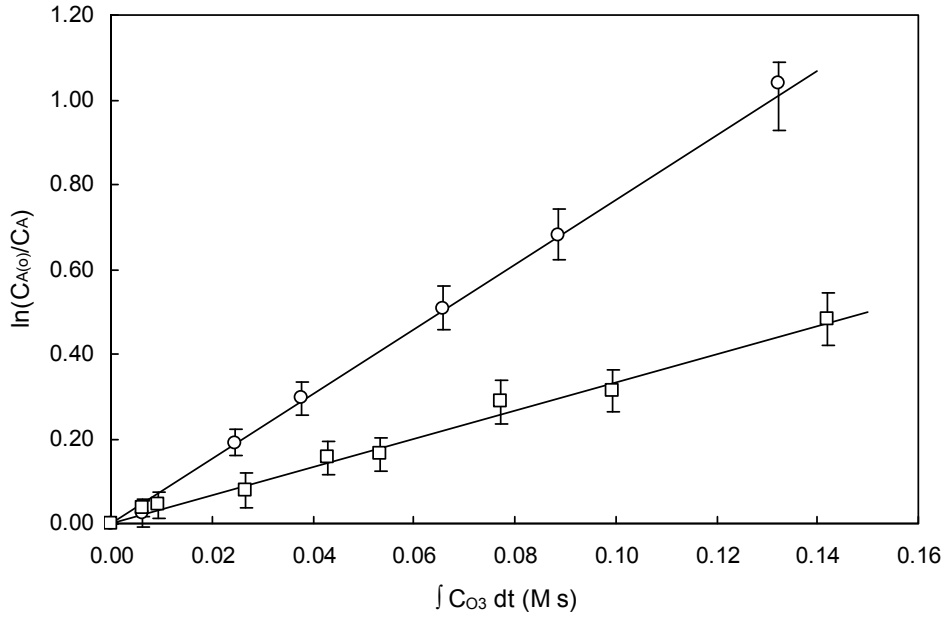

Fig. 5.1. Logarithmic decay of the concentration of fenofibric acid (□) and atrazine (○) in non-catalytic ozonation runs carried out with *t-BuOH* 10 mM as a function of integral ozone exposure (pH 6.5).

The well-known competition method was used with atrazine as reference compound. Assuming a constant hydroxyl radical-to-ozone ratio, the following expression can be derived:

$$\ln\left(\frac{c_{FFA(o)}}{c_{FFA(t)}}\right)=\frac{k^h_{O_3(FFA)}+k^h_{HO\bullet(FFA)}R^h_{ct}}{k^h_{O_3(ATZ)}+k^h_{HO\bullet(ATZ)}R^h_{ct}}\ln\left(\frac{c_{ATZ(o)}}{c_{ATZ(t)}}\right)=m\ln\left(\frac{c_{ATZ(o)}}{c_{ATZ(t)}}\right) \qquad (6)$$

As the direct ozonation rate constants for fenofibric acid and atrazine are low, a plot of $ln(c_{FFAo}/c_{FFA})$ versus $ln(c_{ATZo}/c_{ATZ})$ would yield a straight line with a slope $m = k^h_{HO\bullet(FFA)} / k^h_{HO\bullet(ATZ)}$; this also holds true for non-constant R^h_{ct} [26]. The values reported in the literature for the reaction of atrazine with hydroxyl radical are 3 x 10^9 M^{-1} s^{-1} [27], (2.54 ± 0.22) x 10^9 M^{-1} s^{-1} [28] and 2.4 x 10^9 M^{-1} s^{-1} [29]. Fig. 5.2 shows the experimental relationship the concentration decays of fenofibric acid and atrazine for runs performed in PBW. The value obtained in this study for $k^h_{HO\bullet(FFA)}$ was (6.55 ± 0.33) x

10^9 M^{-1} s^{-1}, which used the value of Balci et al. for $k^h_{HO\bullet(ATZ)}$, the only indicating uncertainty [28]. The boundaries represent 95% confidence intervals and take into account the experimental error for $k^h_{HO\bullet(ATZ)}$ indicated by Balci et al. [28].

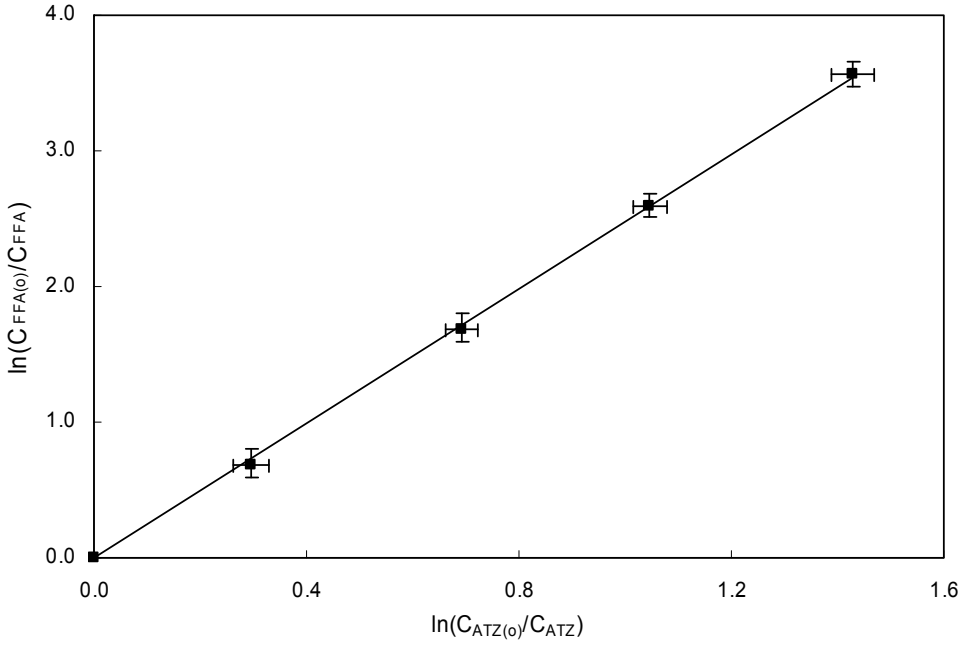

Fig. 5.2. Logarithmic plot of the concentration of fenofibric acid and atrazine in non-catalytic ozonation runs (pH 6.5).

Fig. 5.3 shows the conversion of fenofibric acid and atrazine as a function of integral ozone exposure. The data, particularly those for atrazine, indicate that k^h_R changed in the course of the run. In this case, instead of Eq. 5, a discrete form can be written for short time intervals as follows:

$$\ln\left(\frac{c_{ATZ(t)}}{c_{ATZ(t+\Delta t)}}\right) = \left(k^h_{O_3(ATZ)} + k^h_{HO\bullet(ATZ)}\,\overline{R}^h_{ct}\right)\int_t^{t+\Delta t} c_{O_3}\,dt \qquad (7)$$

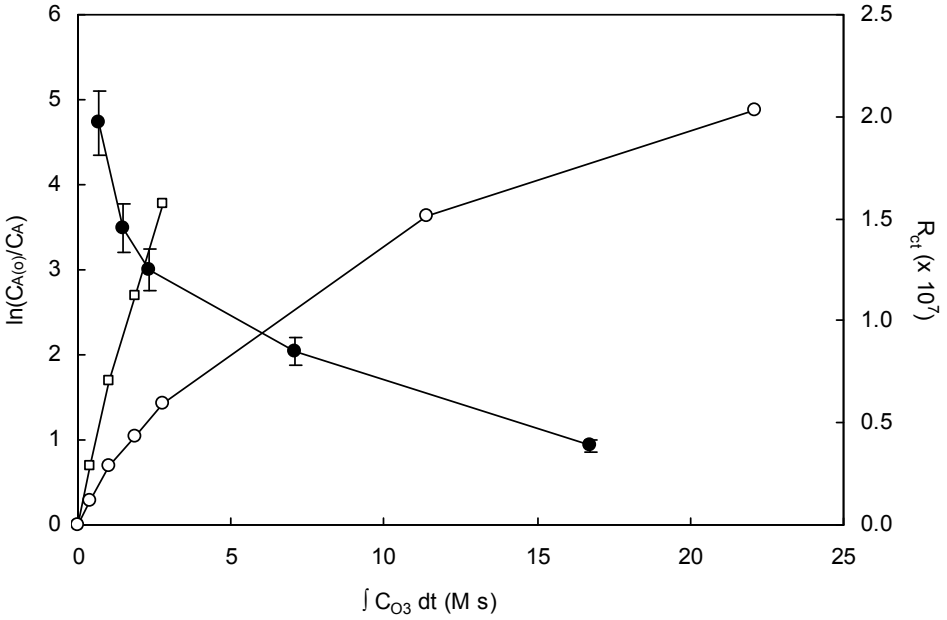

Fig. 5.3. Concentration of fenofibric acid (□) and atrazine(○) during a non-catalytic ozonation process as a function of the integral ozone exposure (pH 6.5). The secondary axis and filled circles represent the average R_{ct} values.

The value $\overline{R}_{ct}^{h}$ represents the average hydroxyl radical-to-ozone ratio within the interval (t, t + Δt) defined as follows:

$$\overline{R}_{ct}^{h} = \frac{\int_{t}^{t+\Delta t} R_{ct}\, c_{O_3}\, dt}{\int_{t}^{t+\Delta t} c_{O_3}\, dt} \tag{8}$$

The experimental set-up allowed accurate and continuous determination of the concentration of dissolved ozone and, therefore, of integral ozone exposure. The results for $\overline{R}_{ct}^{h}$ for the non-catalytic ozonation of fenofibric acid in PBW are also shown in Fig. 5.3 and range from 2 x 10^{-7} at the beginning of the run to 4.7 x 10^{-8} for an integral ozone exposure of 16.5 mM s.

In the experiments performed using wastewater, the reaction mixture was not loaded with phosphate buffer, the pH being controlled by the closed-loop control device described above. The wastewater was spiked with fenofibric and atrazine at the same initial concentrations indicated before. In this case, the logarithmic concentration decays of fenofibric acid and atrazine were linear, as shown in Fig. 5.4. The value of R_{ct}^{h} obtained from Eq. 6 was 9.4 x 10^{-10}, considerably lower than that obtained for pure water or PBW, but within the broad range of usual R_{ct} values, which typically fall in the 10^{-6}–10^{-10} range [30].

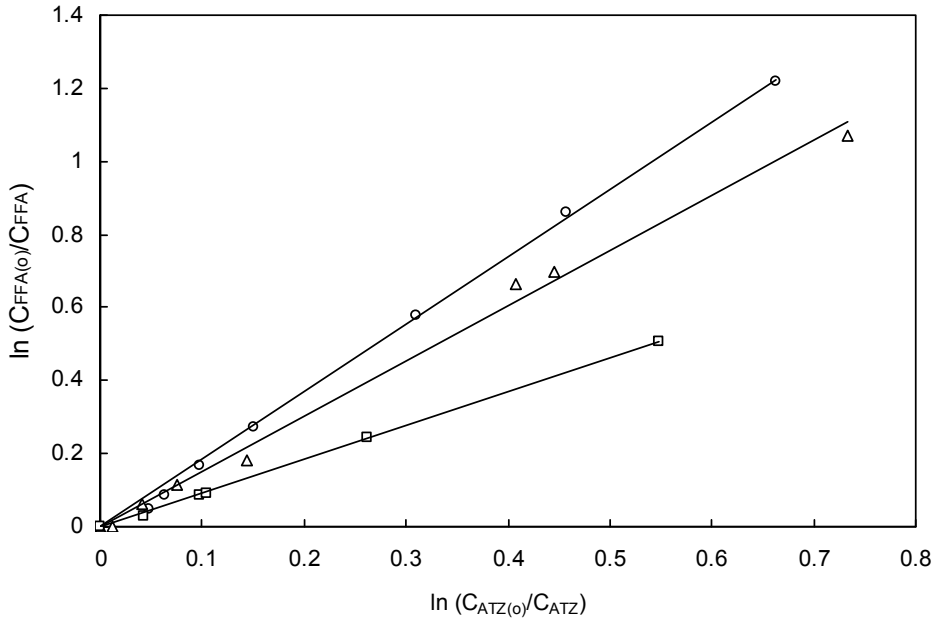

Fig. 5.4. Logarithmic plot of the concentration of fenofibric acid and atrazine in non-catalytic ozonation (□) and using 1 g/L Al_2O_3 (Δ) and 1 g/L MnO_x/Al_2O_3 (○) for initial concentration of fenofibric acid of 15 mg/L in wastewater. (pH 6.5; error bars not shown for clarity).

5.4.2. Catalytic ozonation

In catalytic ozonation, the reaction may take place between organic compounds and hydroxyl radicals with at least one of them being adsorbed. Assuming adsorption equilibrium and low surface coverage, the rate expression becomes linear with the concentration of adsorbate:

$$r_{FFA}^{c} = k_{O_3}^{c}\, c_{FFA}\, c_{O_3} + \left(k_{HO\bullet}^{h}\, R_{ct}^{h}\, c_{FFA}\, c_{O_3} + k_{HO\bullet}^{c}\, R_{ct}^{c}\, c_{FFA}\, c_{O_3} \right) \quad (9)$$

Details concerning the derivation of the former equation are given elsewhere [4, 18]. As stated above, fenofibric acid, even dissociated at the working pH, adsorbed to a very low degree. In addition, the catalysts has no significant effect on the direct ozonation constant in the presence of *t-BuOH*. Consequently, we assumed that the direct ozonation of fenofibric acid was a non-catalytic process and $k_{O_3(FFA)}^{c} = k_{O_3(FFA)}^{h}$.

Indirect ozonation is usually considered to be the combination of a homogeneous and a catalytic process. In this work we used atrazine to derive the hydroxyl radical-to-ozone ratio as indicated in Eq. 7. Atrazine is a neutral compound for which the amount adsorbed on both catalysts was not statistically significant whether in pure water, PBW or wastewater. Therefore, the experimental ratio R_{ct} was measured in the bulk in both catalytic and non-catalytic runs. As a consequence, R_{ct}^{h} and R_{ct}^{c} correspond to the same property and have been represented in what follows by the same symbol, R_{ct}^{hc}:

$$r_{FFA}^{c} = k_{O_3}^{c}\, c_{FFA}\, c_{O_3} + \left(k_{HO\bullet}^{h} + k_{HO\bullet}^{c} \right) R_{ct}^{hc}\, c_{FFA}\, c_{O_3} \quad (10)$$

Taking $k_{HO\bullet}^{hc}$ to denote the apparent kinetic constant for the reaction with hydroxyl radicals in the presence of catalyst, the kinetic equation yields the same mathematical form obtained before for homogeneous ozonation:

$$r_{FFA}^{c} = k_{O_3}^{h}\, c_{FFA}\, c_{O_3} + k_{HO\bullet}^{hc}\, R_{ct}^{hc}\, c_{FFA}\, c_{O_3} \quad (11)$$

The adsorption of reactive species should be reflected in significant differences between $k^{hc}_{HO\bullet}$ and $k^{h}_{HO\bullet}$, which can be checked by means of kinetic data. Combined with the mass balance and on integration, Eq. 11 leads to expressions formally identical to those derived for non-catalytic runs. The results corresponding to the catalytic ozonation of fenofibric acid in spiked wastewater using Al_2O_3 and MnO_x/Al_2O_3 are shown in Fig. 5.4. This plot, representing the competition kinetic method, was linear for both catalysts, but the change in slope for different catalysts and for catalytic runs with respect to non-catalytic ozonation does not necessarily mean that $k^{hc}_{HO\bullet}$ and $k^{h}_{HO\bullet}$ were different. This is shown in Fig. 5.5, where we plotted the slope *m* of Eq. 6 as a function of hydroxyl radical-to-ozone ratio, R_{ct}. The solid line corresponds to $k^{h}_{HO\bullet(FFA)}$ = 6.55 x 10^9 M^{-1} s^{-1}, measured for non-catalytic conditions, so that the results from non-catalytic runs are expected to be distributed along it. The dashed line represents an arbitrary 20% increase in $k^{h}_{HO\bullet(FFA)}$ with respect to the non-catalytic reaction. If the catalytic reaction with hydroxyl radicals involved adsorbed organics, it might be expected that the rate constant $k^{hc}_{HO\bullet}$ would differ from that of the homogeneous system, $k^{h}_{HO\bullet}$. By combining the results of $\overline{R}^{hc}_{ct}$ (Eq. 7) with *m* (Eq. 6), the points corresponding to catalytic and non-catalytic reactions can be located in Fig. 5. The results from catalytic ozonation in the wastewater matrix, represented as empty symbols, show that there was no significant difference between $k^{hc}_{HO\bullet}$ and the homogeneous ratio $k^{h}_{HO\bullet}$.

Stronger evidence may be obtained in a system with enhanced production of hydroxyl radicals, since in this case the discriminating capacity of the ration of rate constants, *m*, is higher. The symbols labelled 1-4 in Fig. 5.5 represent R_{ct}-*m* pairs for reactions carried out in PBW (1-3) and in non-buffered pure water (4). They show that the generation of hydroxyl radicals was considerably enhanced with respect to wastewater. Additionally, in PBW and pure water the hydroxyl radical-to-ozone ratio decreased during the run. The intervals listed in Table 2 and represented in Fig. 5.5 correspond to the first minute and to the period 6.5 ± 1.5 min respectively. For pure water, only the later is shown as there was no ozone in solution during the first 2 min.

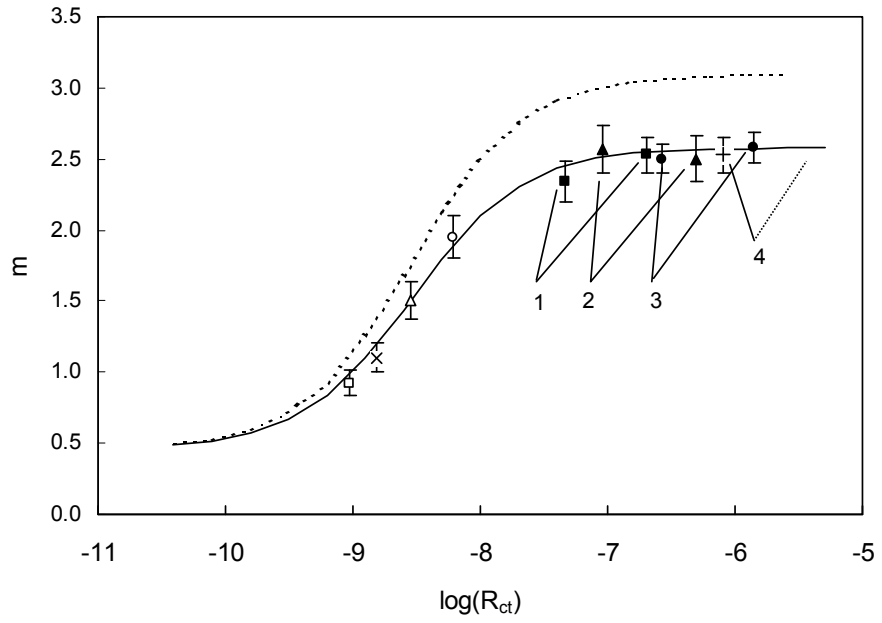

Fig. 5.5. Parameter *m* defined in Eq. 6 as a function of R_{ct} for non catalytic runs (□) and experiments using Al_2O_3 (Δ) and MnO_x/Al_2O_3 (○) in wastewater. Filled symbols represent the same runs in PBW: non-catalytic (1, ■), Al_2O_3 (2, ▲) and MnO_x/Al_2O_3 (3, ●). For these and also for MnO_x/Al_2O_3 (4, +) in pure -not buffered- water (4, +), the span represents the change in R_{ct} from the first minute to the average between 5-8 min. The cross (x) corresponds to ozonation PBW + 1.0 mM *t-BuOH* using MnO_x/Al_2O_3. pH was 6.5 in all cases.

In all cases the experimental value of *m* fell within the theoretical boundaries of $k^h_{HO\bullet(FFA)} / k^h_{HO\bullet(ATZ)} = 2.58 \pm 0.55$. This was true both for runs using MnO_x/Al_2O_3 and Al_2O_3, irrespective of the initial concentration of the organic compound, and for runs either in PBW or in pure water. This result shows no evidence that the catalysts contribute to an increase above its homogeneous value in the rate constant for the reaction between organics and hydroxyl radicals. The reason may be that the surface interaction with fenofibric acid, if any, was too small to activate the organic molecule through surface bonding. The hydroxyl radical-to-ozone ratio, however, was significantly improved by the use of catalysts. Table 5.2 shows that the use of Al_2O_3 increased the ratio by up to three times, whereas MnO_x/Al_2O_3 resulted in a seven-fold increase with respect to non-catalytic ozonation using the same substrate concentration. The values were similar in PBW and

wastewater, the latter also being reported in Table 5.2. Fig. 5.6 shows that in the absence of phosphate, the use of MnO_x/Al_2O_3, whether in PBW or pure water, did not change the slope *m* in Eq. 6. It may be argued that MnO_x/Al_2O_3's failure to affect the rate constant could be attributed to an inhibition of fenofibric acid adsorption due to the phosphate buffer. This behaviour was also observed in pure water making it plain that this is not the case.

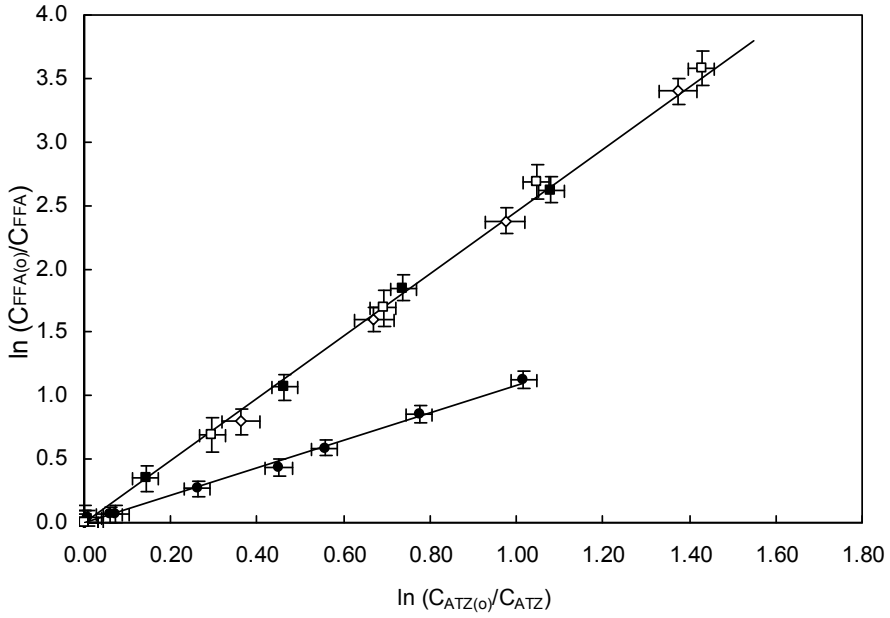

Fig. 5.6. Logarithmic plot of the concentration of fenofibric acid and atrazine in non-catalytic ozonation (□) and using 1 g/L MnO_x/Al_2O_3 in PBW (■), in PBW + 1.0 mM *t-BuOH* (●) and in pure non-buffered water (◊). pH was 6.5 in all cases.

Table 5.2. Rate constants for the decomposition of ozone and ratio of the concentration of hydroxyl radical to ozone in several matrixes (pH 6.5 in all cases).

Homogeneous first order kinetic constant for the decomposition of ozone (s^{-1})

	Non-catalytic	Al_2O_3	MnO_x/Al_2O_3
Pure water	$(3.16 \pm 0.35) \times 10^{-3}$	$(5.50 \pm 0.53) \times 10^{-3}$	$(8.82 \pm 0.46) \times 10^{-3}$
PBW	$(2.10 \pm 0.45) \times 10^{-3}$	$(2.48 \pm 0.61) \times 10^{-3}$	$(3.89 \pm 0.28) \times 10^{-3}$
Wastewater*	$(4.78 \pm 0.72) \times 10^{-3}$	$(5.14 \pm 0.55) \times 10^{-3}$	$(5.79 \pm 0.67) \times 10^{-3}$

Ratio of hydroxyl radical- to-ozone R_{ct}^{h} or $\overline{R}_{ct}^{hc}$

	Non-catalytic	Al_2O_3	MnO_x/Al_2O_3
Pure water (Av. 2-5 min)	-	-	8.2×10^{-7}
PBW (1st min)	2.0×10^{-7}	4.9×10^{-7}	1.4×10^{-6}
PBW (Av. 5-8 min)	4.7×10^{-8}	9.0×10^{-8}	2.7×10^{-7}
PBW + t-BuOH 1.0 mM	-	-	1.6×10^{-9}
Wastewater	9.4×10^{-10}	2.9×10^{-9}	6.2×10^{-9}

* Stopped ozone flow after 30 min of semicontinuous ozonation

The addition of *t-BuOH* 1.0 mM to PBW resulted in apparent kinetic constants that did not change throughout the run. These kinetic constants, k_R, were considerably greater than the direct ozonation constants, k_{O_3}, for fenofibric acid and atrazine, indicating that the amount of *t-BuOH* was insufficient to completely scavenge hydroxyl radicals; but they did not reach the high values of R_{ct} found during the first part of the ozonation runs in the absence of *t-BuOH*. Fig. 5.7 shows the evolution of the concentration of fenofibric acid and atrazine in the presence of *t-BuOH* 1.0 mM on MnO_x/Al_2O_3 as a function of the integral ozone exposure. The corresponding values of R_{ct} and *m* are also shown in Fig. 5.5 and again show no deviation from the solid line drawn using homogeneous rate constants.

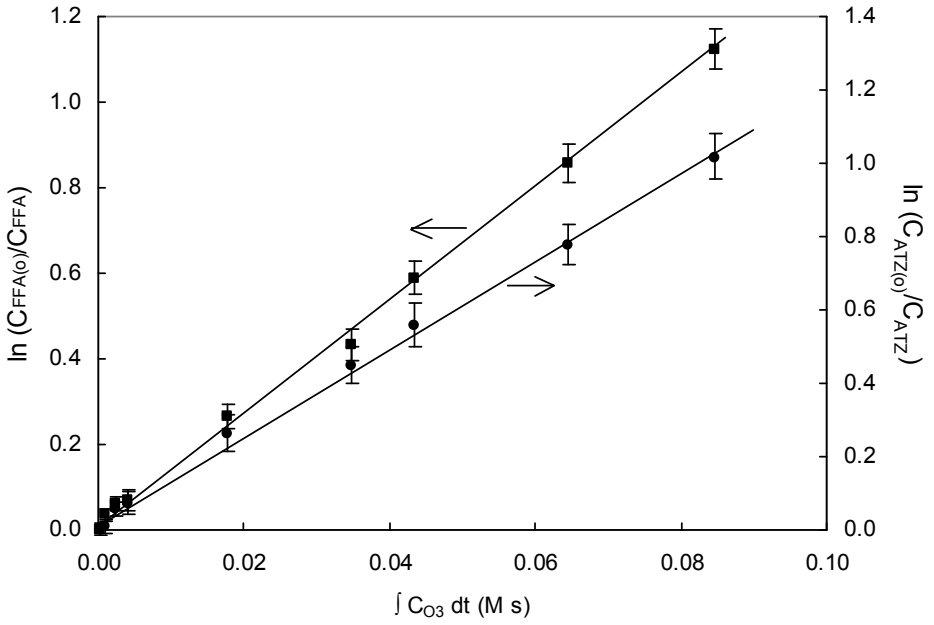

Fig. 5.7. Concentration of fenofibric acid (■) and atrazine(●) as a function of integral ozone exposure during catalytic ozonation using 1 g/L MnO_x/Al_2O_3 in PBW + 1.0 mM *t-BuOH*.

Fig. 5.8 plots the average hydroxyl radical-to-ozone ratio as a function of the concentration of fenofibric acid showing that R_{ct} was approximately linear with the concentration of fenofibric acid. This might be a consequence of a promoting effect of fenofibric acid or an ozonation by-product. It is well known that ozone decomposition, as well as the formation of radicals such as superoxide and hydroperoxyl, can be promoted by the presence of certain substances including compounds commonly found as ozonation by-products. In a previous study we identified 2-hydroxyisubutyric acid and some other acidic compounds to be ozonation by-products of clofibric acid, a fibrate with a relatively similar structure [31].

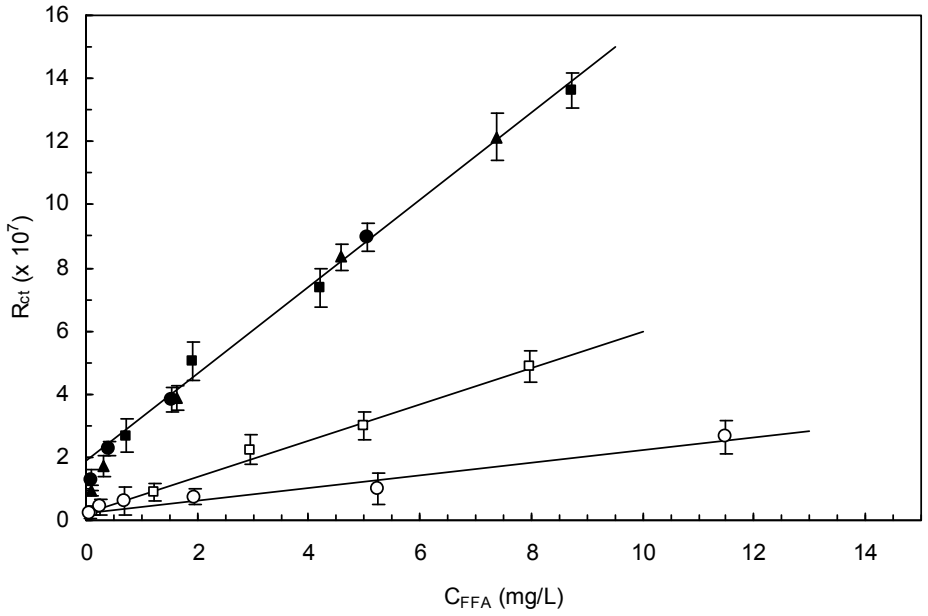

Fig. 5.8. Average hydroxyl radical-to-ozone ratio as a function of the average concentration of fenofibric acid for non-catalytic ozonation (○) and catalytic reaction using 1 g/L Al_2O_3 (□) both with 15 mg/L of initial concentration in PBW. Filled symbols correspond to ozonation with 1 g/L MnO_x/Al_2O_3 at initial concentration of fenofibric acid of 15 (■), 10 (▲) and 5 (●) mg/L in PBW. pH was 6.5 in all cases.

The role of catalytic surface in the heterogeneous decomposition of dissolved ozone was also studied by stopping the gas flow at a given time in order to record the concentration of ozone thereafter until total ozone depletion [18]. In wastewater runs, stopped-flow experiments were performed after 30 min of ozonation to ensure the absence of most reactive compounds. The kinetic constants expressed in pseudo-homogeneous units for a catalyst concentration of 1 g/L at pH 6.5 are shown in Table 5.2 for pure water, PBW and wastewater. In all cases the use of catalysts resulted in an increase of the ozone decomposition rate with greater differences in pure water, but following the same trend in PBW and wastewater. The results showed that both catalysts promoted ozone decomposition. Their effect on ozone decomposition was lower than their effect on promoting the generation of hydroxyl radicals. This is not necessarily contradictory, even considering the fact that the generation of hydroxyl radical stems from the decomposition of ozone, as both results refer to quite different situations: batch homogeneous ozone decomposition versus semicontinuous ozonation of organics while continuously bubbling ozone.

This increase in the hydroxyl-to-ozone ratio in catalytic runs supports the common assumption that surface hydroxyl groups formed from the interaction of water with catalyst sites may react with ozone to form a surface complex [12, 32]. On a similar basis, several authors have proposed that hydroxide ions linked to negatively charged surfaces initiate ozone decomposition and constitute the true active sites for catalytic ozonation [33, 34]. In this study, we have demonstrated that MnO_x/Al_2O_3, negatively charged at pH 6.5, increased the exposure to hydroxyl radicals to a considerably larger extent than activated alumina, whose isoelectric point is 8.2 and was positively charged. This result is consistent with the electrophilic character of the ozone molecule, although the influence of surface charge or the interaction with dissolved ozone is still not clear. The fact that the extent of adsorption did not differ significantly from zero (i.e.: within the uncertainty of the HPLC analytical method) is not fully incompatible with a reaction that takes place between adsorbed species. It is conceivable that a very low concentration of adsorbed fenofibric acid reacts very rapidly with adsorbed hydroxyl radicals but the low rate of adsorption observed in pure water experiments do not support this assumption. Neither does the

lack of effect of catalysts on the kinetic constant of hydroxyl-mediated ozonation.

5.5. Conclusions

Using the competition kinetic method, we determined a rate constant at 20ºC for the non-catalytic ozonation of fenofibric acid of 3.43 ± 0.20 M^{-1} s^{-1}. The rate constant for the reaction of fenofibric acid and hydroxyl radicals was (6.55 ± 0.33) x 10^9 M^{-1} s^{-1}. To our knowledge this is the first time that this rate constant has been reported.

The results of catalytic runs did not show any evidence that the use of Al_2O_3 or MnO_x/Al_2O_3 resulted in an increase in the indirect ozonation rate constant with respect to homogeneous ozonation. This fact suggests the absence of surface interaction with fenofibric acid and may probably indicate that its adsorption did not take place at all. Adsorption data also point in the same direction as neither fenofibric acid nor atrazine adsorb significantly on Al_2O_3 and MnO_x/Al_2O_3 when using PBW and wastewater. Ozonation runs in non-buffered pure water again showed that the tested catalysts had no effect on the indirect ozonation rate constant.

Hydroxyl radical-to-ozone ratio was significantly improved by the use of catalysts. An amount of 1 g/L of Al_2O_3 increased it up to three times whereas MnO_x/Al_2O_3 resulted in a seven-fold increase with respect to non-catalytic ozonation. This holds true for both PBW and wastewater, with a positive effect of both catalysts even in the presence of salts and radical scavengers. The higher rate of hydroxyl radical generation took place on the most active catalyst for the decomposition of dissolved ozone. This fact is consistent with the assumption that the catalysts promoted the generation of hydroxyl radicals, probably through the formation of surface complexes between ozone and surface hydroxyl groups, even if they do not interact significantly with organics.

5.6. Nomenclature

r_{FFA}	fenofibric acid oxidation rate in homogeneous units, mol L^{-1} s^{-1}
k_{O_3}	second order rate constant for direct ozonation reaction, L mol^{-1} s^{-1}
$k_{HO\bullet}$	second order rate constant for the reaction with hydroxyl radicals, L mol^{-1} s^{-1}
c_A	concentration of a given organic compound, mol L^{-1}
$c_{HO\bullet}$	concentration of hydroxyl radical, mol L^{-1}
c_{O_3}	concentration of dissolved ozone, mol L^{-1}
$c^*_{O_3}$	equilibrium concentration of dissolved ozone, mol L^{-1}
Ha	Hatta number, dimensionless
v	stoichiometric coefficient, dimensionless
k_R	second order apparent homogeneous rate constant, L mol^{-1} s^{-1}
D_{O_3}	ozone diffusivity, m^2 s^{-1}
k_L	liquid phase individual mass transfer coefficient, m s^{-1}
k_La	volumetric mass transfer, s^{-1}
R_{ct}	ratio of $c_{HO\bullet}$ to c_{O_3}, dimensionless
$\overline{R}_{ct}$	average value of R_{ct} defined in Eq. 8, dimensionless
m	parameter defined in Eq. 5, dimensionless

5.7. Subscripts and superscripts

FFA	fenofibric acid
ATZ	atrazine
o	initial
t	generic reaction time
*	equilibrium
h	homogeneous reaction
c	catalytic reaction
hc	simultaneous homogeneous and catalytic reaction

5.8. References

[1] M. Stumpf, T.A. Ternes, R.D. Wilken, S.V. Rodrigues, W. Baumann, Polar drug residues in sewage and natural waters in the state of Rio de Janeiro, Brazil, Sci. Total Environ. 225 (1999) 135–141.

[2] T.A. Ternes, J. Stüber, N. Herrmann, D. McDowell, A. Ried, M. Kampmann, B. Teiser, Ozonation: a tool for removal of pharmaceuticals, contrast media and musk fragrances from wastewater? Water Res. 37 (2003) 1976–1982.

[3] J.L. Acero, F.J. Benitez, A.I. Leal, F.J. Real, F. Teva, Membrane filtration technologies applied to municipal secondary effluents for potential reuse, J. Hazard. Mater. 177 (2010) 390-398.

[4] A. Rodríguez, R. Rosal, J.A. Perdigón, M. Mezcua, A. Agüera, M.D. Hernando, P. Letón, A.R. Fernández-Alba, E. García-Calvo, Ozone-based technologies in water and wastewater treatment, in: D. Barceló and M. Petrovic (Eds.), The Handbook of Environmental Chemistry, vol. 5, Part S/2, Emerging contaminants from industrial and municipal waste, Springer: Berlin, 2008, pp 127–175.

[5] R. Rosal, A. Rodríguez, J.A. Perdigón-Melón, A. Petre, E. García-Calvo, M.J. Gómez, A. Agüera, A.R. Fernández-Alba, Occurrence of emerging pollutants in urban wastewater and their removal through biological treatment followed by ozonation, Water Res. 44 (2010) 578-588.

[6] R. Rosal, I. Rodea-Palomares K. Boltes, F. Fernández-Piñas, F. Leganés, S. Gonzalo, A. Petre, Ecotoxicity assessment of lipid regulators in water and biologically treated wastewater using three aquatic organisms, Environ. Sci. Pollut. Res. 17 (2010) 135−144.

[7] I. Muñoz, A. Rodríguez, R. Rosal, A.R. Fernández-Alba, Life Cycle Assessment of urban wastewater reuse with ozonation as tertiary treatment. A focus on toxicity-related impacts, Sci. Tot. Environ. 407 (2009) 1245–1256.

[8] K. Ikehata, N.J. Naghashkar, M.G. El-Din, Degradation of aqueous pharmaceuticals by ozonation and advanced ozonation processes: A review, Ozone: Sci. Eng. 28 (2006) 353−414.

[9] B. Legube, Formation of ozonation by-products, in: A. Nikolay (Ed.) The Handbook of Environmental Chemistry, vol. 5, Part G,

Haloforms and Related Compounds in Drinking Water, Springer: Berlin 2003, pp. 95–116.

[10] F.J. Beltrán, F.J. Rivas, R. Montero, Mineralization improvement of phenol aqueous solutions through heterogeneous catalytic ozonation, J. Chem. Technol. Biotechnol. 78 (2003) 1225–1333.

[11] H. Einaga, S. Futamura, Catalytic oxidation of benzene with ozone over alumina-supported manganese oxides, J. Catal. 227 (2004) 304−312.

[12] L. Yang, C. Hu, Y. Nie, J. Qu, Catalytic Ozonation of Selected Pharmaceuticals over Mesoporous Alumina-Supported Manganese Oxide, Environ. Sci. Technol. 43 (2009) 2525–2529.

[13] B. Kasprzyk-Hordern, M. Ziolek, J. Nawrocki, Catalytic ozonation and methods of enhancing molecular ozone reactions in water treatment, Appl. Catal. B: Environ. 46 (2003) *46*, 639–669.

[14] C.M. Jonsson, C.L. Jonsson, D.A. Sverjensky, H.J. Cleaves, R.M. Hazen, Attachment of L -Glutamate to Rutile (□-TiO_2): A Potentiometric, Adsorption, and Surface Complexation Study, Langmuir, 25 (2009) 12127–12135.

[15] R. Rosal, A. Rodríguez, M.S. Gonzalo, E. García-Calvo, Catalytic ozonation of naproxen and carbamazepine on titanium dioxide, Appl. Catal. B: Environ. 84 (2008) 48–57.

[16] F.J. Beltrán, Ozone Reaction Kinetics for Water and Wastewater Systems, CRC Press LLC: Florida, 2004, pp. 124–125.

[17] M.O. Buffle, J. Schumacher, E. Salhi, M. Jekel, U. von Gunten, Measurement of the initial phase of ozone decomposition in water and wastewater by means of a continuous quench-flow system: Application to disinfection and pharmaceutical oxidation, Water Res. 40 (2006) 1884−1894.

[18] R. Rosal, A. Rodríguez, M.S. Gonzalo, E. García-Calvo, Ozonation of clofibric acid catalyzed by titanium dioxide, J. Hazard. Mater. 169 (2009) 411–418.

[19] P.H. Calderbank, M.B. Moo-Young, The continuous phase heat and mass transfer properties of dispersions, Chem. Eng. Sci. 16 (1961) 39–54.

[20] R. Rosal, A. Rodríguez, J.A. Perdigón-Melón, A. Petre, E. García-Calvo, Oxidation of dissolved organic matter in the effluent of a sewage treatment plant by ozone combined with hydrogen peroxide (O_3/H_2O_2), Chem. Eng. J. 149 (2009) 311−318.

[21] W.S. Kijlstra, E.K. Poels, A. Bliek, B.M. Weckhuysen, R.A. Schoonheydt, Characterization of Al_2O_3-supported manganese oxides by electron spin resonance and diffuse reflectance spectroscopy, J. Phys. Chem. B 101 (1997) 309–316.

[22] T. Morimoto, S. Kittaka, Isoelectric point of manganese oxide. Bull. Chem. Soc. Jpn. 47 (1974) 1586−1588.

[23] H. Einaga, M. Harada, S. Futamura, Structural changes in alumina-supported manganese oxides during ozone decomposition, Chem. Phys. Lett. 408 (2005) 377–380.

[24] M.S. Elovitz, U. von Gunten, Hydroxyl radical/ozone ratios during ozonation processes. I. The Rct concept, Ozone Sci. Eng. 21 (1999) 239–260.

[25] U. von Gunten, Ozonation of drinking water: Part I. Oxidation kinetics and product formation, Wat. Res. 37 (2003) 1443–1467.

[26] F.J. Beltrán, J.F. Garcia-Araya, P.M. Alvarez, F.J. Rivas, Aqueous degradation of atrazine and some of its main by-products with ozone/hydrogen peroxide, J. Chem. Technol. Biotechnol. 71 (1998) 345−355.

[27] J.L. Acero, K. Stemmler, U. von Gunten, Degradation kinetics of atrazine and its degradation products with ozone and OH radicals: a predictive tool for drinking water treatment, Environ. Sci. Technol. 34 (2000) 591–597.

[28] B. Balci, N. Oturan, R. Cherrier, M.A. Oturan, Degradation of atrazine in aqueous medium by electrocatalytically generated hydroxyl radicals. A kinetic and mechanistic study, Water Res. 43 (2009) 1924–1934.

[29] G.U. Buxton, C.L. Greenstock, W.P. Helman, A.B. Ross, Critical review of rate constants for reactions of hydrated electrons, hydrogen atoms and hydroxyl radicals ($HO^{\bullet}/O^{\bullet -}$) in aqueous solution, J. Phys. Chem. Ref. Data 17 (1988) 513–886.

[30] N.K. Vel Leitner, B. Roshani, Kinetic of benzotriazole oxidation by ozone and hydroxyl radical. Water Res. 44 (2010) 2058–2066.

[31] R. Rosal, M.S. Gonzalo, K. Boltes, P. Letón, J.J. Vaquero, E. García-Calvo, Identification of intermediates and ecotoxicity assessment of the oxidation products generated during the ozonation of clofibric acid. J. Hazard. Mater. 172 (2009), 1061−1068.

[32] H. Jung, H. Choi, Catalytic decomposition of ozone and para-Chlorobenzoic acid (pCBA) in the presence of nanosized ZnO, Appl. Catal. B: Environ. 66 (2006) 288–294.

[33] J. Ma, N.J.D. Graham, Degradation of atrazine by manganese-catalysed ozonation: Influence of humic substances, Water Res. 33 (1999) 785–793.

[34] F.J. Belltrán, J. Rivas, P. Álvarez, R. Montero, Kinetics of heterogeneous catalytic ozone decomposition in water on an activated carbon, Ozone: Sci. Eng. 24 (2002) 227−237.

CHAPTER 6

CATALYTIC OZONATION OF ATRAZINE AND LINURON ON MNO_X/AL_2O_3 AND MESOPOROUS MNO_X/SBA-15 IN A FIXED BED REACTOR

(Chemical Engineering Journal, In Press, 2010)

6. Catalytic ozonation of atrazine and linuron on MnO_x/Al_2O_3 and mesoporous MnO_x/SBA-15 in a fixed bed reactor

(Chemical Engineering Journal, In Press, 2010)

6.1. Abstract

The catalytic ozonation of the herbicides atrazine and linuron was studied in a fixed-bed reactor using alumina-supported manganese oxide catalysts. Two manganese oxides were supported, one on activated alumina, MnO_x/Al_2O_3, the other, MnO_x/SBA-15, after impregnating mesoporous silica by the minimum volume method. The adsorption of both compounds was not significant and the kinetic data indicated that the reaction with molecular ozone was a non-catalytic process which took place in homogeneous phase. The results of catalytic runs also showed no evidence that any of the catalysts increased the rate of the hydroxyl-mediated ozonation. Both catalysts, however, considerably increased the ozone decomposition rate constant, particularly MnO_x/SBA-15 for which a MnO_x bed load of 1.0% wt. as MnO_2 resulted in a 30 fold increase with respect to the homogeneous rate. The catalysts also improved the efficiency in the production of hydroxyl radicals from ozone with an average hydroxyl radical-to-ozone ratio as high as 10^{-6} for MnO_x/Al_2O_3 and 3.0 x 10^{-6} for MnO_x/SBA-15. The catalysts also led to a lower ozone consumption per mole of converted organic compound, whether or not bicarbonate was present in the solution. Best results were obtained in all cases for MnO_x/SBA-15, most probably due to a better distribution of the active phase on a larger surface.

Keywords: Heterogeneous catalytic ozonation; Fixed bed; Manganese oxide; SBA-*15* supported catalyst*; Hydroxyl radicals.*

6.2. Introduction

There is a growing need for treatment technologies that can provide safe treated effluents from wastewater treatment plants (WWTP) in order to enhance wastewater reuse. Organic compounds, particularly those belonging to emerging groups such as pharmaceuticals and personal care products, severely endanger water reuse in many applications even if they are present in very low amounts. Besides affecting reuse strategies, micropollutants from WWTP are currently discharged to surface bodies, thus jeopardising the environmental protection of water bodies. In this regard, Member States of the European Union have been urged to introduce policies under the EC Water Framework Directive with a view to achieving good ecological water status in terms of the presence of chemicals from human activity in a period covering fifteen years from 2015, the date this Directive comes into force [1].

The available technologies for the removal of micropollutants include many oxidation processes carried out alone or in combination with membrane separations. A wide variety of oxidation processes have been proposed for the removal of organic compounds from WWTP, most of them belonging to the category of advanced oxidation processes (AOP). AOP are those oxidation processes based on the generation of highly reactive species, particularly hydroxyl radicals, whose use has been proposed for the degradation of many classes of organic compounds, especially when their chemical stability makes them difficult to degrade otherwise [2]. AOP is a growing family of technologies that differ in the way they generate the primary oxidant species, the hydroxyl radical. They include a number of combined processes in which the simultaneous use of several technologies aims at increased economic efficiency or better suitability to certain streams [3, 4].

Among them, considerable research effort has recently been centred on investigating heterogeneous catalytic ozonation. In this process, a solid catalyst may (i) adsorb and decompose ozone, thereby leading to the formation of active species which then react with non-chemisorbed

organics; and (ii) adsorb organic molecules with further reaction with oxidants either adsorbed and surface-generated or from the bulk [5]. Apart from these general ideas, the exact mechanism of catalytic ozonation is still not clear. In metals or metal oxides, the catalytic reaction might involve the adsorption of organic molecules or ions with subsequent oxidation by Eley-Rideal or Langmuir-Hinshelwood interaction with oxidant species. It is well known that the adsorption of neutral compounds on oxides in aqueous solutions has to overcome the competitive adsorption of water molecules and that adsorption is relatively favoured for ionizable compounds if the surface is charged [5]. Although it is generally true that the extent of adsorption considerably decreases under the unfavourable electrostatic conditions that take place on charged surfaces, it has been pointed out that small but significant adsorption may occur even in this case through surface complexation reactions [6]. In a previous paper, we determined that the use of Al_2O_3 or MnO_x/Al_2O_3 catalysts did not result in an increase in the indirect ozonation rate constant of fenofibric acid with respect to homogeneous ozonation, a fact that suggests the absence of surface interaction with fenofibric acid, a compound completely dissociated in working conditions [7].

The use of three-phase beds for heterogeneous catalytic ozonation was originally developed as part of the Ecoclear process, and originally intended for the use of granular activated carbon (GAC) to remove chlorinated hydrocarbons in contaminated groundwater [8]. From then on, most applications of catalytic ozonation which used fixed or fluidized beds were linked to GAC or metal/metal oxides supported on GAC. [9, 10]. Recently, there have been reports of the use of activated carbon fibers for the ozonation of phenol in an aqueous fluidized bed reactor in which a significant reduction of the isoelectric point (IEP) of the surface took place as a consequence of the production of surface oxygen-containing groups [11]. Contrary to agitated reactors, that exhibit a high liquid-to-catalyst ratio, fixed-bed reactors can limit parallel homogeneous reactions such as polymerisation or the formation of other by-products. In this work, we studied the ozonation of the herbicides atrazine and linuron, two non-polar pollutants commonly encountered in wastewater from agricultural activities. The complexity of gas-liquid-solid reactions is a well-known factor that complicates the use of reactors operating in packed-bubble or trickle-bed modes. Accordingly, in this work we used a two-phase heterogeneous catalytic reactor operating with an ozone-preloaded aqueous buffer that

facilitated our goal of studying the efficiency of production of hydroxyl radicals of two manganese-based catalysts using a low-liquid-to-catalyst ratio. For this purpose we compared a classic manganese oxide supported on activated alumina with a mesoporous MnO_x/SBA-15 catalyst.

In spite of the considerable research in the field of catalytic ozonation performed during last years, the mechanism of catalytic processes is still essentially unknown. It has been demonstrated that several catalysts enhance the efficiency of ozonation but the mechanism of this process, particularly concerning the production of hydroxyl radicals, is required prior to introduce this technique to water treatment at an industrial scale. There are two major gaps in understanding catalytic ozonation. First, is not completely clear whether catalysts cause ozone decomposition leading to the formation of hydroxyl radicals. Some recent papers used electron paramagnetic resonance to show that the presence of metal oxides accelerates the generation of hydroxyl radicals during ozonation [12]. However, there is still no direct evidence of ozone adsorption on metal oxides in the presence of water and whether the decomposition of ozone leads to the formation of surface-bound radicals or other surface oxidizing species [13]. Second, it is not known whether the adsorption of organics on the surface of catalyst plays a role in the process. Certain authors reported high adsorption of organic molecules on catalysts, but the presence of salts and other competing compounds makes it difficult to assess the importance of the adsorption of organic molecules during catalytic ozonation.

The purpose of our work was to use kinetic data to determine whether the adsorption of organic molecules results or not in an interaction between adsorbate and catalytic surface leading to an energetically favoured pathway. Besides, this study aimed to determine the influence of MnO_x on the increase of hydroxyl radicals produced from ozone and the effect of a greater surface dispersion of the oxide when using SBA as support instead of activated alumina.

6.3. Materials and methods

6.3.1 Materials

Atrazine, linuron, potassium indigotrisulfonate and sodium thiosulfate were high-purity analytical grade reagents supplied by Sigma-Aldrich. The formulation of buffers and pH adjustments were made with analytical grade reagents from Merck or Sigma-Aldrich. MiliQ ultrapure water with a resistivity of at least 18 MΩ cm at 25ºC was obtained from a Milipore system.

The heterogeneous catalysts used in this study were alumina supported manganese oxide (MnO_x/Al_2O_3) and manganese oxide supported on mesoporous SBA-15. As to the former, the activated alumina was purchased from Sigma-Aldrich and used as received. It is an activated porous aluminium oxide, with a surface area of 155 $m^2\ g^{-1}$, determined by nitrogen adsorption, and an average particle size of 100 μm. The MnO_x/Al_2O_3 catalyst was prepared by incipient wetness impregnation of the aforementioned dried Al_2O_3 using an aqueous solution of $Mn(CH_3COO)_2{\cdot}4H_2O$ (Sigma-Aldrich). The catalyst was subsequently dried in air at 423 K and calcined at 773 K for 3 hours. The catalyst was washed twice in phosphate buffered water (PBW) to avoid further leaching of manganese. The amount of manganese corresponded to a 10.2% wt. expressed as MnO_2 and calculated by weight difference after washing and calcination. The BET surface area was 119 m^2/g for the manganese oxide catalyst with an average pore size of 6 nm which has been calculated using the Broekhoff and de Boer (BdB) method.

MnO_x/SBA-15 was prepared by the impregnation of silica SBA-15. The method of obtaining silica SBA-15 was as follows. Pluronic P123 (Aldrich $EO_{20}PO_{70}EO_{20}$, EO: ethylene oxide, PO: propylene oxide, MW = 5800) and tetraethoxysilane (TEOS 98% GC Aldrich) were used as received. In a typical synthesis, 6 g of Pluronic P123 were stirred at 308 K in 45 g of water and 180 g of 2 M HCl solution until total dissolution. TEOS (12.5 g) was added to the solution and stirred at 308 K for 20 hours. The mixture was aged at 373 K for 24 hours. The white powder was recovered through filtration, washed with water and dried at 323 K overnight. The product was calcined at 773 K for 12 hours with a heating rate of 1 K min^{-1}. The impregnation of the SBA-15 was carried out by the minimum volume

method. In a typical impregnation the desired amount of manganese precursor, Manganese nitrate tetrahydrate (Fluka) 2.01 g was dissolved in 30 mL of water and the solution poured slowly over 5 g of calcined SBA-15 while being stirred. The stirring was continuous for 10 hours and the solid dried out at 323 K overnight. The catalyst was activated under calcinations at 773 K for 12 hours, with heating rate of 1 K min^{-1}. The prepared catalysts presented 11.9% wt of MnO_2 measured after washing with PBW and calcination. MnO_x/SBA-15 had a particle size of 1.3 ± 0.2 μm as determined by DLS using a Malvern Zetasizer instrument. BET surface area was 650 m^2/g as measured by nitrogen adsorption. We obtained a narrow pore size distribution around 5 nm using the BdB method.

The IEP of catalysts was obtained by measuring the ζ-potential in aqueous solutions at 25ºC and at various pH values after adjusting ionic strength to 10^{-3} M with NaCl. The value of IEP for MnO_x/Al_2O_3 as prepared was 7.3, which fell to 3.0 after contact with bubbling ozone in aqueous slurry for 30 min. For MnO_x/SBA-15 ζ-potential was low at working conditions, with a value of -1.3 ± 0.8 mV at pH 6.5 indicating an almost neutral surface that became negatively charged after contact with bubbling ozone. The decrease of ζ-potential during ozonation could be attributed to the production of negatively-charged surface oxygen-containing groups [11], but it is also relevant for the possible adsorption of organics through ion-exchange.

6.3.2. Ozonation procedure

The runs were performed using ozone stock solution stored in a tank kept at 25ºC in which ozone was continuously bubbled using a diffuser. The stock was kept at pH 6.5 using 0.1 M PBW. The reason for using phosphate buffer was to ensure a constant pH inside the reactor where external adjustments are not possible. pH in the feed tank was continuously monitored by means of a Eutech alpha-pH100 feed-back control device. The concentration of ozone in the stock tank varied in the 5.0-10.0 mg/L range according to the prescribed dose for each run. The ozone solution was delivered to the reactor at a flow-rate of 2.0-4.5 mL/min using a HPLC Shimadzu pump. The experiments were conducted using stock solutions of 4.5 mg/L of atrazine (20.9 mM) and 5.0 mg/L of linuron (20.1 mM) at a flow-rate of 0.6-1.6 mL/min, which represented a maximum dilution factor of 7.5 in the PBW charged with ozone. The solution containing organics was delivered using a Harvard Dual Syringe Pump, which also pumped the quenching agent that stopped reaction.

In preliminary runs, we monitored the temperature and the inlet, outlet and inside the bed with no significant deviations (± 1.5 ºC) from the stock temperature of 25 ºC. The tee located at the reactor head was provided with two PVDF internal tubes in order to avoid the mixing of ozone charged water with the solution containing the organic reagent before reaching the catalytic bed. Details on the experimental set-up are given in Fig. 6.1.

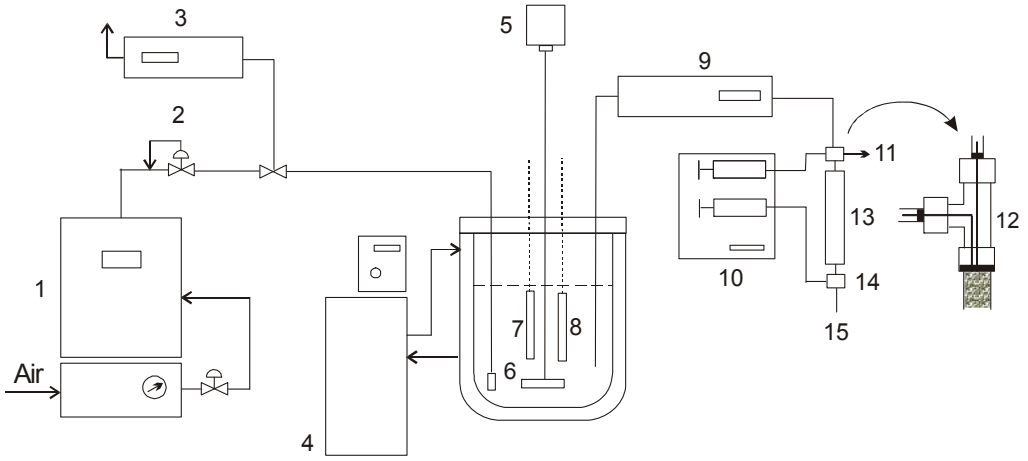

Fig. 6.1. Experimental equipment: 1, ozone generator; 2, flow control; 3, gas-phase UV ozone analyser; 4, thermostatic unit; 5, stirrer; 6, gas diffuser; 7, ozone amperometric sensor; 8, pH electrode; 9, HPLC pump; 10, dual-channel syringe pump; 11, sampling device; 12, detail of tubing inserts; 13, fixed-bed reactor; 14, low dead-volume mixer, 15, sampling device.

All reactions were performed with an excess of ozone. The residual oxidant in the exit mixture was quenched with the indigo reagent so that the reaction immediately stopped and the concentration of ozone could be determined. As an alternative, sodium thiosulfate was used for ozone quenching to ensure the absence of interferences in HPLC measurements. The length of the columns filled with catalyst was either 90 or 50 mm with an inside diameter or 4.6 mm. Both MnO_x/Al_2O_3 and MnO_x/SBA-15 were diluted with Al_2O_3 and SBA-15 of the same granulometry at 2.5% and 10%, leading to 0.25% and 1.0% of MnO_2 with respect to the whole bed. For higher loads, and due to the low liquid-to-catalyst ratio used in this work, no residual ozone could be observed in the exit stream. In all cases, after establishing the desired flow-rates, the concentration of ozone at the reactor inlet was determined using a sample valve as indicated below. All runs using the same concentration of catalyst were performed with the same column, which had been

preconditioned with ozone for at least 2 h before performing the first measurement. By periodically checking with reference conditions, no loss of efficiency or deactivation could be measured for any of the catalytic beds used in this work during their service period. Additional bath runs were performed to determine the rate constants for direct ozonation in the presence of t-BuOH following a procedure described elsewhere [7].

6.3.3. Analyses

The concentration of ozone dissolved in the aqueous phase was monitored with an amperometric Rosemount 499AOZ analyzer periodically calibrated using the Indigo Colorimetric Method (SM 4500-O3 B). The same colorimetric method was used to determine the ozone at the reactor inlet and outlet. The analyses of atrazine and linuron were performed by HPLC using a Hewlett Packard 1200 Series device (Agilent Technologies, Palo Alto, USA) equipped with a reversed phase Kromasil 5u 100A C18 analytical column. The mobile phase was a mixture of acetonitrilo (60%) and water (40%). UV detection was carried out at 210 nm (linuron) and 228 nm (atrazine). Nitrogen adsorption isotherms were measured at 77 K using a Beckman-Coulter SA3100 system on samples that were previously outgassed overnight at 200ºC.

6.4. Results and discussion

It is well known that the presence of particles smoothes out the laminar velocity profile and results in a uniform profile provided that the wall effects and axial dispersion are negligible. The effect of higher bed porosity in the vicinity of the reactor wall can be neglected if the ratio of the reactor diameter to the particle diameter is larger than 10. Similarly, the axial dispersion can be neglected by using a ratio of reactor length to particle diameter of over 50 [14]. In this work and for the most unfavourable case the aforementioned ratios were 44 and 480 respectively. Bed porosity was estimated in line with Haughey and Beveridge [15].

Prior to ozonation runs, the adsorption of atrazine and linuron was assessed in batch runs. After 24 h in contact with any of the catalysts used in this work, the amount adsorbed was below statistical significance in PBW. In a previous work we obtained similar results for fenofibric acid on

MnO_x/Al_2O_3 both in PBW and wastewater [7]. Other studies have reported the lack of significant adsorption of organics on various catalysts including supported manganese oxide at several pH values, a result which may suggest that the reaction probably occurs mainly in the aqueous phase and not on the catalyst surface [16].

The rate of depletion of a given organic compound in an ozonation process is the consequence of its second order parallel reaction with dissolved ozone and with hydroxyl radicals as indicated in Eq. 1. According to Elovitz and von Gunten's hypothesis, the ozonation process is characterized by R_{ct}, the ratio of the concentration of hydroxyl radicals and ozone, that represents the efficiency of the system in generating hydroxyl radicals [17].

$$r_A\left(mol\,L^{-1}\,s^{-1}\right) = k^h_{O_3}\,c_A\,c_{O_3} + k^h_{HO\bullet}\,c_A\,c_{HO\bullet} = \left(k^h_{O_3} + k^h_{HO\bullet}\,R^h_{ct}\right) c_A\,c_{O_3} \qquad (1)$$

The preceding equation has been written in homogeneous units; a superscript "h" indicating homogeneous reaction. In what follows we assumed an average value for the ratios R_{ct} and R^c, the last defined below. Although both parameters may change during an ozonation reaction, the conversion of atrazine and linuron was in all cases low enough to accept that these values could be representative of the first part of the ozonation, where there is still a considerable amount of the parent compounds in solution. Additional details on this point are given elsewhere [7]. In the presence of a solid catalyst, the rate of ozonation is also the result of parallel direct and hydroxyl-mediated oxidation on the catalyst surface in a reaction that may involve adsorbed species. Assuming adsorption equilibrium and low surface coverage, the rate expression becomes linear with the concentration of organic adsorbate [18]. The interaction of ozone and catalytic surface has been shown to increase the amount of surface hydroxyl groups that have been recognized as the active sites for ozone decomposition on transition metal oxides [19]. As a consequence of this interaction, ozone-adsorbed species $S\text{-}OH(O_3)_s$ or the product of the evolution of hydroxyl radicals or oxygen, $S\text{-}O_3^{\bullet}$ or $S\text{-}O^{\bullet}$ respectively, where “S” refers to surface of the catalyst [16]. The primary formation of oxidised surface sites in then due to the following reaction:

$$O_3 + S - OH \overset{K}{\rightleftarrows} S - OH\left(O_3\right)_s \qquad (2)$$

Considering this equilibrium, and c_s being the concentration of surface sites available for ozone binding, is, the concentration of dissolved ozone determines the amount of oxidised surface sites [20]:

$$c_{(O_3)_s} = K\, c_{O_3}\, c_s = \frac{K\, c_{O_3}\, c_t}{1 + K\, c_{O_3}} \tag{3}$$

where c_t is the total concentration of surface sites and it was assumed that the adsorption of organics do not interfere with the interaction of the surface with ozone. For $K\, c_{O_3} >> 1$, Eq. 3 reverts to an expression similar to the definition of R_{ct} in homogeneous systems in which we considered that the concentration of dissolved ozone at the catalyst surface equals the ozone concentration in the bulk doe to its low reaction rate:

$$c_{(O_3)_s} = R^c\, c_{O_3} \tag{4}$$

Without loss of generality, $c_{(O_3)_s}$ may be substituted by the concentration of oxidized surface, c_{ox}, sites yielding the following overall rate constant expression for a catalytic process:

$$\begin{aligned} r_A^c \left(mol\, kg^{-1}\, s^{-1} \right) &= k_{O_3}^c\, c_A\, c_{O_3} + k_{ox}^c\, c_A\, c_{ox} = k_{O_3}^c\, c_A\, c_{O_3} + k_{ox}^c\, R^c\, c_A\, c_{O_3} = \\ &\left(k_{O_3}^c + k_{ox}^c\, R^c \right) c_A\, c_{O_3} \end{aligned} \tag{5}$$

where the superscript "c" stands for catalytic reactions. This equation is valid either for the interaction with an organic molecule in the liquid phase by an Eley-Rideal mechanism or for the reaction between adsorbed species provided the adsorption equilibrium constant is low [18]. The rate of ozonation can be obtained combining Eqs. 1 and 5 and expressed in heterogeneous units are as follows:

$$\begin{aligned} r_A &= \left(\frac{\varepsilon}{\rho_b}\, k_{O_3}^h + k_{O_3}^c \right) c_A\, c_{O_3} + \left(\frac{\varepsilon}{\rho_b}\, k_{HO\bullet}^h\, c_{HO\bullet} + k_{ox}^c\, c_{ox} \right) c_A = \\ &\left(\frac{\varepsilon}{\rho_b}\, k_{O_3}^h + k_{O_3}^c + \frac{\varepsilon}{\rho_b}\, k_{HO\bullet}^h\, R_{ct}^h + k_{ox}^c\, R^c \right) c_A\, c_{O_3} = k_1\, c_A\, c_{O_3} \end{aligned} \tag{6}$$

where ε and ρ_b are bed porosity and bulk density respectively. The decomposition of ozone also takes place following parallel catalytic and homogeneous processes.

$$r_{O_3}\left(mol\,kg^{-1}\,s^{-1}\right)=\frac{\varepsilon}{\rho_b}r_{O_3}^{h}+r_{O_3}^{c}=\frac{\nu\,\varepsilon}{\rho_b}k_{o_3}^{h}\,c_A\,c_{O_3}+\nu\,k_{o_3}^{c}\,c_A\,c_{O_3}+\frac{\varepsilon}{\rho_b}k_d^{h}\,c_{O_3}+k_d^{c}\,c_{O_3}$$

$$=\nu\left(\frac{\varepsilon}{\rho_b}k_{o_3}^{h}+k_{o_3}^{c}\right)c_A\,c_{O_3}+\left(\frac{\varepsilon}{\rho_b}k_d^{h}+k_d^{c}\right)c_{O_3}=k_2\,c_A\,c_{O_3}+k_3\,c_{O_3} \qquad (7)$$

where v is the stoichiometric coefficient for the direct reaction between the organic compound and ozone. The mass balance to a differential reactor volume yields the following equations:

$$\frac{dW}{F_o}=-\frac{dc_A}{r_A} \qquad (8)$$

$$\frac{dW}{F_o}=-\frac{dc_{O_3}}{r_{O_3}} \qquad (9)$$

The combination of the integrated forms of the preceding equations with the expanded forms of r_A and r_{O_3} allows the experimental determination of the constants k_1, k_2 and k_3, which represent a combination of the fundamental kinetic parameters governing the ozonation process, as explained below. The mass balance to a differential reactor volume can also be expressed as follows:

$$\frac{dc_A}{dc_{O_3}}=\frac{r_A}{r_{O_3}}=\frac{k_1\,c_A\,c_{O_3}}{k_2\,c_A\,c_{O_3}+k_3\,c_{O_3}} \qquad (10)$$

If there are more than one organic oxidizable compound, a similar equation can be written for both, which is the basis of the competitive method of kinetic analysis

$$\frac{dc_A}{dc_B}=\frac{r_A}{r_B} \qquad (11)$$

In a first series of runs, we determined the rate of catalytic decomposition of ozone in the absence of organic compounds. The rate constant for the homogeneous decomposition of ozone in PBW was determined in semicontinuous experiments using PBW previously loaded with ozone and following a procedure described elsewhere [21]. The value obtained was k_d^h = (2.10 ± 0.45) x 10^{-3} s^{-1}. The value of k_d^c, derived from Eq. 4, was 0.0044 ± 0.00020 L kg^{-1} s^{-1} for Al_2O_3 and 0.0023 ± 0.0031 L kg^{-1} s^{-1} for SBA-15, where the boundaries represent 95% confidence intervals, the last not differing significantly from zero. The incorporation of manganese forming MnO_x/Al_2O_3 or MnO_x/SBA-15 resulted in a considerable increase in the catalytic rate of ozone decomposition as shown in Fig. 6.2. With 10% MnO_x/SBA-15 (1.0 % wt. of bed as MnO_2), the kinetic constant increased up to 0.123 ± 0.004 L kg^{-1} s^{-1}. Expressed in pseudo-homogeneous units (s^{-1}) this amounts a 30 fold increase with respect to the constant for non-catalytic ozone decomposition. The corresponding kinetic constant for MnO_x/Al_2O_3 loaded with 10% MnO_2 (1.0% wt. of bed as MnO_2) was 0.0155 ± 0.0015 L kg^{-1} s^{-1}. The relative efficiency for ozone decomposition of MnO_x/SBA-15 and MnO_x/Al_2O_3 is somewhat larger than that expected from their respective surface areas. This may reflect a better dispersion of MnO_x on silica, probably as a consequence of the differences in the metal oxide-support interaction. Moreover, the uniform pore-size distribution in the ordered mesoporous materials could allow for a better particle size control of the active phase.

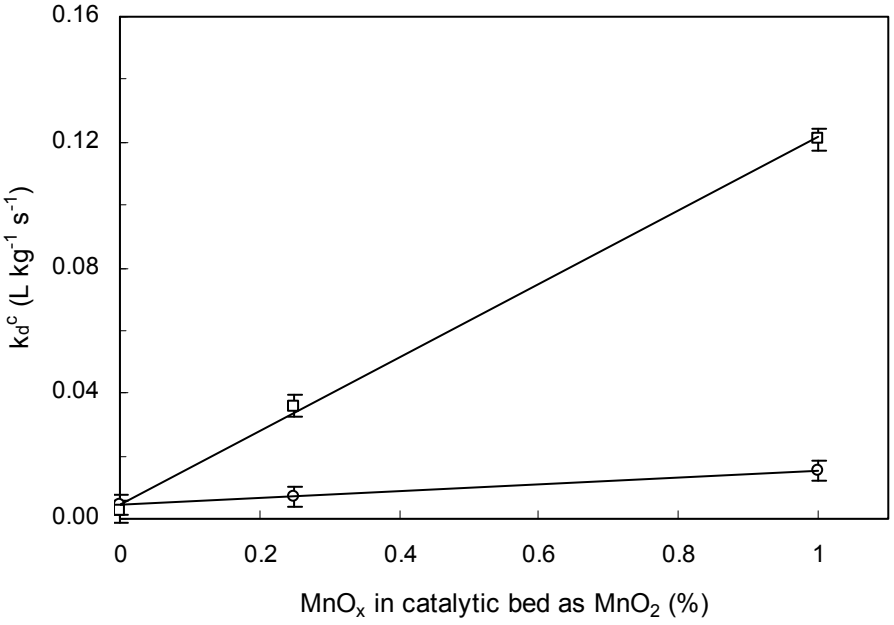

Fig. 6.2. Rate constant for the catalytic decomposition of ozone on MnO_x/Al_2O_3 (○) and MnO_x/SBA-15 (□) as a function of the content of manganese oxide in the catalytic bed calculated as MnO_2.

During the ozonation of a given organic compound, Eq. 10 can be integrated along the reactor to yield the following expression:

$$\frac{k_2}{k_1}\left(c_{Ao}-c_{As}\right)+\frac{k_3}{k_1}\ln\left(\frac{c_{Ao}}{c_{As}}\right)=\left(c_{O_3o}-c_{O_3s}\right) \tag{12}$$

Using experimental values for the concentrations of organic compound and ozone from runs performed at different spatial velocities, a regression analysis yields values for k_2/k_1 and k_3/k_1. The ratio k_2/k_1 can be rearranged from Eqs. 6 and 7 as follows:

$$\frac{k_2}{k_1}=\frac{\frac{\nu\,\varepsilon}{\rho_b}k_{O_3}^h+\nu\,k_{O_3}^c}{\frac{\varepsilon}{\rho_b}k_{O_3}^h+k_{O_3}^c+\frac{\varepsilon}{\rho_b}k_{HO\bullet}^h R_{ct}^h+k_{ox}^c R^c} \tag{13}$$

The compounds tested in this work have a low value of $k_{O_3}^h$ that is 6 $M^{-1}s^{-1}$ for atrazine [22], and 1.9 $M^{-1}s^{-1}$ for linuron [23]. Batch runs performed in the presence of t-BuOH 10 mM, a well-known radical scavenger, allowed the calculation of the direct catalytic rate constants for degradation of atrazine and linuron, $k_{O_3}^c$. We found no evidence that these values were significantly different from zero, the conversion of both compounds being completely explained by the homogeneous direct ozonation reaction. This result agrees with the negligible extent of adsorption observed for both compounds, as indicated before, and is also consistent with a low interaction between surface and neutral organics. Using these results, Eq. 13 transforms as follows:

$$\frac{k_2}{k_1} = \frac{\frac{\nu\,\varepsilon}{\rho_b} k_{O_3}^h + \nu\, k_{O_3}^c}{\frac{\varepsilon}{\rho_b} R_{ct}^h \left(k_{HO\bullet}^h + k_{ox}^c \frac{R^c}{R_{ct}^h} \frac{\rho_b}{\varepsilon} \right)} = \frac{\frac{\nu\,\varepsilon}{\rho_b} k_{O_3}^h + \nu\, k_{O_3}^c}{\frac{\varepsilon}{\rho_b} R_{ct}^h\, k_{HO\bullet}^{hc}} \tag{14}$$

where $k_{HO\bullet}^{hc}$ represents the apparent kinetic constant for the reaction with hydroxyl radicals in the presence of catalyst expressed in heterogeneous units. It is not a true kinetic constant, as depends on the efficiency of the system in producing homogeneous hydroxyl radicals and oxidized surface sites, but it can be readily computed and compared with the homogeneous constant $k_{HO\bullet}^h$. The same rearrangements for k_3/k_1 lead to the following expression:

$$\frac{k_3}{k_1} = \frac{\frac{\varepsilon}{\rho_b} k_d^h + k_d^c}{\frac{\varepsilon}{\rho_b} R_{ct}^h\, k_{HO\bullet}^{hc}} \tag{15}$$

In all cases and under the conditions tested in this work, with atrazine or linuron as organic compounds, Eq. 12 yielded experimental values for k_2/k_1 that did not differ significantly from zero. This is clearly due to the low value of the direct ozonations constants for both compounds. The value of k_3 can be obtained from the experimental data for ozone concentration the same runs by combining and integrating Eqs. 7 an 9. As a result, k_1 can be derived from

Eq. 15 and, from it, the experimental values of $k_{HO\bullet}^{hc} R_{ct}^{h}$ have been computed. The effect of catalyst could result in an enhancement of the rate of hydroxyl radical production from ozone, R_{ct}^{h}, an increase in the catalytic rate constant between organics and hydroxyl radicals, included in $k_{HO\bullet}^{hc}$, or both. In order to gain further insight on this point, we performed a series of simultaneous ozonation runs of atrazine and linuron in PBW and in the presence of bicarbonate 10^{-3} M and 5 x 10^{-3} M. The competitive kinetic method applied to a differential section of the fixed bed yields:

$$\frac{dc_A}{dc_B} = \frac{r_A}{r_B} = \frac{k_{1,A}\, c_A\, c_{O_3}}{k_{1,B}\, c_B\, c_{O_3}} = \frac{c_A\, k_{HO\bullet,A}^{hc}}{c_B\, k_{HO\bullet,B}^{hc}} \tag{16}$$

And integrating between inlet and outlet compositions:

$$\ln\left(\frac{c_{A.o}}{c_{A,s}}\right) = \frac{k_{HO\bullet,A}^{hc}}{k_{HO\bullet,B}^{hc}} \ln\left(\frac{c_{B.o}}{c_{B,s}}\right) \tag{17}$$

In order to derive Eqs. 16 and 17, $k_{O_3}^{h}$ was considered as being low for both atrazine and linuron, as indicated earlier. Fig. 6.3 shows the results of six series of runs performed with mixtures of atrazine (A) and linuron (B) using different amounts of bicarbonate, a well-known radical scavenger that should affect R_{ct} but not $k_{HO\bullet}$. The ratio of the logarithmic concentration decays of atrazine and linuron across the catalytic bed yielded a value for $k_{HO\bullet(A)}^{hc} / k_{HO\bullet(B)}^{hc}$ of 0.49 ± 0.05, a value that is not significantly different from the ratio determined using the homogeneous second order rate constants published elsewhere and obtained at 20ºC, namely, $k_{HO\bullet(A)}^{h} / k_{HO\bullet(B)}^{h}$ = 0.43 ± 0.04 [22-24]. This result offers no evidence that any of the catalysts may contribute to an increase in the second order rate constant for the reaction between organics and hydroxyl radicals. To be more precise, the experimental results show no evidence that $k_{ox}^{c} \frac{R^c}{R_{ct}^{h}} \frac{\rho_b}{\varepsilon}$ is significantly different from zero. If the catalytic reaction with hydroxyl radicals involved adsorbed organics, it might be expected that the rate constant $k_{HO\bullet}^{hc}$, due to the effect of k_{ox}^{c}, would differ from that of the homogeneous system, $k_{HO\bullet}^{h}$ and

that this difference would also affect their ratio. There is the possibility that the rate constant could increase both for atrazine and linuron cancelling the effect on the ratio of rate constants, but our previous findings pointed to a low degree of interaction between surface and organics if any. For it, the ozonation of fenofibric acid in several matrixes had already demonstrated that neither Al_2O_3 nor MnO_x/Al_2O_3 had any observable effect on its indirect ozonation rate constant even when hydroxyl radical-to-ozone ratio was significantly improved by both catalysts [7].

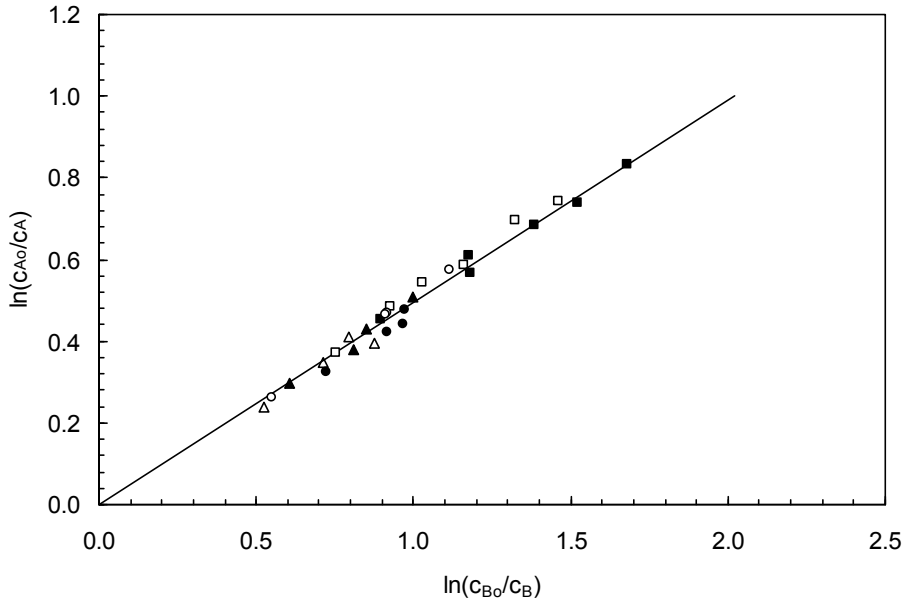

Fig. 6.3. Logarithmic decay of concentrations of atrazine (A) and linuron (B) in ozonation runs of mixtures of both compounds using MnO_x/Al_2O_3 (□) and MnO_x/SBA-15 (■) in PBW and MnO_x/Al_2O_3 10^{-3} M $NaHCO_3$ (○), MnO_x/Al_2O_3 5 x 10^{-3} M $NaHCO_3$ (Δ), MnO_x/SBA-15 10^{-3} M $NaHCO_3$ (●) and MnO_x/SBA-15 5 x 10^{-3} M $NaHCO_3$ (▲). (1.0 wt. % of MnO2 in all beds).

In what follows, we used the result that $k_{HO\bullet}^{hc}$ did not differ from their corresponding homogeneous values, $k_{HO\bullet}^{h}$ for atrazine and linuron in order to derive average values for R_{ct}^{h} from the experimental values of k_3/k_1 using Eq. 15. It must be noted that the conclusion concerning the lack of interaction of atrazine and linuron with the catalytic surface is not dependent on the particular values of R_{ct}^{h} or R^{c}. Fig. 6.4 plots the average hydroxyl radical-to-

ozone ratio within the reactor for ozonation runs of atrazine as a function of the moles of ozone consumed per mole of atrazine. The values were obtained in several reactors containing Al_2O_3, SBA-15 and two different amounts of MnO_x loaded on both supports. The plot shows that R_{ct}^h decreased with the moles of ozone consumed, whose higher values also corresponded to higher atrazine conversions. This behaviour may be a consequence of the disappearance from solution of the parent aromatic compounds. In fact, it has been stated that the decomposition of ozone and the production of hydroxyl radicals are strongly promoted by aromatic solutes due to the formation of hydrogen peroxide as an intermediate product [25]. Other compounds such as oxoacetic acids, typically found as ozonation by-products, contribute to ozone decomposition and to the formation of radicals such as superoxide and hydroperoxyl, and may contribute to this effect [26].

Fig. 6.4 also shows that R_{ct}^h was considerably promoted by MnO_x/Al_2O_3 with values near or over 10^{-6} whereas the maximum value obtained for Al_2O_3 was 3.7 x 10^{-7} for atrazine conversions < 10%. A much higher effect could be appreciated when MnO_x was incorporated into SBA-15, with R_{ct}^h as high as 3.0 x 10^{-6} while in similar conditions SBA-15 alone hardly surpassed 10^{-7}. This represented an average 30 fold increase in R_{ct} when using MnO_x/SBA-15 with respect to SBA-15 alone, whereas MnO_x/Al_2O_3 increased the efficiency in generation hydroxyl radicals by an average factor of 2.7 with respect to Al_2O_3. For MnO_x/SBA-15, R_{ct} increased threefold with respect to MnO_x/Al_2O_3 under similar conditions.

The use of catalyst also led to lower ozone consumption per mole of converted organic compound as observed in Fig. 6.5, which gives R_{ct}^h for runs performed using mixtures of linuron and atrazine on MnO_x/Al_2O_3 and MnO_x/SBA-15 in PBW loaded with different concentrations of bicarbonate. The increase in R_{ct}^h was parallel to the decrease in the moles of ozone consumed and was more intense for the case of MnO_x/SBA-15 catalyst. The lower ozone consumption corresponded to runs with high space velocities and, therefore, lower conversions, typically less than 10% ozone conversions for runs with efficiencies near 1.5 moles of ozone per mole of converted parent organic, atrazine or linuron.

a)

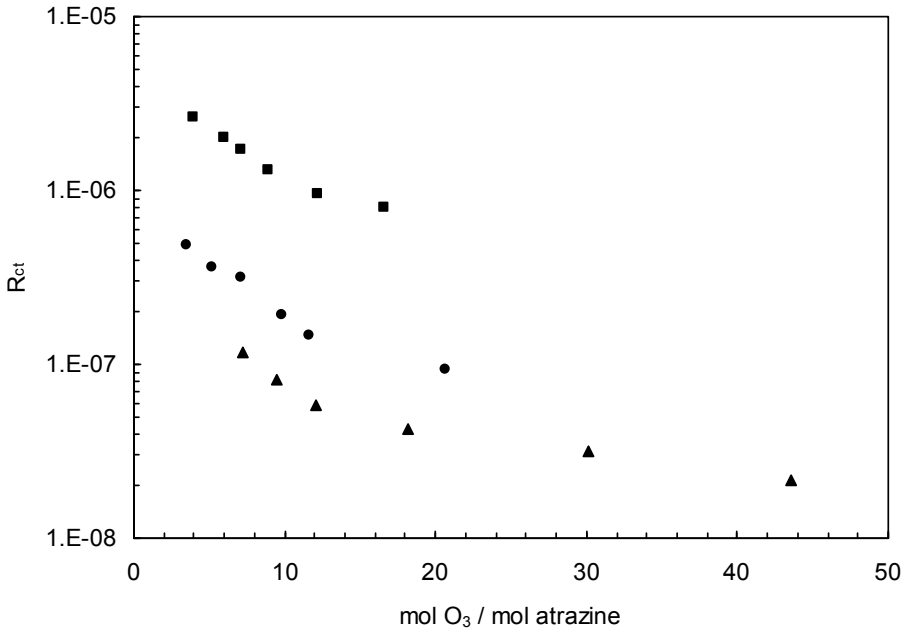

b)

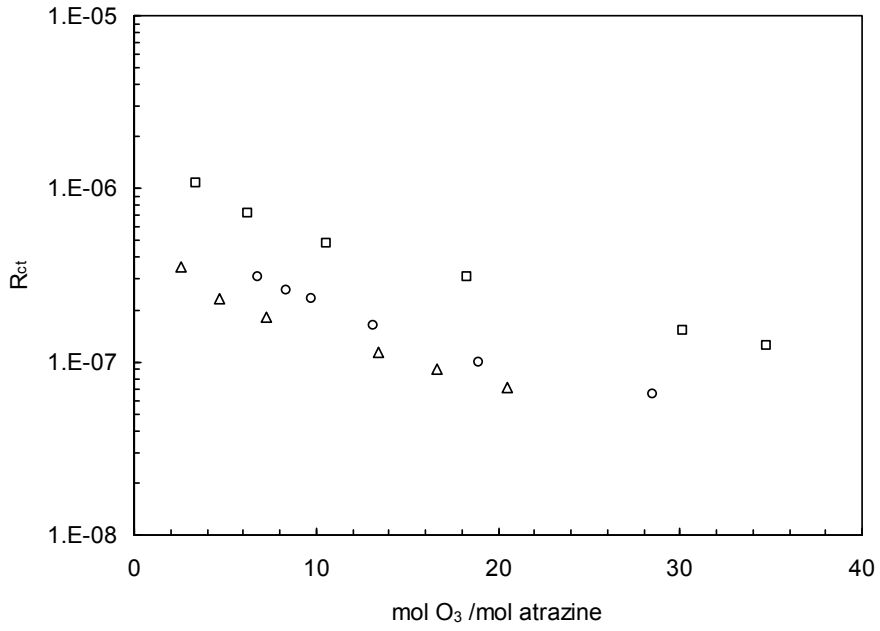

Fig. 6.4. Hydroxyl-radical-to-ozone ratio, R_{ct}, for the catalytic ozonation of atrazine on MnO_x/SBA-15 (a, filled symbols) and MnO_x/Al_2O_3 (b, empty symbols) using a MnO_2 load of 1.0% wt. (squares), 0.25% wt. (circles) and 0% (Al_2O_3 or SBA-15, triangles).

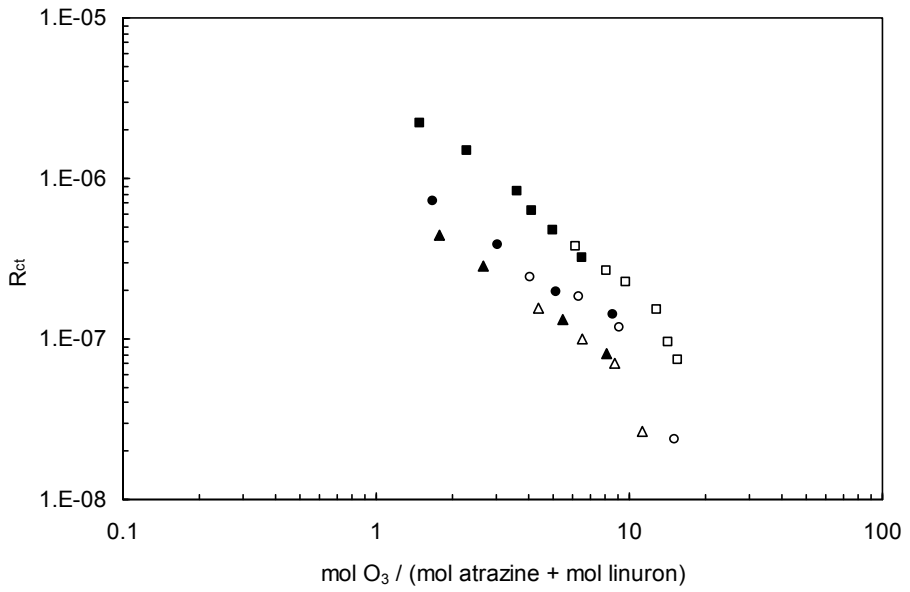

Fig. 6.5. Hydroxyl-radical-to-ozone ratio, R_{ct}, for the catalytic ozonation of mixtures of atrazine and linuron as a function of the moles of ozone consumed per mole of atrazine or linuron oxidized. MnO_x/Al_2O_3 (□) and MnO_x/SBA-15 (■) in PBW; MnO_x/Al_2O_3 10^{-3} M $NaHCO_3$ (○),MnO_x/SBA-15 10^{-3} M $NaHCO_3$ (●); MnO_x/Al_2O_3 5 x 10^{-3} M $NaHCO_3$ (Δ), and MnO_x/SBA-15 5 x 10^{-3} M $NaHCO_3$ (▲). (1.0 wt. % of MnO_2 in all beds).

6.5. Conclusions

A kinetic study of the catalytic ozonation of atrazine and linuron was carried out in a two-phase fixed-bed reactor operating in excess of ozone with ozone-preloaded phosphate buffered water. A catalyst with a larger specific surface, MnO_x/SBA-15, improved the rate of ozone decomposition with a kinetic constant of 0.123 ± 0.004 L kg^{-1} s^{-1} for a total metal bed load of 1.0 % expressed as MnO_2. In the same conditions, the ozone decomposition rate constant was 0.0155 ± 0.0015 L kg^{-1} s^{-1} for MnO_x/Al_2O_3. The incorporation of MnO_x to SBA-15 (1.0% as MnO_2) resulted in a 30 fold increase in the rate constant with respect to the non-catalytic ozone decomposition constant in the same matrix.

Neither atrazine nor linuron adsorbed significantly on any of the catalysts in PBW. Consistent with this result, we found that the direct catalytic ozonation constant did not differ significantly from zero in any case, the reaction with molecular ozone being essentially the non-catalytic process taking place in homogeneous phase. The results of catalytic runs on both

catalysts and using different concentrations of bicarbonate did not show any evidence that MnO_x/Al_2O_3 or MnO_x/SBA-15 increased the indirect, hydroxyl-mediated, ozonation rate constant with respect to homogeneous ozonation. This result suggests the absence of surface interaction with atrazine and linuron and may indicate that their adsorption did not take place at all. In any case, a possible adsorption of organics did not result in an energetically favoured route for the catalytic reaction with hydroxyl radicals.

The efficiency of hydroxyl radical production from ozone was significantly improved by the use of catalysts with average hydroxyl radical-to-ozone ratio within the reactor near 10^{-6} for MnO_x/Al_2O_3 and up to 3.0 x 10^{-6} for MnO_x/SBA-15. This represented a considerable - up to 30 fold - increase in the average value for R_{ct}^{h} with respect to the support alone for MnO_x/SBA - 15. R_{ct} for MnO_x/SBA-15 was about three times its value for MnO_x/Al_2O_3 under similar conditions. The use of catalyst also led to lower ozone consumption per mole of converted organic compound, whether or not bicarbonate was present in the solution, the highest efficiency being obtained for MnO_x/SBA-15. The relative efficiency of MnO_x/SBA-15 with respect to MnO_x/Al_2O_3 is most probably the consequence of a better distribution of the active phase on a larger surface.

6.6. Nomenclature

r_A	rate of ozonation of a given compound, mol L^{-1} s^{-1} or mol kg^{-1} s^{-1}
r_{O_3}	rate of reaction of ozone, mol L^{-1} s^{-1} or mol kg^{-1} s^{-1}
k_{O_3}	second order rate constant for direct ozonation reaction, L mol^{-1} s^{-1} (homogeneous) or L^2 mol^{-1} kg^{-1} s^{-1} (catalytic)
k_{ox}	second order rate constant of surface reaction, L mol^{-1} s^{-1}
k_d	rate constant for the decomposition of ozone, s^{-1} (homogeneous) or L kg^{-1} s^{-1} (catalytic)
$k_{HO\bullet}$	second order rate constant for the reaction with hydroxyl radicals, L mol^{-1} s^{-1}
c_A , c_B	concentration of organic compounds, mol L^{-1}
$c_{HO\bullet}$	concentration of hydroxyl radical, mol L^{-1}
c_{O_3}	concentration of dissolved ozone, mol L^{-1}
$c_{(O_3)_s}$	concentration of adsorbed ozone, mol kg^{-1}
c_s	concentration of free active centers at the catalyst surface, mol kg^{-1}
c_{ox}	concentration of oxidized surface sites, mol kg^{-1}
c_t	total concentration of active sites, mol kg^{-1}
K	equilibrium constant of ozone adsorption, L mol^{-1}
R_{ct}	ratio of $c_{HO\bullet}$ to c_{O_3}, dimensionless
R^c	ratio of $c_{(O_3)_s}$ and c_{O_3}, L kg^{-1}
W	mass of catalyst, kg
F_o	liquid flow-rate in reactor feed, L s^{-1}

6.7. Greek letters

v	stoichiometric coefficient, dimensionless
ε	bed porosity, dimensionless
ρ_b	bed bulk density, g L^{-1}

6.8. Subscripts and superscripts

o	reactor inlet
s	reactor outlet
h	homogeneous reaction
c	catalytic reaction
hc	simultaneous homogeneous and catalytic reaction

6.9. References

[1] EC, Directive of the European Parliament and of the Council 2000/60/EC establishing a framework for community action in the field of water policy, Official Journal, 2000, C513, 23/10/2000.

[2] R. Andreozzi, V. Caprio, A. Insola, R. Marotta, Advanced oxidation processes (AOP) for water purification and recovery, Catal. Today 53 (1999) 51–59.

[3] P.R. Gogate, A.B. Pandit, A review of imperative technologies for wastewater treatment I: oxidation technologies at ambient conditions, Adv. Environ. Res. 8 (2004) 501–551.

[4] P.R. Gogate, A.B. Pandit, A review of imperative technologies for wastewater treatment II: hybrid methods, Adv. Environ. Res. 8 (2004) 553–597.

[5] B. Kasprzyk-Hordern, M. Ziolek, J. Nawrocki, J., Catalytic ozonation and methods of enhancing molecular ozone reactions in water treatment, Appl. Catal. B: Environ. 46 (2003) 639–669.

[6] C.M. Jonsson, C.L. Jonsson, D.A. Sverjensky, H.J. Cleaves, R.M. Hazen, Attachment of L -glutamate to rutile (□-TiO_2): a potentiometric, adsorption, and surface complexation study, Langmuir, 25 (2009) 12127–12135.

[7] R. Rosal, M.S. Gonzalo, A. Rodríguez, E. García-Calvo, Catalytic ozonation of fenofibric acid over alumina-supported manganese oxide, J. Hazard. Mater., 183 (2010) 271–278.

[8] J.P. Kaptijn, The Ecoclear® process. Results from full-scale installations, Ozone Sci. Eng. 19 (1997) 297–305.

[9] Lin, S.H., Lai, C.L., Kinetic characteristics of textile wastewater ozonation in fluidized and fixed activated carbon beds, Water Res. 34 (2000) 763–772.

[10] J. Ma, M. Sui, T. Zhang, C. Guan, Effect of pH on MnO_x/GAC catalyzed ozonation for degradation of nitrobenzene, Water Res. 39 (2005) 779–786.

[11] X. Qu, J. Zhenga, Y. Zhanga, Catalytic ozonation of phenolic wastewater with activated carbon fiber in a fluid bed reactor, J. Colloid. Interface Sci. 309 (2007) 429–434.

[12] Y. Yangm J. Ma, Q. Qin, X. Zhai, Degradation of nitrobenzene by nano-TiO_2 catalyzed ozonation, J. Mol. Catal. A: Chem., 267 (2010) 41-48.

[13] J. Nawrocki, B. Kasprzyk-Hordern, The efficiency and mechanisms of catalytic ozonation, Appl. Catal. B: Environ., 99, (2010) 27–42.

[14] Y. Schuurman, Aspects of kinetic modeling of fixed bed reactors, Catal. Today 138 (2008) 15–20.

[15] D.P. Haughey, G.S.G. Beveridge, Local voidage variation in a randomly packed bed of equal-sized spheres. Chem. Eng. Sci. 21 (1966) 905−916.
[16] L. Yang, C. Hu, Y. Nie, J. Qu, Catalytic Ozonation of Selected Pharmaceuticals over Mesoporous Alumina-Supported Manganese Oxide, Environ. Sci. Technol. 43 (2009) 2525–2529.
[17] M.S. Elovitz, U. von Gunten, Hydroxyl radical/ozone ratios during ozonation processes. I. The R_{ct} concept, Ozone Sci. Eng. 21 (1999) 239–260.
[18] A. Rodríguez, R. Rosal, J.A. Perdigón, M. Mezcua, A. Agüera, M.D. Hernando, P. Letón, A.R. Fernández-Alba, E. García-Calvo, Ozone-based technologies in water and wastewater treatment, in: D. Barceló, M. Petrovic (Eds.), The Hand- book of Environmental Chemistry, vol. 5, Part S/2, Emerging Contaminants from Industrial and Municipal Waste, Springer, Berlin, 2008, pp. 127–175.
[19] L. Zhao, J. Ma, Z. Sun, H. Liu, Mechanism of heterogeneous catalytic ozonation of nitrobenzene in aqueous solution with modified ceramic honeycomb, Appl. Catal. B: Environ. 89 (2009) 326-334.
[20] F.J. Beltrán, F.J. Rivas, R. Montero, Catalytic ozonation of oxalic acid in an aqueous TiO_2 slurry reactor, Appl. Catal. B: Environ. 39 (2002) 221–231
[21] R. Rosal, A. Rodríguez, M.S. Gonzalo, E. García-Calvo, Catalytic ozonation of naproxen and carbamazepine on titanium dioxide, Appl. Catal. B: Environ. 84 (2008) 48–57.
[22] U. von Gunten, Ozonation of drinking water: Part I. Oxidation kinetics and product formation, Water Res. 37 (2003) 1443–1467.
[23] F.J. Benítez, F.J. Real, J.L. Acero, C. Garcia, Kinetics of the transformation of phenyl-urea herbicides during ozonation of natural waters: Rate constants and model predictions, Water Res. 41 (2007) 4073–4084.
[24] B. Balci, N. Oturan, R. Cherrier, M.A. Oturan, Degradation of atrazine in aqueous medium by electrocatalytically generated hydroxyl radicals. A kinetic and mechanistic study, Water Res. 43 (2009) 1924–1934.
[25] Pi, Y., Schumacher, J., Jekel, M., Decomposition of aqueous ozone in the presence of aromatic organic solutes, Water Res. 39 (2005) 83–88.
[26] J. Staehelin, J. Hoigné, Decomposition of ozone in water in the presence of organic solutes acting as promoters and inhibitors of radical chain reactions. Environ. Sci. Technol. 19 (1985) 1206–1213.